Discovery and Preclinical Characterization of 5-[4,6-Bis({3-oxa-8-azabicyclo[3.2.1]octan-8-yl})-1,3,5-triazin-2-yl]-4-(difluoromethyl)pyridin-2-amine (PQR620), a Highly Potent and Selective mTORC1/2 Inhibitor for Cancer and Neurological Disorders

Denise Rageot,[†] Thomas Bohnacker,[†] Anna Melone,[†] Jean-Baptiste Langlois,[†] Chiara Borsari,[†] Petra Hillmann,[‡] Alexander M. Sele,[†] Florent Beaufils,[†] Marketa Zvelebil,[†] Paul Hebeisen,[‡] Wolfgang Löscher,[§] John Burke,[∥] Doriano Fabbro,[‡] and Matthias P. Wymann*,[†]

[†]Department of Biomedicine, University of Basel, Mattenstrasse 28, 4058 Basel, Switzerland

[‡]PIQUR Therapeutics AG, Hochbergerstrasse 60, 4057 Basel, Switzerland

[§]Department of Pharmacology, Toxicology, and Pharmacy, University of Veterinary Medicine Hannover, and Center for Systems Neuroscience, 30559 Hannover, Germany

[∥]Department of Biochemistry and Microbiology, University of Victoria, Victoria, British Columbia V8W 2Y2, Canada

Ⓢ *Supporting Information*

ABSTRACT: Mechanistic target of rapamycin (mTOR) promotes cell proliferation, growth, and survival and is overactivated in many tumors and central nervous system disorders. PQR620 (**3**) is a novel, potent, selective, and brain penetrable inhibitor of mTORC1/2 kinase. PQR620 (**3**) showed excellent selectivity for mTOR over PI3K and protein kinases and efficiently prevented cancer cell growth in a 66 cancer cell line panel. In C57BL/6J and Sprague−Dawley mice, maximum concentration (C_{max}) in plasma and brain was reached after 30 min, with a half-life ($t_{1/2}$) > 5 h. In an ovarian carcinoma mouse xenograft model (OVCAR-3), daily dosing of PQR620 (**3**) inhibited tumor growth significantly. Moreover, PQR620 (**3**) attenuated epileptic seizures in a tuberous sclerosis complex (TSC) mouse model. In conclusion, PQR620 (**3**) inhibits mTOR kinase potently and selectively, shows antitumor effects in vitro and in vivo, and promises advantages in CNS indications due to its brain/plasma distribution ratio.
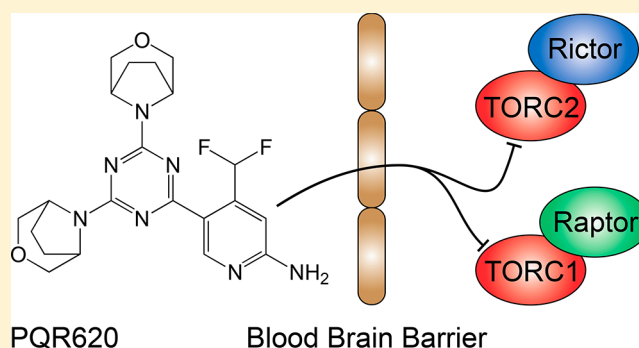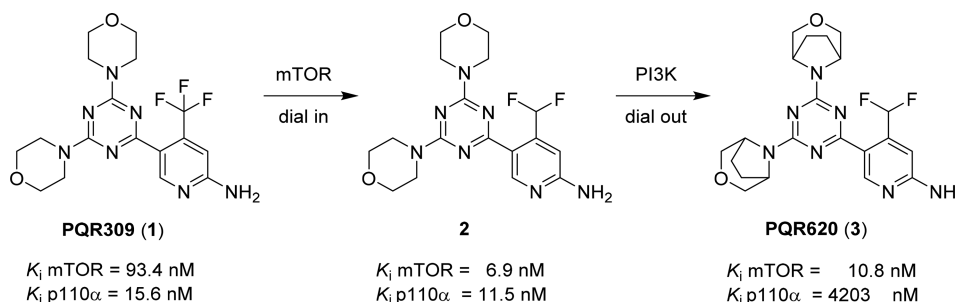
INTRODUCTION

The mechanistic target of rapamycin (mTOR, earlier mammalian TOR) operates downstream of phosphoinositide 3-kinase (PI3K) and protein kinase B (PKB/Akt). The PI3K/mTOR pathway is a key regulator of metabolism, cell growth, proliferation, and survival and is frequently overactivated in cancer and neurodegenerative disease.[1,2] The mTOR kinase is part of two main TOR complexes (TORC1 and TORC2). TORC1 integrates signals from cell surface receptors, energy status, stress, and availability of oxygen and amino acids. Cell surface receptors activate PI3K to produce PtdIns(3,4,5)P_3, which serves as a docking site for PKB/Akt and 3-phosphoinositide-dependent protein kinase 1 (PDK1). PKB/Akt is phosphorylated by PDK1 on Thr308 and by mTOR kinase integrated in TORC2 in the hydrophobic motif on Ser473.[3] Fully activated, PKB/Akt phosphorylates tuberous sclerosis 2 (TSC2, tuberin) in the tuberous sclerosis complex (TSC) and blocks its GTPase-activating protein (GAP) activity, which leads to the accumulation of GTP-loaded Rheb-GTPase (homologue enriched in brain) and assembly of

active TORC1 on endomembranes.[2] TORC2 is linked to PI3K activation by the Sin1 PH domain, as the Sin1-PtdIns(3,4,5)P_3 interaction unlocks TORC2 kinase activity after membrane translocation.[4] The phosphorylation of S6 kinase (S6K) by TORC1 is key to control cellular protein and lipid synthesis. TORC1 activity also impacts lysosome dynamics and autophagy, and TORC2 promotes metabolic activity, cell cycle, and cytoskeletal rearrangements.[2]

Rapamycin (sirolimus), its more soluble rapamycin-derivative (rapalog) RAD001 (everolimus), as well as CCI-779 (temsirolimus)[5] block TORC1 specifically by the formation of a TORC1/rapalog/FK506 binding protein 12 (FKBP12) complex.[6] Rapamycin has a long history as an immunosuppressive agent in organ transplant recipients,[7] and rapalogs have been exploited to prevent restenosis based on their anti-inflammatory and antiproliferative effects.[8]

PQR309 (1)

K_i mTOR = 93.4 nM
K_i p110α = 15.6 nM

2

K_i mTOR = 6.9 nM
K_i p110α = 11.5 nM

PQR620 (3)

K_i mTOR = 10.8 nM
K_i p110α = 4203 nM

Figure 1. Schematic design and optimization cascade leading to the mTOR kinase-selective ATP-binding site inhibitor PQR620 (**3**). Binding affinity for mTOR kinase was increased by the substitution of the trifluoromethyl group in PQR309 (**1**) with a difluoromethyl group in compound **2**. The introduction of substituted morpholino groups was then explored to reduce PI3K binding, resulting in PQR620 (**3**).

In 2007, temsirolimus (CCI-779) was approved for the treatment of renal cell carcinoma (RCC), followed by a phase III trial of everolimus in an advanced stage of the disease.[9] Everolimus has been approved for advanced pancreatic, lung, and gastrointestinal neuroendocrine tumors, mantle cell lymphoma, endometrial cancer, noncancerous kidney tumors in patients with TSC, pediatric subependymal giant cell astrocytoma (SEGA), and advanced ER+/HER2-negative breast cancer.[10]

In spite of the clinical success of rapalogs in the above indications, overall response rates to rapalogs as a single agent in major solid tumors have been modest.[11] Reasons for this are: (i) adverse effects of rapamycin due to its immune-suppressive action, limiting the maximal tolerated dose, but also (ii) the attenuation of drug action by a rapamycin-mediated suppression of a negative feedback loop, where TORC1 activates S6K and Grb10 to negatively control PI3K activation by receptors for insulin and growth factors. In the presence of rapalogs, TORC1 is thus inhibited, but class IA PI3Ks are overactivated, resulting in a TORC2-dependent increase in PKB/Akt activity.[1,2] Compounds targeting both TORC1 and TORC2 are therefore expected to provide a more efficient block of growth factor and PI3K downstream signaling.

ATP-competitive inhibitors have therefore been developed to target TORC1 and TORC2 protein kinase activities.[12] Sapanisertib (INK128 (**73**), MLN0128, TAK-228)[13] is in multiple clinical trials including advanced solid tumors, non-Hodgkin's lymphoma, breast cancer, multiple myeloma, and Waldenstrom's macroglobulinaemia, while CC-223 (**77**)[14] is being explored in malignancies such as non-Hodgkin's lymphoma, multiple myeloma, and diffuse large B-cell and follicular lymphoma. Vistusertib [AZD2014 (**78**)][15] is currently evaluated in a range of advanced tumors and has progressed to phase II clinical trials as a single agent in nonresponders to chemotherapy with mutated TSC (for more studies see clinicaltrials.gov). Moreover, preclinically charac-terized chemical probes with different potency and selectivity for TOR kinase, such as Torin1, PP242 (**75**), Ku-0063794, WAY-600, WYE-687, WYE-354, Palomid 529, and more have been described (for a review see ref 5.).

The overactivation of the mTOR pathway is not only important in malignant cancer but also promotes the development of hyperplastic lesions. In autosomal-dominant tuberous sclerosis complex (TSC), mutations in either TSC1 (hamartin) or TSC2 (tuberin) lead to a loss of control of mTOR signaling and the formation of initially benign hamartomas. These occur in multiple organs such as skin,

heart, kidneys, lung, and brain. Some form of impaired CNS function is frequent in TSC and includes epileptic seizures in ~90% patients, which dominates TSC morbidity to a high degree.[16]

Rapalogs have recently been explored to alleviate epileptic seizures triggered by loss-of-function mutations in the mTOR pathway. In a mouse model where TSC1 was selectively eliminated in neurons, sirolimus (rapamycin) and everolimus (RAD001) significantly improved the survival of neuronal-specific Tsc1 null mice and attenuated TORC1 downstream signaling.[17] A similar action of rapalogs could be achieved in TSC patients,[18,19] finally culminating in the approval of everolimus for TSC-associated seizures in April 2018. Rapalogs are, however, not generally effective in the whole TSC population, as resistance and considerable adverse side effects lead to treatment termination and dose reduction.[18,20]
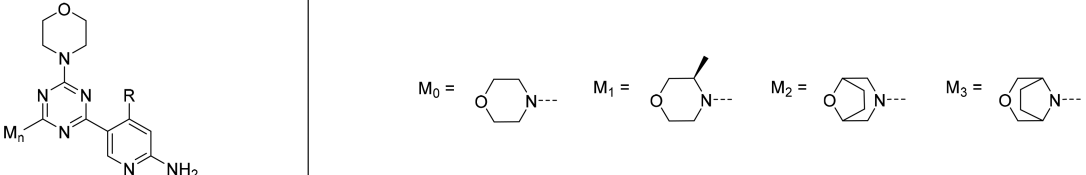
Targeting mTOR has also been proposed to be beneficial in Alzheimer's disease,[21] Huntington's disease,[22] and Parkinson's disease,[16] mostly based on the observation that inhibition of mTOR promoted removal of toxic protein complexes by the induction of autophagy. As rapalogs display limited brain permeability, there is a lack of molecules targeting mTOR in the CNS.

We have recently reported on PQR309 (**1**),[23] a pan-PI3K/mTOR inhibitor with excellent brain penetration and oral bioavailability, which is currently in phase II clinical trials for the treatment of lymphoma and solid tumors. This compound served as a starting point for the development and rational design of selective and highly brain penetrable mTOR kinase inhibitors. By introducing substituents with specific steric demands and defined electronic properties, we were able to derive a compound class with increased affinity for mTOR and much reduced binding of PI3K (Figure 1). From this series, we developed the highly selective and potent ATP-competitive mTOR inhibitor PQR620 (**3**), targeting TORC1 and TORC2.

■ RESULTS AND DISCUSSION

The transition from a pan-PI3K to an mTOR inhibitor was initiated by the elucidation of the binding mode of PQR309 (**1**) in the ATP-binding pocket of PI3K and mTOR kinases, where PQR309 (**1**) showed a 6-fold selectivity for PI3Kα over mTOR kinase (K_i for PI3Kα was 15.6 nM and K_i for mTOR was 93.4 nM). The binding mode of PQR309 (**1**) in PI3Kγ involves a hydrogen bond interaction in the hinge region between the backbone amide of Val882 and the morpholine oxygen atom. Additional interactions occur between Asp836 and Asp841 and the 2-aminopyridine moiety in the affinity pocket.[23,24] An analogous binding mode of PQR309 (**1**) is

Table 1. SAR Study of Selected R-Substituted Triazine Core Compounds

| compd | R | M_n | IC$_{50}$ [nM][a] | | K$_i$ [nM][b] | | ratio K$_i$ |
			pPKB/Akt	pS6	p110α	mTOR	p110α/mTOR
4[c]	H	M_0	404	382	94.0	46.1	2.0
5[d]	CH$_3$	M_0	401	939	61.2	609	0.10
PQR309 (**1**)[c]	CF$_3$	M_0	178	194	15.6	93.4	0.17
2	CHF$_2$	M_0	102	118	11.5	6.9	1.7
6	CH$_2$F	M_0	397	218	68.6	54.3	1.3
7	CH$_2$OH	M_0	341	528	81.3	74.5	1.1
8	CH(OCH$_3$)$_2$	M_0	1198	2109	129	474	0.27
9	OCH$_3$	M_0	1848	1918	693	483	1.4
10	CHF$_2$	M_1	147	138	20.8	9.6	2.1
11	CHF$_2$	M_2	144	112	23.7	3.4	7.0
12	CHF$_2$	M_3	156	113	25.8	11.2	2.3

[a]Phosphorylation of PKB/Akt on Ser473 and ribosomal protein S6 on Ser235/236 were analyzed in A2058 cells exposed to the indicated inhibitors and subsequent detection of phosphoproteins in an in-cell Western assay.[23] [b]Compounds were tested in vitro for binding to the catalytic subunit of PI3Kα (p110α) and mTOR using a commercially available time-resolved FRET (TR-FRET) displacement assay (LanthaScreen). Means of K$_i$s are shown. Standard errors of the mean (SEM) are depicted in Supporting Information, Table S9. [c]Extended from ref 23. [d]Derived from ref 23.
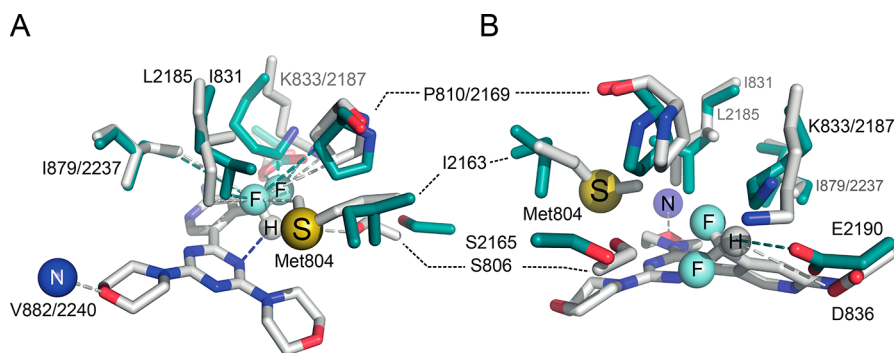
Figure 2. Predicted interactions of compound **2** with the catalytic core of PI3Kγ (gray) and mTOR kinase (teal). Displayed are amino acids in close contact with the inhibitor; three-digit numbers refer to PI3Kγ, four-digit codes to mTOR kinase. Labeled spheres: N, nitrogen atom of the hinge region Val (882/2240); S, sulfur atom of Met804; F and H, difluoromethyl group. (A) One morpholine group (left) of **2** interacts with the nitrogen atom of the hinge region Val. Here the hydrogen atom of the difluoromethyl group is oriented to form an intramolecular interaction with the triazine core. (B) The hinge region valine interaction is oriented toward the back, and the hydrogen atom of the difluoromethyl group is well positioned to form an interaction with Glu2190 of mTOR. (A,B) Compound **2** in PI3Kγ was modeled based on a PQR309 (**1**)−PI3Kγ complex[23] (PDB 5OQ4; resolution of 2.7 Å), and the mTOR−compound **2** complex was derived from a 3.6 Å resolution structure of PI103 bound to mTOR (PDB 4JT6) by docking as described in ref 23. A comparative listing of amino acid residues depicted here across PI3K isoforms can be found in Supporting Information, Table S1.

assumed in mTOR, involving residues Val2240 and Asp2190/2357.

Optimization of mTOR Affinity. To assess the influence of the trifluoromethyl moiety at the C4-position of the aminopyridine (R-substituent), toward selective mTOR inhibition, we prepared a series of compounds replacing the trifluoromethyl moiety with various substituents and tested them in cellular and enzymatic assays (Table 1). Physicochemical properties, such as clogP and PSA, were calculated for all studied compounds (see Supporting Information, Table S9). Substitutions on the heteroaromatic ring (compounds **1**, **2**, and **4**−**9**) had a major impact on the balance between hydrophilicity and lipophilicity (clogP variations from 1.08 to 2.72).

Among this bismorpholino-substituted triazine series, compound **2** with a difluoromethyl substituent (R = CHF$_2$) was found to be the most potent compound in vitro (K$_i$ for mTOR of 6.9 nM) and in cells (IC$_{50}$ for phosphorylated PKB = 102 nM, for phosphorylated S6, IC$_{50}$ = 118 nM). In general, the affinity toward mTOR increased as a function of R in the order: CH$_3$ ≈ CH(OCH$_3$)$_2$ ≈ OCH$_3$ < CF$_3$ ≈ CH$_2$OH ≈ CH$_2$F ≈ H < CHF$_2$. For compound **2** the cellular data displayed both efficient inhibition of TORC1 upstream of ribosomal protein S6 kinase (see IC$_{50}$ value for pS6 in Table 1), and TORC2 activity upstream of PKB phosphorylation (see IC$_{50}$ for pPKB in Table 1). The low mTOR affinities of compounds **8** and **9** can only in part be attributed to bulky substituents as the affinity differences in CF$_3$-, CHF$_2$-, CH$_2$F, and CH$_3$-substituted compounds point to an importance of the

Table 2. SAR of Symmetrically Substituted 4-(Difluoromethyl)-5-(1,3,5-triazin-2-yl)pyridine-2-amines

| compd | M_n | IC$_{50}$ [nM][a] | | K$_i$ [nM][b] | | ratio K$_i$ |
		pPKB	pS6	p110α	mTOR	p110α/mTOR
13	M_1	364	310	633	12.6	50
14	M_2	630	301	1297	13.9	93
PQR620 (3)	M_3	190	85.2	4203	10.8	389
15	M_4	4037	1565	>20000	18.5	>1000
16	M_5	17685	12572	4632	308	15
17	M_6	17851	5768	>20000	551	49
18	M_7	354	209	32.2	13.6	2.4
19	M_8	252	160	141	3.5	40
20	M_9	3570	1189	>20000	79.9	>250
21	M_{10}	379	294	64.0	21.1	3.0
22	M_{11}	20872	10380	15364	650	24
23	M_{12}	4815	2329	8787	73.4	120
24	M_{13}	942	526	632	32.8	19
25	M_{14}	357	275	2379	31.0	77
26	M_{15}	1212	1298	>20000	60.2	>330

[a]Phosphorylation of PKB/Akt on Ser473 and ribosomal protein S6 on Ser235/236 were analyzed in A2058 cells exposed to the indicated inhibitors and subsequent detection of phosphoproteins in an *in-cell* Western assay.[23] [b]Compounds were tested in vitro for binding to the catalytic subunit of PI3Kα (p110α) and mTOR using a commercially available time-resolved FRET (TR-FRET) displacement assay (LanthaScreen). Means of K$_i$s are shown. SEMs are depicted in Supporting Information, Table S9.

dipole moment of CHF$_2$ group in R in mTOR, but less so in PI3Kα.

The CHF$_2$ group was recently proposed to act as a lipophilic hydrogen donor[25] and has as such two possible conformational interaction modes in PI3K and mTOR: as depicted in Figure 2A, the proton of the CHF$_2$-group could (i) interact with a triazine core nitrogen in an intramolecular fashion, or (ii) form interactions with Asp836 in PI3Kγ or Glu2190 in mTOR (Figure 2B). An intramolecular proton−nitrogen interaction with the core does not disturb the overall orientation of the inhibitor, although in class I PI3K the CHF$_2$ group is in close proximity to a methionine (Met804 in PI3Kγ, distance ca. 3.3 Å), while mTOR presents an isoleucine (Ile2163, >7 Å) at this position. Turned toward Glu2190 (mTOR) or Asp836 (PI3Kγ), the CHF$_2$ group appears to be closer to the negative side chain in mTOR than in PI3Kγ. This, and the slightly more hydrophobic nature of the pocket in mTOR (see Ile2163), is likely to enforce a CHF$_2$ proton−Glu2190 hydrogen bond and thus explains the pronounced increase in mTOR affinity for CHF$_2$-substituted compounds.

Increasing Selectivity for mTOR, Dialing Out PI3K. As many of the above R-substituents maintained low K$_i$ values for PI3Kα (see PQR309 (1), 2, 5, and 6; Table 1), we introduced various morpholine derivatives as M$_n$ substituents, such as (R)-3-methylmorpholine (M$_1$), 8-oxa-3-azabicyclo[3.2.1]octane (M$_2$), and 3-oxa-8-azabicyclo[3.2.1]octane (M$_3$, Table 1). Morpholine derivatives M$_1$, M$_2$, and M$_3$ with increased steric demands were examined to determine whether the interaction in the hinge region of mTOR occurs with the oxygen atom of

the morpholine M$_0$ or of the substituted morpholine (M$_{1−3}$). The effect of various substitution of morpholines on mTOR versus PI3K selectivity has been reported for pyrazolopyrimidines,[26] showing a profound loss in PI3Kα activity leading to a >1000-fold selectivity for mTOR over PI3Kα when morpholine M$_0$ was replaced with the 2,6- or 3,5-ethylene bridged morpholine (M$_2$ and M$_3$). Likewise, the introduction of (R)-3-methylmorpholine (M$_1$) improved the selectivity for mTOR.

Consequently, we prepared analogues of compound 2 (with R = CHF$_2$) with selected substituted morpholines. Among M$_n$ substituents, morpholine M$_2$ showed the highest affinity and selectivity for mTOR in 11 (K$_i$ for mTOR = 3.4 nM, and ratio of K$_i$ of p110α/mTOR ∼7). Inhibitors 10, 11, and 12 with substituents M$_n$ = M$_1$, M$_2$, and M$_3$, respectively, proved to be all excellent inhibitors for mTOR and PI3K in vitro and in cells (Table 1). These results underline that the increase in mTOR activity is dominated by the 4-(difluoromethyl)pyridin-2-amine group rather than from substitutions of one morpholine group. Compounds 10−12 maintain most likely affinity for PI3K as they all bear one unsubstituted morpholine (M$_0$), which is able to bind to the hinge region of the ATP-binding site of PI3K. The bulky morpholines (M$_{1−3}$) would then be solvent exposed and have a negligible effect on PI3K or mTOR binding.

These observations prompted us to focus our SAR study on symmetrically substituted triazines (Table 2). Introduction of methyl groups, methylene, or ethylene bridges into morpholine groups (see 13−17) did not significantly affect the clogP. Bulky alkylic substitutions on the morpholine yielded,
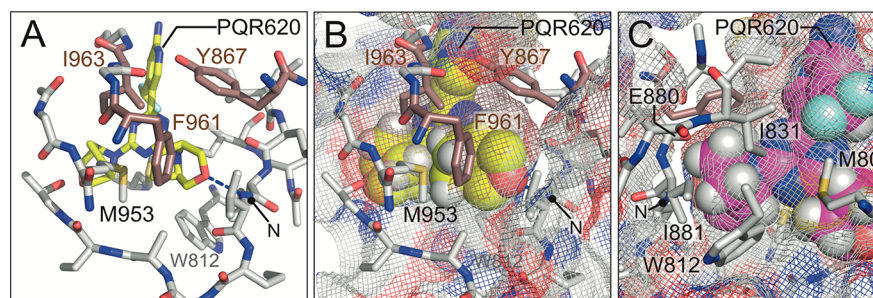
Figure 3. Steric clashes of PQR620 (**3**) docked into PI3Kγ (light gray). Two opposite conformations of the ethylene bridges of the morpholines of PQR620 (**3**) that allow the morpholine oxygen to form a hydrogen bond with the hinge Val882 nitrogen (N) are shown. (A) In the "bridge-up" conformation, the ethylene bridge of PQR620 (**3**) (yellow) points toward Met953 and is flanked by a rigid part of PI3Kγ,[27] represented by Tyr867, Phe961, and Ile963 (colored in brown). (B) When the surface of PI3Kγ is depicted as a mesh and PQR620 (**3**) as space filling model (atom size set to 0.9 times of van der Waals radii), steric clashes become visible as penetrations of the PI3Kγ surface mesh. (C) In the "bridge-down" conformation (pink), steric clashes imposed by the ethylene bridges in PQR620 (**3**) occur with the backbone of Ile881 and Glu880 and side chains of Ile831 and Ile881. As for Figure 2, the models were derived from coordinates of a PQR309 (**1**)−PI3Kγ complex[23] (PDB 5OQ4; resolution of 2.7 Å). A comparative listing of amino acid residues depicted here across PI3K isoforms can be found in Supporting Information, Table S2.

however, more lipophilic compounds (compounds **18−24** and **26**; see Supporting Information, Table S9). Many of these compounds showed excellent mTOR activity in vitro ($K_i \leq 30$ nM for PQR620 (**3**), **13−15**, **18−19**, **21**, and **24−25**). The affinity for mTOR was reduced when both, the C2- and C6-morpholine positions were substituted with a methyl-group (K_i of 650 nM for compound **22**), whereas methyl-substitution at both the C3- and C5-position showed only a minor effect on mTOR binding. Excellent in vitro (>100-fold) selectivity for mTOR versus PI3Kα were obtained for compounds PQR620 (**3**, M_3), **15** (M_4), **20** (M_9), and **26** (M_{15}); good selectivity (>70-fold) for compounds **14** (M_2), **23** (M_{12}), and **25** (M_{14}).

Compounds containing 3,5-dimethylmorpholines (M_8, M_9, and M_{10}) showed relevant differences in cellular potency and in selectivity for mTOR versus PI3Kα. Whereas compound **20** (M_9) showed good selectivity (K_i of p110α/mTOR > 250) and no inhibition of mTOR/PI3K in cells, its enantiomer **21** (M_{10}) was much less selective (K_i of p110α/mTOR ∼3) and was slightly more active in cells. The enantiomeric pair **15** and **16** (M_4 and M_5) showed poor potency in cellular assays (IC_{50} > 1000 nM), although a remarkable difference in affinity for mTOR between them (K_i = 18.5 nM for **15** vs K_i = 308 nM for **16**).

Generally, the symmetrically substituted derivatives in Table 2 displayed reduced cellular activities as compared to unsymmetrically substituted analogues (Table 1, compounds **10−12**), with the exception of the selected compound PQR620 (**3**). Compound PQR620 (**3**) was the most potent in biochemical and cellular assays (K_i for mTOR = 10.8 nM; IC_{50} for pPKB = 190 nM and IC_{50} for pS6 = 85.2 nM) and very selective for mTOR versus PI3K (389-fold selectivity).

Elucidation of Binding Modes to PI3K and mTOR. Computational modeling studies were used to elucidate the binding mode of PQR620 (**3**) and ultimately provided structural features defining the compounds high selectivity toward mTOR versus PI3K. Exploiting the 2.7 Å resolution X-ray structure of PQR309 (**1**) in PI3Kγ (PDB code 5OQ4), we substituted the inhibitor for PQR620 (**3**). Energy minimization calculations of the resulting PI3Kγ−ligand complex maintained important interactions such as hydrogen bonds between the aminopyridine and Asp836/964 as well the one between one morpholine oxygen atom and the backbone amine of Val882 (as present in the parental structure with PQR309 (**1**)). In PQR620 (**3**), the ethylene bridge of the morpholine pointing toward Val882 can take two main conformations, with the bridge oriented toward Met953 ("bridge-up", Figure 3A,B) or toward Ile881 ("bridge-down", Figure 3C). The bridge-up conformation induces steric clashes within a region of the ATP-binding pocket that has previously been identified as very rigid in PI3Kγ and is defined by residues Tyr867, Phe961, and Ile963.[27]

The "bridge-down" conformation of PQR620 (**3**) generates steric clashes with the backbone of Ile881 and Glu880 and side chains of Ile831 and Ile881. All these steric clashes can only be minimized when the distance between the Val882 and the morpholine O atom is significantly increased to >3.5 Å, as compared to a 2.5 Å distance in the PQR309 (**1**)−PI3Kγ complex, and therefore no longer represents a strong hydrogen bond. Steric clashes, and as a consequence the weakening of the essential hydrogen bond to the PI3K hinge region explain the reduced affinity of PQR620 (**3**) for PI3K.

Analogous computational modeling studies were performed for a PQR620 (**3**)−mTOR kinase complex starting with the 3.6 Å resolution structure of the PI103−mTOR complex (PDB 4JT6). After a ligand exchange, the oxygen atom of one bridged morpholine of PQR620 (**3**) forms a hydrogen bond with the hinge region Val2240 backbone nitrogen and the 2-amino moiety interacts with Asp2195/2357 side chains in the affinity binding pocket of mTOR. The binding pocket of mTOR is deeper due to the presence of the flexible Leu2354 replacing the rigid Phe961 in PI3Kγ (see Figure 2). As a result, an ethylene-bridged morpholine (M_3) can be easily accommodated in the pocket pointing toward Val2240. Although these modeling efforts suggest some preference for the "bridge-up" conformation in mTOR, the low resolution of the mTOR template structure prevents a precise placement of the ethylene bridge in the morpholine pointed toward Val2240 (Supporting Information, Figure S1).

Glu2190 in mTOR can be superimposed with Asp836 of PI3Kγ, but Glu2190 has a different vector allowing it to interact with the 2-amino moiety (3.1 Å) and the dipole of the CHF_2 group (3.4 Å). This view is supported by biological data pointing to an important role of the CHF_2 substituent in the selectivity of mTOR binding. The combination of the Glu2190 CHF_2 group dipole interaction in mTOR and the steric clashes in PI3K explain the enhanced binding affinity for mTOR and the reduced affinity of PQR620 (**3**) for PI3K as compared to PQR309 (**1**).

Table 3. SAR Study of Selected Pyrimidine Core Compounds
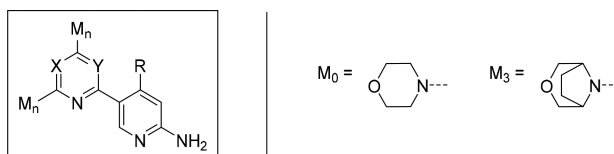
compd	R	M_n	X	Y	IC$_{50}$ [nM][a]		K_i [nM][b]		ratio of K_is
					pPKB/Akt	pS6	p110α	mTOR	p110α/mTOR
BKM120 (**27**)	CF$_3$	M$_0$	N	CH	416	553	20	199	0.10
28	CHF$_2$	M$_0$	N	CH	207	184	18	35	0.51
29[c]	CF$_3$	M$_0$	CH	N	729	926	41	911	0.045
30	CHF$_2$	M$_0$	CH	N	243	256	29	42	0.69
31	CF$_3$	M$_3$	N	CH	520	318	2190	30	73.0
32	CHF$_2$	M$_3$	N	CH	287	164	2090	12	174
33	CF$_3$	M$_3$	CH	N	3318	1944	5668	435	13.0
34	CHF$_2$	M$_3$	CH	N	650	395	2230	60	37.2

[a]Phosphorylation of PKB/Akt on Ser473 and ribosomal protein S6 on Ser235/236 were analyzed in A2058 cells exposed to the indicated inhibitors and subsequent detection of phosphoproteins in an in-cell Western assay.[23] [b]Compounds were tested in vitro for binding to the catalytic subunit of PI3Kα (p110α) and mTOR using a commercially available time-resolved FRET (TR-FRET) displacement assay (LanthaScreen). Means of K_is are shown. [c]Compound is referred to as BKM120-R1 (regio-isomer of BKM120) in ref 24. SEMs are depicted in Supporting Information, Table S9.

Scheme 1. Synthesis of Trisubstituted Compounds with Triazine and Pyrimidine Core[a]
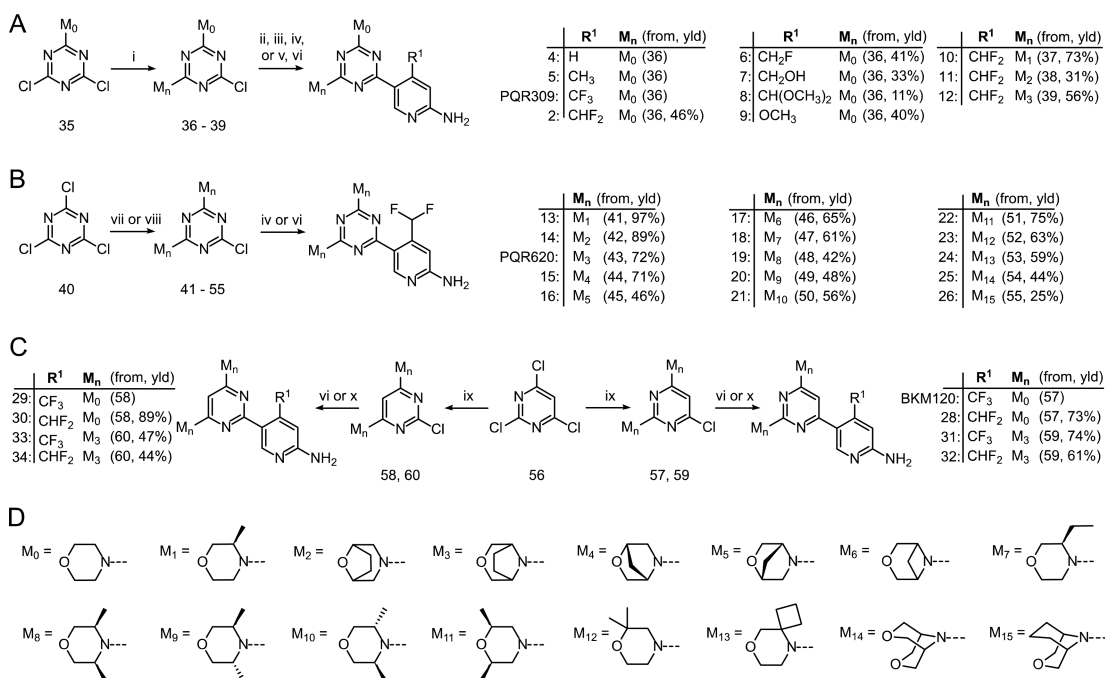
[a]Reagents and conditions: (i) morpholine derivative (M_n-H), DIPEA, EtOH, 0 °C → rt, o/n (for **37–39**); (ii) 2-aminopyridine-5-boronic acid pinacol ester or 2-amino-4-methyl-pyridine-5-boronic acid pinacol ester, Pd(dppf)Cl$_2$ (cat.), Na$_2$CO$_3$, 1,2-dimethoxyethane/H$_2$O, 90 °C, 16 h (for **4, 5**); (iii) (1) boronic ester **72**, Pd(OAc)$_2$/PPh$_3$ (cat.), K$_2$CO$_3$, THF/H$_2$O, 55 °C, 2 h, (2) HCl, H$_2$O, 55 °C, 16 h (for PQR309); (iv) boronic ester **64**, XPhosPdG2 (cat.), K$_3$PO$_4$, dioxane/H$_2$O, 95 °C, o/n (for **10, 11, 12, 14, 17, 18, 23, 24,** PQR620); (v) boronic ester generated in situ, XPhosPdG2 (cat.), K$_3$PO$_4$, dioxane/H$_2$O, 95 °C, 3.5 h, (2) TFA, CH$_2$Cl$_2$, add. at 0 °C, rt, 6 h (for **8**); (vi) (1) boronic ester **64** or **72** or boronic ester generated in situ, XPhosPdG2 (cat.), K$_3$PO$_4$, dioxane/H$_2$O, 95 °C, 3–16 h, (2) HCl, dioxane/H$_2$O, 60 °C, 3–16 h (for **2, 6, 7, 13, 15, 16, 19–22, 25, 26, 28, 30–34**; for **9** the reaction was carried out in ethanol at 80 °C); (vii) M_n-H, DIPEA, CH$_2$Cl$_2$, 0 °C → rt, o/n (for **41–47, 52, 53, 55**); (viii) M_n-H, DIPEA, THF, add at 0 °C, 70 °C, o/n (for **48–51, 54**); (ix) morpholine derivative (M_n-H), DIPEA, EtOH, Δ, o/n (for **57–60**); (x) (1) boronic ester **72**, Pd(OAc)$_2$/PPh$_3$ (cat.), K$_2$CO$_3$, dioxane/H$_2$O, 80 °C, 16 h, (2) HCl, H$_2$O, 60 °C, 18 h (for BKM120, **29**[24]).

To ascertain the choice for a lead compound, the SAR study was extended to pyrimidine core analogues of PQR620 (**3**) (Table 3). Therefore, we prepared BKM120 (**27**), its regioisomer **29**,[24] and the corresponding 4-(difluoromethyl)-pyridin-2-amine analogues **28** and **30**. Replacement of trifluoromethyl by difluoromethyl as R-substituent improved

mTOR binding by a factor of 5−20 for pyrimidine analogues in vitro (Table 3), validating the CHF$_2$−dipole mTOR interactions discussed above. Still, both pyrimidine core regioisomers **28** and **30** showed reduced potency compared to their triazine analogue **2** (compare Table 1).

Table 4. mTOR and Lipid Kinase Binding Constants of PQR620 (3) and Reference Compounds

| | kinases | | | | | | | fold selectivity |
| | inhibitor binding constants[a] K_d, [nM] | | | | | | | |
	mTOR	PI3Kα	PI3Kβ	PI3Kδ	PI3Kγ	PI4Kβ	VPS34	PI3Kx/mTOR[c]
PQR620 (3)[d]	0.27	**1000**	22000	23000	18000	>30000	2750	~3700×
INK128 (73)	0.092	15	81	30	**3.7**	n.d.	8200	~40×
SB2602 (74)	0.85	2700	20000	>30000	22000	>30000	8300	~3100×
PP242 (75)[b]	3	150	120	**31**	42	940	nd	~10×
CC223 (77)	28	**2300**	18000	6200	7100	39	2500	~80×
AZD2014 (78)	0.14	**33**	3300	1500	8400	>30000	23000	~230×

[a]Dissociation constants (K_d) were determined using ScanMax technology (DiscoveRx) with 11-point 3-fold serial dilutions of the indicated compounds. K_d is the mean value from experiments performed in duplicate and were calculated from standard dose response curves using the Hill equation ($n \geq 2$). [b]Dissociation constants (K_d) of PP242 (75) are reprinted from ref 28. with the consent of DiscoverX Corporation. nd: not determined. [c]Fold selectivity: ratio of K_d of most sensitive class I PI3K isoform (displayed in bold type) over K_d for mTOR. [d]A preliminary data set has been compared with rapamycin and everolimus (K_ds for the FKBP12 site were 0.6 and 2 nM, respectively) in ref 29. Standard deviations are reported in Supporting Information, Table S3, except for cited values of PP242.

Pyrimidine core derivatives of PQR620 (3), such as compounds 32 and 34, displayed higher selectivity for mTOR as compared to their CF₃-substituted analogues (31 and 33). The pyrimidine core compounds bearing substituted morpholines were inactive toward PI3K, but triazine-based PQR620 (3) surpassed its pyrimidine analogue 32 regarding selectivity and potency toward mTOR in vitro and in cells.

Chemical Synthesis. Triazine analogues described above and substituted with two unsubstituted morpholines (M_0) (PQR309 (1), 2, 4−9) or with one morpholine M_0 and a $M_{1−3}$ morpholine (compounds 10−12) were prepared according to the synthetic route A depicted in Scheme 1 starting from commercially available 4-(4,6-dichloro-1,3,5-triazin-2-yl)-morpholine (35). Morpholine derivatives were introduced as M_n substituents by nucleophilic aromatic substitution reaction (for intermediates 37−39, with $M_n \neq M_0$) and a subsequent palladium catalyzed Suzuki coupling between the desired organoboronic ester and cholorotriazine intermediate 36−39 gave the inhibitors PQR309 (1), 2, and 4−12. The synthetic strategy B was used to prepare di-M_n-substituted triazines (PQR620 (3) and compounds 13−26) and route C to synthesize pyrimidine core analogues (compound 28−34). All three synthetic routes only differ by the reaction conditions used. Overall, this strategy represents a robust and modular synthetic route giving access to a broad variety of compounds.

Enzymatic and Cellular Profiling, Determination of Selectivity, and in Vitro ADME. Because of its superior activity and mTOR selectivity PQR620 (3) was chosen for further characterization. DiscoverX KINOMEscan assays confirmed PQR620 (3)'s excellent mTOR selectivity: PQR620 (3) was ~3700-fold more potent for mTOR as compared to class I and class III PI3K isoforms and did not inhibit PI4Kβ even at excessive concentrations (Table 4). The selectivity of PQR620 (3) for mTOR over PI3K thus exceeds competitor compounds such as INK128 (73) (~40×), CC223 (77) (~80×), and AZD2104 (78) (~230×) and is closely followed by SB2602 (74) with a selectivity of ~3100-fold.

Moreover, compound PQR620 (3) showed negligible off-target effects when screened against a DiscoverX scanMAX kinase assay panel containing a set of 456 diverse wild-type kinases (Supporting Information, Figure S2). At a concentration of 10 μM, PQR620 (3) and SB2602 (74) reached outstanding selectivity scores (S(10) of 0.005 and 0.003, respectively; Supporting Information, Table S4), while values of INK128 (73) and PP242 (75) exceeded 0.1 for S(10)

[S(10) = number of hits/number of tested kinases (at a threshold of 10% of control; see Supporting Information, Table S4)].

The in vitro pharmacology profile of PQR620 (3) at 10 μM was determined in a panel of assays covering a broad range of targets including receptors, ion channels, transporters, enzymes, and second messengers. No off-target binding activities were identified and PQR620 (3) showed excellent selectivity versus unrelated receptors and ion channels including hERG (Supporting Information, Figure S3). Detectable signals for COX1 and PDE4D2 inhibition remained below 50% (Supporting Information, Figure S4).

Cellular Activities. Compound PQR620 (3) was tested in vitro across a panel of tumor cell lines including glioblastoma (A-172, T98G, and "U-87 MG"), neuroblastoma (SK-N-AS and SK-N-FI) and malignant melanoma (A375, COLO 829, and RPMI-7951) cancer cell lines (Figure 4 and Supporting
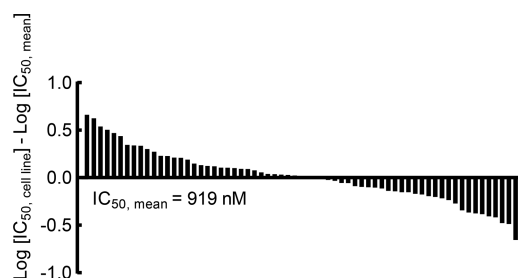

Figure 4. Waterfall plot representing the potency of PQR620 (3) in a full NTRC (Netherlands Translational Research Center BV) Oncolines cell panel of 66 cancer cell lines. Concentrations of half-maximal growth inhibition (IC_{50}) for PQR620 (3) were obtained from dose−response growth curves, and individual IC_{50} values of a cell line was related to the mean IC_{50} of all cells lines; cell lines were sorted by lowest to highest sensitivity for PQR620 (3) from left (SK-N-FI) to right (A-498). Individual cell lines and values (IC_{50} and GI_{50}) are given in Supporting Information, Table S6.

Information, Table S6). Growth inhibitory activity was evaluated after an exposure time of 72 h with inhibitor concentrations ranging from $10^{−9}$ to $10^{−5}$ M. Compound PQR620 (3) showed potency across these cell lines with a mean IC_{50} value of 0.92 μM for growth inhibition. An analysis of the most frequently mutated cancer genes in the cell panel did not yield a significant and relevant association of mutations

and susceptibility to the mTOR inhibitor (Supporting Information, Figure S6).

When compared with other mTOR kinase inhibitors such as PP242 (75), SB2602 (74), and the PI3K inhibitor GDC0941 (76), PQR620 (3) shows a very similar potential to prevent cell growth and proliferation in two reference cell lines A2058 and SKOV3 (Figure 5). INK128 (73) is more potent but exceeds the expected ca. 3-fold difference defined by its in vitro potency for mTOR by far, which could indicate that PI3K inhibition (Table 4) or other off target kinase actions
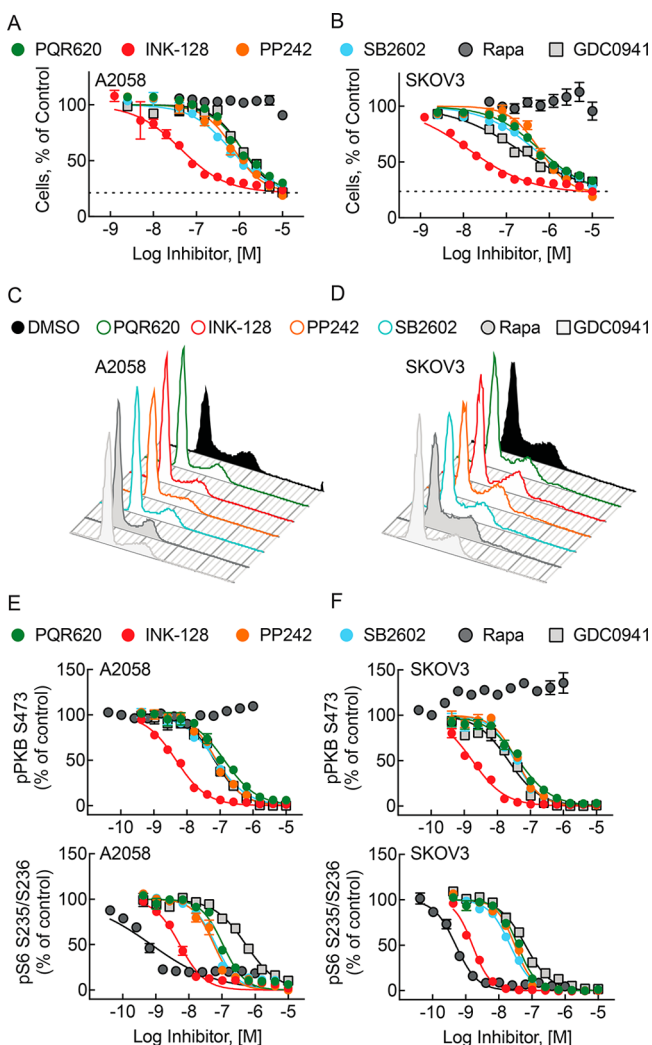
Figure 5. Proliferation, cell cycle, and cellular signaling. A2058 (A) and SKOV3 (B) cells were exposed to indicated inhibitors for 72 h; cell numbers are shown as % of DMSO controls. The dashed line indicates cell numbers at $t = 0$ h, as % of cells of DMSO control at 72 h ($n = 9$, three independent experiments (ie); rapamycin and GDC0941 (76) $n = 6$; 2 ie; each data point measured at least in triplicate, mean ± SEM. Cell cycle distribution of (C) A2058 and (D) SKOV3 cells after 24 h exposure to (C) 5 μM or (D) 2 μM of drugs or DMSO. After Hoechst33342 staining, cell cycle profiles were determined by FACS. Quantification and statistics are provided in Supporting Information, Figure S5. (E) A2058 and (F) SKOV3 cells were incubated for 1 h with compounds and then subjected to in cell western detection of phosphorylation of PKB/Akt and S6. Phospho-protein signals are presented as % of DMSO controls ($n = 3$, mean ± SEM); immunoblots of phospho-PKB/Akt, S6, S6K, and 4E-BP1 are in Supporting Information, Figure S5.

(Supporting Information, Figure S2) contribute to its antiproliferative potential.

Because of a loss of PTEN (phosphatase and tensin homologue) and an activating B-Raf mutation A2058 cells are rather resistant to PI3K inhibition,[23,30] while growth of SKOV3 cells is promoted by a constitutively activated PI3Kα, rendering these cells more sensitive to PI3K and mTOR kinase inhibitors. Even for excessive concentrations of rapamycin (10 μM), no attenuation of cell proliferation could be observed, indicating that the inhibition of mTORC1 is insufficient to block proliferation of A2058 and SKOV3. Cell cycle analysis revealed that all tested PI3K and mTOR kinase inhibitors accumulated cells in G1, diminishing cell numbers in S and G2/M cell cycle phases (Figure 5 and Supporting Information, Figure S5). Moreover, at 10 μM PQR620 (3) did not show cytotoxicity in 65 of 66 cell lines of the NTCR panel, a typical feature for the blockage of the PI3K/mTOR pathway.[24]

Growth inhibition goes hand in hand with the inhibition of mTORC1 and mTORC2 targets, where PQR620 (3), INK128 (73), PP242 (75), SB2602 (74), and GDC0941 (76) efficiently block the phosphorylation of S6, S6K, 4E-BP1, and PKB/Akt (Figure 5 and Supporting Information, Figure S5). As observed earlier for PI3K inhibitors,[24] the mTOR inhibitors also yield half-maximal growth inhibition only when mTOR targets are close to 90% inhibited. While rapamycin is highly efficient to block phosphorylation of mTORC1 targets such as S6K (and therefore S6) and 4E-BP1, it leads to an increase of pPKB/Akt in A2058 and SKOV3 cells. This corresponds to a previously reported feedback loop, where rapalog-dependent mTORC1 and S6K inactivation enforces surface receptor to PI3K signaling,[31] which explains the reduced antiproliferative activity of rapalogs as compared to mTOR kinase inhibitors.

Metabolic Stability. To predict the metabolic stability of PQR620 (3), the compound was incubated in vitro with microsomes and hepatocytes from different animal species. Compound PQR620 (3) was found to be very stable in rat liver microsomes (no metabolites detected), whereas it was moderately metabolized in mouse liver microsomes (~70% remaining PQR620 (3) after a 30 min incubation, Table 5).

Table 5. Stability of Compound PQR620 (3)

microsome stability,[a] [% remaining after 30 min]		hepatocyte			
		-clearance [μL/min/10⁶ cells][b]		-stability $t_{1/2}$ [min][b]	
rat	mouse	rat	mouse	rat	mouse
108 ± 3.3	70.2 ± 0.33	1.85	2.67	468.4	324.4

[a]Experiments were carried out by Aphad Srl with rat and mouse liver microsomes (Xenotech). Each experiment performed $n = 2$. [b]Experiments were carried out by Pharmacelsus GmbH using cryopreserved hepatocytes.

Similarly, compound PQR620 (3) was more stable in rat hepatocytes (RH) than in mouse hepatocytes (MH) (CL_{hep} = 1.850 μL/min/10⁶ cells for RH and CL_{hep} = 2.671 μL/min/10⁶ cells for MH).

In addition, PQR620 (3) showed moderate passive permeability (52.23 ± 7.35 nm/s) in a PAMPA assay (parallel artificial membrane permeability assay), suggesting nonlimiting cellular permeability. As a further indicator for bioavailability the thermodynamic solubility was assessed over a range of pH, as well as in fasted and fed state simulated intestinal fluids

Table 6. Physicochemical Properties of Compound PQR620 (3)

permeability P_{app} [nm/s]	thermodynamic solubility, [μM]					log D pH 7.4	clogP[c]	mol wt [g/mol]	CNS MPO score
	pH 1.2	pH 4.5	pH 6.8	FaSSIF[a]	FeSSIF[b]				
52.23 ± 7.35	19967 ± 6487	78.2 ± 15.5	33.7 ± 4.3	66.0 ± 3.2	335 ± 148	3.47	3.06	445.47	3.8

[a]FaSSIF: fasted simulated intestinal fluid. [b]FeSSIF: fed simulated intestinal fluid. [c]clogP values were calculated using MarvinSketch. Solubility assays were performed by Aphad Analytical Solutions.

(FaSSIF and FeSSIF). The solubility of compound PQR620 (3) was 20.0 ± 6.5 mM at pH 1.2, 33.7 ± 4.3 μM at pH 6.8, and reached 335 ± 148 μM in FeSSIF buffer (Table 6). Overall, PQR620 (3) displays good ADME properties and promising physicochemical characteristics, such as the experimental log D value (3.47 in PBS buffer pH 7.4), the partition coefficient clogP (3.06), and molecular weight (445.47). Moreover, the CNS MPO score, an algorithm used to estimate blood−brain barrier permeability, was 3.8 for PQR620 (3), which suggests good penetration to the brain.

In Vivo Pharmacokinetic and Pharmacodynamic Evaluation. Compound PQR620 (3) was then profiled in vivo in rats and mice to evaluate PK and PD. After a single oral dose of PQR620 (3) (10 mg/kg) given to healthy female Sprague−Dawley (SD) rats, PQR620 (3) concentrations in plasma and brain were monitored over time (Figure 6): the maximal concentration (C_{max}) of PQR620 (3) was reached in plasma and brain after 30 min (1355 and 1310 ng/g, respectively). After 8 h, the total exposure AUC_{0-8} was 409 μg·h/mL in plasma and 404 μg·h/mL in brain. A comparison with SB2602 (74) showed that its plasma C_{max} exceeded the one of PQR620 (3), while plasma AUC levels were relatively comparable. Brain levels of PQR620 (3) were maintained at ca. 900 ng/g for >8 h, for SB2602 (74) they dropped to ca. 170 ng/g after 4 h. PQR620 (3) displayed approximately a ∼1:1 distribution in brain/plasma, while brain access of SB2602 (74) was limited (brain/plasma levels ∼1:5.6; Figure 6).

Dosed at 50 mg/kg in mice, a single oral application of PQR620 (3) yielded a C_{max} of 4835 ng/g in plasma and 7706 ng/g in brain (see Supporting Information, Table S7), confirming the excellent brain penetration of PQR620 (3) (brain/plasma levels ∼1.6:1). A brain tissue binding assay revealed an f_u (fraction unbound) value of 3%, which matches the levels of compounds with established brain activity in the same assay (see diazepam; f_u ∼4%, Supporting Information, Table S8A). Brain penetration data are also in accordance with MDCK permeability assays, which document a rapid, passive diffusion, independent of P-gp (P-glycoprotein 1, MDR1) transport (see Supporting Information, Table S8B).

As reported earlier, inhibitors targeting PI3Kα trigger an acute peak of plasma insulin.[23] PQR620 (3) and SB2602 (74) did not lead to an increase of plasma insulin concentrations in rats and mice as compared to background levels, while the pan-PI3K inhibitor PQR309 (1) at the same dose produced a prominent insulin peak. In rats, glucose levels could not be distinguished from background after PQR620 (3) administration, while PQR309 (1) led to a slow glucose increase, which even extends beyond the 8 h measurements presented here.[23] In contrast, an elevated dose and exposure of PQR620 (3) in mice caused an elevation of glucose plasma levels that were delayed in comparison to the increase triggered by PQR309 (1). While PQR309 (1) response pattern with a glucose and insulin increase can be explained by the induction of insulin resistance by suppression of GLUT4 in muscle and
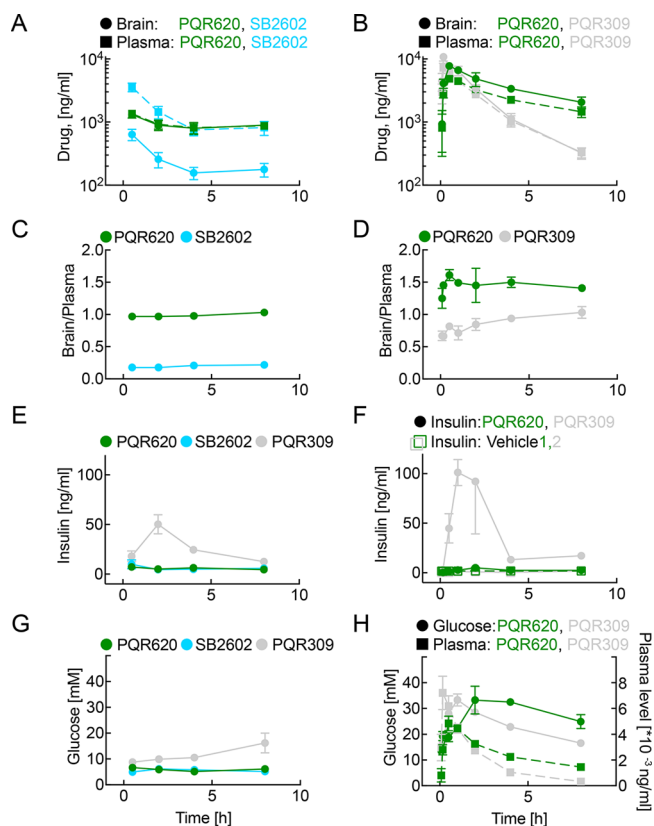
Figure 6. PK and PD in female Sprague−Dawley rats (left panels) and male C57BL/6JRj mice (right panels). (A,B) Plasma and brain levels (broken lines) of indicated drugs determined after a single dose po of 10 mg/kg in rats, and 50 mg/kg in mice.* (C,D) Brain/plasma ratio over time calculated from values above. Plasma (E,F) insulin and (G,H) glucose levels measured in animals above. All experiments depicted as mean ± SEM (n = 3); error bars are omitted where smaller than symbols. *PQR620 data in (B) was compared to rapamycin and everolimus in ref 29

adipocytes, the glucose increase triggered by mTOR kinase inhibitors is less well-defined. It was proposed that mTOR kinase inhibitors acutely cause hyperglycemia via TORC2-mediated regulation of glycolysis in skeletal muscle.[32] PQR620 (3) displayed a good exposure after oral dosing and excellent brain permeability, which makes this compound suitable as potential agent for CNS cancer indications and neurological diseases.

Evaluation of in Vivo Efficacy. The in vivo efficacy of compound PQR620 (3) was preclinically evaluated in a xenograft tumor model (Figure 7). Compound PQR620 (3) showed very good tolerability in mice (MTD ∼ 150 mg/kg) and was well tolerated in a 14-day toxicological study in rats, where the MTD was defined to be ∼30 mg/kg. PQR620 (3) was efficacious in an OVCAR-3 human ovarian cancer xenograft model, where BALB/C nude mice were inoculated
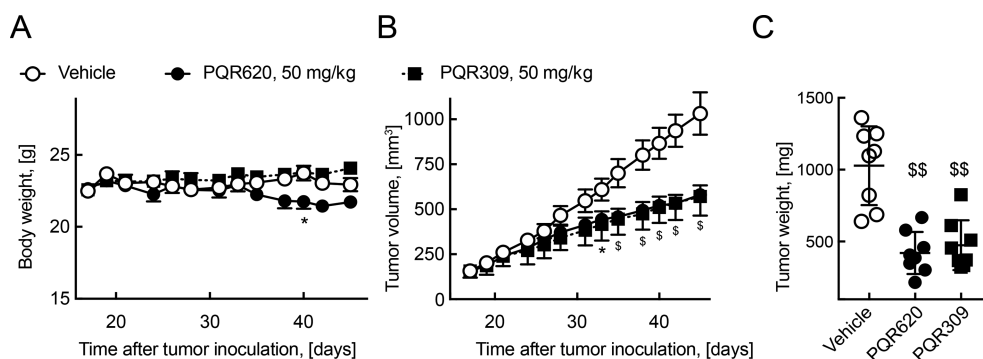
Figure 7. OVCAR-3 human ovarian cancer xenograft model in BALB/c nude mice: tumor cells were subcutaneously inoculated at day 0, and daily oral application of the indicated agents was started at day 17 (28 × QD). (A) Body weight was determined at the depicted time points. Body weight loss of >10% was observed in one mouse (of 8) in the PQR620 (**3**) treatment group. (B) The tumor size was measured and calculated as described in the Experimental Section. (C) The tumor weight was determined at day 45 after inoculation. Statistics: (*$p < 0.05$; $^\$p < 0.001$; $^{\$\$}p < 0.0001$; $n = 8$; (A,B) Two-Way ANOVA with Bonferroni or Dunnett's correction for multicomparisons, mean ± SEM; (C) mean ± SD, One-Way ANOVA with Tukey's correction for multicomparisons.

subcutaneously with cisplatin resistant OVCAR-3 cells. Compound PQR620 (**3**) and PQR309 (**1**) at 50 mg/kg were well tolerated in tumor bearing mice and did not cause a significant body weight loss, except for an outlier in the PQR620 (**3**) treatment group (1 out of 8 mice) where one mouse lost >10% of its weight (Figure 7). Tumor growth and terminal tumor weight were attenuated by treatment with compounds PQR620 (**3**) and PQR309 (**1**) by >50%. This demonstrates that mTOR kinase inhibition can be equivalent to the inhibition of upstream PI3K in some settings.

Attenuation of Neurological Disease. It has been previously reported that Tsc1GFAP conditional knockout mice (Tsc1$^{flox/flox}$ × GFAP-Cre) with targeted disruption of the Tsc1 gene in glial fibrillary acidic protein containing cells (mostly neurons) show a high incidence of spontaneous postnatal epilepsy. Treatment with rapamycin reduced the number of seizures and mortality.[33]

Here we evaluated the capacity of PQR620 (**3**) and PQR309 (**1**) to rescue the neuronal loss of function Tsc1 phenotype: mice treated with vehicle (postnatal days 21−55) suffered robust electrographic seizures, while a daily treatment of PQR620 (**3**) (100 mg/kg, po) eliminated seizures almost completely (Figure 8). The reduction of seizures by PQR309 (**1**) did not reach significance. It is tempting to speculate PQR309's (**1**) capacity to inhibit mTOR was insufficient and that targeting of class I PI3Ks cannot remedy the TSC phenotype. It is possible, however, that it is PQR309's (**1**) short half-life in mice that contributes to diminish its effectiveness. The protective effect of PQR620 (**3**) demonstrates clearly that targeting TORC1 and TORC2 mTOR kinase activity efficiently counteracts TSC-dependent over-activation of the mTOR pathway and thereby caused epileptic seizures.

CONCLUSIONS

In summary, we demonstrated that lead compound PQR620 (**3**) potently inhibits mTORC1/2 in vitro and in vivo. A >1000-fold selectivity toward mTOR over PI3Kα in binding assays is obtained by the introduction of a difluoromethyl-substituent and sterically demanding 3,5-ethylene bridged morpholines. PQR620 (**3**) exhibits excellent selectivity over a wide panel of protein and lipid kinases, as well as excellent selectivity versus unrelated receptor enzymes and ion channels.
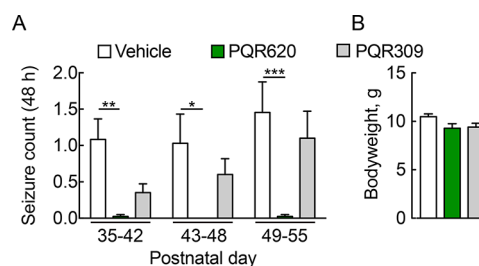
Figure 8. Effects of mTOR and PI3K inhibition on frequency of electrographic seizures caused by neuron-specific elimination of TSC1.[33] (A) Tsc1^{GFAP} conditional knockout mice were treated from postnatal days 21−53 with vehicle, PQR620 (**3**) (100 mg/kg), or PQR309 (**1**) (50 mg/kg). In three observation intervals, EEG traces were recorded, and the number of seizures were determined (depicted as seizure count/48 h; mean ± SEM, $n = 30−48$. Two-Way ANOVA test with Dunnet's multiple comparison related to vehicle control; *$p = 0.032$; **$p = 0.0021$; ***$p = 0.0002$). (B) Body weights averaged over the whole observation time in the three treatment groups (mean ± SEM, $n \geq 13$).

PQR620 (**3**) demonstrates its potency to inhibit cancer cell line proliferation with a potential comparable to pan-PI3K inhibition. The physicochemical properties (log D, solubility, liver microsomal stability ($t_{1/2}$), and apparent permeability) of compound PQR620 (**3**) resulted in a good exposure in both plasma and brain following oral administration. PQR620 (**3**) shows significant antitumor effects in a xenograft mouse model, is well tolerated in rats and mice, and lacks some of the adverse mechanism-based side effects of pan-PI3K inhibitors. The almost complete elimination of seizures in the mouse TSC null model above, and a significantly increased seizure threshold in a mouse model of chronic epilepsy[29] demonstrate the efficiency of PQR620 (**3**) in the CNS. The excellent brain/plasma partitioning promises a therapeutic potential in a wider range of neurodegenerative diseases and epilepsy with a reduced impact on host defense responses as compared to competitor compounds that require higher plasma levels to reach mTOR inhibition in brain tissue. Altogether, the preclinical data support a further development of this compound.

■ EXPERIMENTAL SECTION

General Information. Reagents were purchased at the highest commercial quality from Acros, Sigma-Aldrich, or Fluorochem and used without further purification. Solvents were purchased from Acros Organics in AcroSeal bottles over molecular sieves. Cross coupling reactions were carried out under nitrogen atmosphere in anhydrous solvents, and glassware was oven-dried prior to use. Thin layer chromatography (TLC) plates were purchased from Merck KGaA (Polygram SIL/UV254, 0.2 mm silica with fluorescence indicator) and UV light (254 nm) was used to visualize the compounds. Column chromatographic purifications were performed on Merck KGaA silica gel (pore size 60 Å, 230−400 mesh particle size). Alternatively, flash chromatography was performed with Isco CombiFlash Companion systems using prepacked silica gel columns (40−60 μm particle size RediSep). ^{1}H and ^{13}C NMR spectra were recorded on a Bruker Avance 400 spectrometer. NMR spectra were obtained in deuterated solvents, such as CDCl$_3$, (CD$_3$)$_2$SO, or CD$_3$OD. The chemical shift (δ values) are reported in ppm and corrected to the signal of the deuterated solvents (7.26 ppm (^{1}H NMR) and 77.16 ppm (^{13}C NMR) for CDCl$_3$, 2.50 ppm (^{1}H NMR) and 39.52 ppm (^{13}C NMR) for (CD$_3$)$_2$SO, and 3.31 ppm (^{1}H NMR) and 49.00 ppm (^{13}C NMR) for CD$_3$OD). Coupling constants, when given, are reported in hertz (Hz). High resolution mass spectra (HRMS) were recorded on a Thermo Fisher Scientific LTQ Orbitrap XL (ESI-MS) spectrometer. MALDI-ToF mass spectra were obtained on a Voyager-De Pro measured in m/z. The chromatographic purity of final compounds was determined by high performance liquid chromatography (HPLC) analyses on an Ultimate 3000SD System from ThermoFisher with LPG-3400SD pump system, ACC-3000 autosampler and column oven, and DAD-3000 diode array detector. An Acclaim-120 C18 reversed-phase column from ThermoFisher was used as stationary phase. Gradient elution (5:95 for 0.2 min, 5:95 → 100:0 over 10 min, 100:0 for 3 min) of the mobile phase consisting of CH$_3$CN/MeOH:H$_2$O$_{(10:90)}$ was used at a flow rate of 0.5 mL/min at 40 °C. The purity of all final compounds was >95%.

General Procedure 1. The free amine or the corresponding HCl salt (2.0−2.3 equiv) was dissolved in CH$_2$Cl$_2$ (approximately 1 mL/0.8 mmol) and N,N-diisopropylamine (2.2−6.0 equiv) was added. The resulting solution was cooled to 0 °C and then added dropwise to a solution of cyanuric chloride (1.0 equiv) in CH$_2$Cl$_2$ (approximately 1 mL/0.4 mmol) at 0 °C. The resulting reaction mixture was stirred overnight, while it was allowed to warm up to room temperature. Additional CH$_2$Cl$_2$ (approximately 1 mL/0.5 mmol) was added, and the organic layer was washed with an aq satd solution of NaHSO$_4$ (2×). The organic layer was dried over anhydrous Na$_2$SO$_4$ and filtered, and the solvent was evaporated under reduced pressure. The crude product was purified by column chromatography on silica gel.

General Procedure 2. To a solution of the amine or the corresponding HCl salt (2.0−2.1 equiv) and N,N-diisopropylethylamine (4.0−4.2 equiv) in tetrahydrofuran (approximately 1 mL/0.1 mmol), cyanuric chloride (1.0 equiv) was added at 0 °C. The resulting mixture was stirred at reflux overnight. The mixture was then allowed to cool down to room temperature, washed with aq satd NaHSO$_4$ (2×), dried over anhydrous Na$_2$SO$_4$, and filtered, and the solvent was evaporated under reduced pressure. The crude product was purified by column chromatography on silica gel.

General Procedure 3. To a solution of the morpholine derivative (1.1 equiv) and N,N-diisopropylethylamine (2.0−2.1 equiv) in ethanol (approximately 1 mL/0.2 mmol) at 0 °C, 4-(4,6-dichloro-1,3,5-triazin-2-yl)morpholine (**35**, 1.0 equiv) was added portionwise. The resulting mixture was stirred at room temperature overnight. The solvent was then removed under reduced pressure, and the residue was purified by column chromatography on silica gel.

General Procedure 4. Monochlorotriazine derivative (1.0 equiv), boronic acid pinacol ester **64** (1.0−1.2 equiv), K$_3$PO$_4$ (2.0 equiv), and chloro(2-dicyclohexylphosphino-2′,4′,6′-triisopropyl-1,1′-biphenyl)-[2-(2′-amino-1,1′-biphenyl)]-palladium(II) (XPhos Pd G2, 0.05 equiv) were charged in a flask. Under nitrogen atmosphere, 1,4-dioxane (approximately 1 mL/0.2 mmol) and deionized H$_2$O

(approximately 1 mL/0.4 mmol) were added, and the resulting mixture was placed into an oil bath preheated at 95 °C and stirred at this temperature overnight. Deionized H$_2$O was added and the aqueous layer was extracted with CH$_2$Cl$_2$ (3×). The combined organic layers were dried over anhydrous Na$_2$SO$_4$ and filtered, and the solvent was evaporated under reduced pressure. The crude product was purified by column chromatography on silica gel.

General Procedure 5. Monochlorotriazine derivative (1.0 equiv), boronic acid pinacol ester **64** or **72** (1.0−1.1 equiv), K$_3$PO$_4$ (2.0 equiv), and chloro(2-dicyclohexylphosphino-2′,4′,6′-triisopropyl-1,1′-biphenyl)[2-(2′-amino-1,1′-biphenyl)]palladium(II) (XPhos Pd G2, 0.05 equiv) were charged in a flask. Under nitrogen atmosphere, 1,4-dioxane (approximately 1 mL/0.2 mmol) and deionized H$_2$O (approximately 1 mL/0.4 mmol) were added and the resulting mixture was placed into an oil bath preheated at 95 °C and stirred at this temperature for 2−5 h. After this time, the reaction mixture was allowed to cool down to room temperature, a 3 M aq HCl-solution (>10 equiv) was added, and the resulting mixture was stirred at 60 °C for 3−15 h. The pH was adjusted to 10 by addition of a 2 M aq NaOH solution, and the aqueous layer was then extracted with EtOAc (3×). The combined organic layers were dried over anhydrous Na$_2$SO$_4$ and filtered, and the solvent was evaporated under reduced pressure. The crude product was purified by column chromatography on silica gel.

General Procedure 6. Step 1: Bis(pinacolato)diboron (1.5 equiv), KOAc (3.0 equiv), [1,1′-bis(diphenylphosphino)-ferrocene]-dichloropalladium(II) (Pd(dppf)Cl$_2$, 0.10 equiv), and the respective bromo derivative (1.0 equiv) were dissolved in abs dioxane (approximately 1 mL/0.1 mmol) under nitrogen atmosphere. The resulting mixture was stirred at 95 °C for 6−8 h. The mixture was allowed to cool down to room temperature. Step 2: 4,4′-(6-Chloro-1,3,5-triazine-2,4-diyl)dimorpholine (**36**, 1.1 equiv), chloro(2-dicyclo-hexylphosphino-2′,4′,6′-triisopropyl-1,1′-biphenyl)[2-(2′-amino-1,1′-biphenyl)]palladium(II) (XPhos Pd G2, 0.05 equiv), and K$_3$PO$_4$ (2.0 equiv) were added. The resulting reaction mixture was placed in a preheated oil bath at 95 °C and stirred for 3−16 h. Then the mixture was allowed to cool down to room temperature, deionized H$_2$O was added, and the mixture was extracted with CH$_2$Cl$_2$ (3×). The combined organic layers were washed with brine (2×), dried over anhydrous Na$_2$SO$_4$, filtered, and reduced to dryness under reduced pressure. Step 3: The above residue was dissolved in dioxane (approximately 1 mL/0.1 mmol) and an aqueous solution of HCl (3 M, 10−15 equiv) was added. The reaction mixture was stirred at 60 °C for 2 h. The mixture was diluted with deionized H$_2$O and washed with EtOAc (1×). The aqueous layer was basified to pH = 10 and then extracted with EtOAc (3×). The combined organic layers were dried over anhydrous Na$_2$SO$_4$ and filtered, and the solvent was evaporated under reduced pressure. The crude product was purified by column chromatography on silica gel.

General Procedure 7. To a solution of di-*tert*-butyl dicarbonate (2.5−3.0 equiv) in tetrahydrofuran (approximately 1 mL/0.4 mmol), the respective amine was added (1.0 equiv) at 0 °C. Then, 4-(dimethylamino)pyridine (0.30 equiv) was added and the resulting mixture was stirred overnight, while it was allowed to warm up to room temperature. The solvent was evaporated under reduced pressure. The residue was dissolved in CH$_2$Cl$_2$, and the resulting organic layer was washed with an aq satd NH$_4$Cl solution, dried over anhydrous Na$_2$SO$_4$, and filtered. The solvent was evaporated under reduced pressure, and the crude product was purified by column chromatography on silica gel.

5-[4,6-Bis(morpholin-4-yl)-1,3,5-triazin-2-yl]-4-(trifluoromethyl)-pyridin-2-amine (PQR309 (1)). **1** was prepared according to the literature.[24]

5-[4,6-Bis(morpholin-4-yl)-1,3,5-triazin-2-yl]-4-(difluoromethyl)-pyridin-2-amine (2). **2** was prepared according to general procedure 5 from intermediate **36** (355 mg, 1.24 mmol, 1.0 equiv) and boronic ester **64** (422 mg, 1.30 mmol, 1.0 equiv). Purification by column chromatography on silica gel (cyclohexane/EtOAc 1:0 →1:3) gave compound **2** (225 mg, 572 μmol, 46%) as a colorless solid. ^{1}H NMR (400 MHz, CDCl$_3$): δ 9.02 (s, 1 H), 7.65 (t, [2]$J_{H,F}$ = 55 Hz, 1 H), 6.84

(s, 1 H), 4.85 (br s, 2 H), 3.90−3.78 (m, 8 H), 3.78−3.71 (m, 8 H). ^{13}C{^{1}H} NMR (101 MHz, (CD$_3$)$_2$SO): δ 168.9 (s, 1 C), 164.1 (s, 2 C), 161.6 (s, 1 C), 152.1 (s, 1 C), 142.1 (t, $^2J_{C,F}$ = 22 Hz, 1 C), 118.2 (t, $^3J_{C,F}$ = 4.4 Hz, 1 C), 111.8 (t, $^1J_{C,F}$ = 237 Hz, 1 C), 103.1 (t, $^3J_{C,F}$ = 8.4 Hz, 1 C), 66.0 (s, 4 C), 43.3 (s, 4 C). ESI-HRMS (m/z): [M + H]$^+$ calcd for C$_{17}$H$_{22}$F$_2$N$_7$O$_2$ 394.1798, found 394.1787. HPLC: t_R = 7.18 min (96.5% purity).

5-[4,6-Bis({3-oxa-8-azabicyclo[3.2.1]octan-8-yl})-1,3,5-triazin-2-yl]-4-(difluoromethyl)pyridin-2-amine (PQR620 (3)). 3 was prepared according to general procedure 4 from intermediate 43 (396 mg, 1.17 mmol, 1.0 equiv) and boronic acid pinacol ester 64 (420 mg, 1.29 mmol, 1.1 equiv). Purification by column chromatography on silica gel (cyclohexane/EtOAc 1:0 → 2:3) gave compound PQR620 (3) (375 mg, 842 μmol, 72%) as a colorless solid. ^{1}H NMR (400 MHz, CDCl$_3$): δ 9.04 (s, 1 H), 7.71 (t, $^2J_{H,F}$ = 55 Hz, 1 H), 6.83 (s, 1 H), 4.83 (br s, 2 H), 4.75−4.60 (m, 4 H), 3.83−3.72 (m, 4 H), 3.70−3.58 (m, 4 H), 2.14−1.92 (m, 8 H). ^{13}C{^{1}H} NMR (101 MHz, CDCl$_3$): δ 169.8 (s, 1 C), 163.3 (s, 2 C), 160.2 (s, 1 C), 152.5 (s, 1 C), 143.7 (t, $^2J_{C,F}$ = 22 Hz, 1 C), 121.5 (t, $^3J_{C,F}$ = 4.9 Hz, 1 C), 111.5 (t, $^1J_{C,F}$ = 238 Hz, 1 C), 104.1 (t, $^3J_{C,F}$ = 8.0 Hz, 1 C), 72.0 (s, 2 C), 71.7 (s, 2 C), 55.0 (s, 2 C), 54.6 (s, 2 C), 27.1 (s, 2 C), 27.0 (s, 2 C). ESI-HRMS (m/z): [M + H]$^+$ calcd for C$_{21}$H$_{26}$F$_2$N$_7$O$_2$ 446.2111, found 446.2101. HPLC: t_R = 8.15 min (99.4% purity).

5-[4,6-Bis(morpholin-4-yl)-1,3,5-triazin-2-yl]pyridin-2-amine (4) and 5-[4,6-Bis(morpholin-4-yl)-1,3,5-triazin-2-yl]-4-methylpyridin-2-amine (5). 4 and 5 were prepared according to the literature.[23]

5-[4,6-Bis(morpholin-4-yl)-1,3,5-triazin-2-yl]-4-(fluoromethyl)-pyridin-2-amine (6). 6 was prepared according to general procedure 6 from intermediate 36 (71.0 mg, 248 μmol, 1.1 equiv) and N′-(5-bromo-4-(fluoromethyl)pyridin-2-yl)-N,N-dimethylformimidamide (67, 58.6 mg, 225 μmol, 1.0 equiv). Purification by column chromatography on silica gel (cyclohexane/EtOAc 1:0 →1:3) gave compound 6 (34.3 mg, 91.4 μmol, 41%) as a colorless solid. ^{1}H NMR (400 MHz, CDCl$_3$): δ 9.07 (s, 1 H), 6.75 (s, 1 H), 5.89 (d, $^2J_{H,F}$ = 49 Hz, 2 H), 4.78 (br s, 2 H), 3.90−3.79 (m, 8 H), 3.79−3.71 (m, 8 H). ^{13}C{^{1}H} NMR (101 MHz, CDCl$_3$): δ 170.0 (s, 1 C), 164.8 (s, 2 C), 160.3 (d, $^4J_{C,F}$ = 3.0 Hz, 1 C), 151.8 (s, 1 C), 149.5 (d, $^2J_{C,F}$ = 17 Hz, 1 C), 120.2 (d, $^3J_{C,F}$ = 4.0 Hz, 1 C), 130.2 (d, $^3J_{C,F}$ = 19 Hz, 1 C), 82.9 (d, $^1J_{C,F}$ = 172 Hz, 1 C), 66.9 (s, 4 C), 43.8 (br s, 4 C). ESI-HRMS (m/z): [M + H]$^+$ calcd for C$_{17}$H$_{23}$FN$_7$O$_2$ 376.1892, found 376.1882. HPLC: t_R = 7.06 min (95.9% purity).

{2-Amino-5-[4,6-bis(morpholin-4-yl)-1,3,5-triazin-2-yl]pyridin-4-yl}methanol (7). 7 was prepared according to general procedure 6 from intermediate 36 (421 mg, 1.47 mmol, 1.1 equiv) and N′-[5-bromo-4-{[tert-butyl(dimethyl)silyl]oxymethyl]-2-pyridyl}-N,N-dimethyl-formamidine (68, 500 mg, 1.34 mmol, 1.0 equiv). Purification by column chromatography on silica gel (CH$_2$Cl$_2$/CH$_3$OH 1:0 → 9:1) gave compound 7 (163 mg, 437 μmol, 33%) as a colorless solid. ^{1}H NMR (400 MHz, CDCl$_3$): δ 9.08 (s, 1 H), 6.45 (s, 1 H), 4.81 (br s, 2 H), 4.62 (s, 2 H), 3.87−3.80 (m, 8 H), 3.80−3.72 (m, 8 H). ^{13}C{^{1}H} NMR (101 MHz, CDCl$_3$): δ 170.3 (s, 1 C), 164.4 (s, 2 C), 160.2 (s, 1 C), 152.9 (s, 1 C), 151.1 (s, 1 C), 122.1 (s, 1 C), 108.4 (s, 1 C), 66.7 (s, 4 C), 64.4 (s, 1 C), 43.8 (s, 4 C). ESI-HRMS (m/z): [M + H]$^+$ calcd for C$_{17}$H$_{24}$N$_7$O$_3$ 374.1935, found 374.1948. HPLC: t_R = 5.59 min (99.9% purity).

5-[4,6-Bis(morpholin-4-yl)-1,3,5-triazin-2-yl]-4-(dimethoxymethyl)pyridin-2-amine (8). 8 was prepared from intermediate 36 (211 mg, 738 μmol, 1.1 equiv) and tert-butyl N-[5-bromo-4-(dimethoxymethyl)pyridin-2-yl]-N-[(tert-butoxy)carbonyl]-carbamate (70, 301 mg, 673 μmol, 1.0 equiv) following steps 1 and 2 of general procedure 6. Step 3.: The residue was dissolved in CH$_2$Cl$_2$ (5 mL), and trifluoroacetic acid (500 μL, 6.53 mmol, 9.7 equiv) was added at 0 °C. The reaction mixture was stirred at room temperature for 6 h. Then the reaction was quenched with 2 M aq NaOH-solution and diluted with CH$_2$Cl$_2$. The organic layer was separated, and the aqueous layer was extracted with CH$_2$Cl$_2$ (2×). The combined organic layers were dried over Na$_2$SO$_4$ and filtered, and the solvent was evaporated under reduced pressure. Purification by column chromatography on silica gel (cyclohexane/EtOAc 1:0 →0:1) gave compound 8 (32.0 mg, 76.7 μmol, 11%) as a yellowish solid. ^{1}H

NMR (400 MHz, CDCl$_3$): δ 8.70 (s, 1 H), 6.81 (s, 1 H), 6.41 (s, 1 H), 4.70 (br s, 2 H), 3.95−3.80 (m, 8 H), 3.78−3.67 (m, 8 H), 3.32 (s, 6 H). ^{13}C{^{1}H} NMR (101 MHz, CDCl$_3$): δ 171.3 (s, 1 C), 164.9 (s, 2 C), 159.6 (s, 1 C), 151.7 (s, 1 C), 147.7 (s, 1 C), 123.3 (s, 1 C), 105.6 (s, 1 C), 99.8 (s, 1 C), 67.0 (s, 4 C), 54.0 (s, 2 C), 43.8 (s, 4 C). ESI-HRMS (m/z): [M + H]$^+$ calcd for C$_{19}$H$_{28}$N$_7$O$_4$ 418.2197, found 418.2188. HPLC: t_R = 6.41 min (96.1% purity).

5-[4,6-Bis(morpholin-4-yl)-1,3,5-triazin-2-yl]-4-methoxypyridin-2-amine (9). Step 1: tert-Butyl N-(5-bromo-4-methoxypyridin-2-yl)-N-[(tert-butoxy)carbonyl]carbamate (71, 910 mg, 2.26 mmol, 1.0 equiv), tetrahydroxydiboron (607 mg, 6.77 mmol, 3.0 equiv), KOAc (665 mg, 6.77 mmol, 3.0 equiv), 2-dicyclohexylphosphino-2′,4′,6′-triisopropylbiphenyl (XPhos, 108 mg, 226 μmol, 0.10 equiv), and chloro(2-dicyclohexylphosphino-2′,4′,6′-triisopropyl-1,1′-biphenyl)-[2-(2′-amino-1,1′-biphenyl)]palladium(II) (XPhos Pd G2, 89.0 mg, 113 mmol, 0.05 equiv) were charged in a flask, and abs ethanol (23 mL) was added under nitrogen atmosphere. The resulting mixture was heated at 80 °C for 1 h. Step 2: The mixture was allowed to cool down to room temperature and intermediate 36 (643 mg, 2.26 mmol, 1.0 equiv) was added, followed by K$_3$PO$_4$ (1.44 g, 6.77 mmol, 3.0 equiv). The resulting reaction mixture was stirred at 80 °C for 3.5 h. An aq satd NH$_4$Cl solution was added to quench the reaction, and the mixture was extracted with EtOAc (3×). The combined organic layers were washed with brine (2×), dried over anhydrous Na$_2$SO$_4$, filtered, and reduced to dryness under reduced pressure. Step 3: The above residue was dissolved in dioxane (2 mL), and a 3 M aq HCl solution (3.0 mL, 12.0 mmol, 5.3 equiv) was added. The reaction mixture was stirred at 60 °C for 2 h. The mixture was then diluted with deionized H$_2$O, basified to pH = 10, and extracted with CH$_2$Cl$_2$ (3×). The combined organic layers were dried over anhydrous Na$_2$SO$_4$, filtered, and reduced to dryness under reduced pressure. Purification by column chromatography on silica gel (CH$_2$Cl$_2$/CH$_3$OH 1:0 → 95:5) gave compound 9 (336 mg, 900 μmol, 40%) as a colorless solid. ^{1}H NMR (400 MHz, CDCl$_3$): δ 8.65 (s, 1 H), 6.01 (s, 1 H), 4.75 (br s, 2 H), 3.91−3.78 (m, 11 H), 3.78−3.69 (m, 8 H). ^{13}C{^{1}H} NMR (101 MHz, CDCl$_3$): δ 169.8 (s, 1 C), 166.7 (s, 1 C), 165.0 (s, 2 C), 161.3 (s, 1 C), 152.2 (s, 1 C), 115.4 (s, 1 C), 90.2 (s, 1 C), 67.0 (s, 4 C), 55.6 (s, 1 C), 43.7 (s, 4 C). ESI-HRMS (m/z): [M + H]$^+$ calcd for C$_{17}$H$_{24}$N$_7$O$_3$ 374.1935, found 374.1924. HPLC: t_R = 5.67 min (>95.0% purity).

4-(Difluoromethyl)-5-{4-[(3R)-3-methylmorpholin-4-yl]-6-(mor-pholin-4-yl)-1,3,5-triazin-2-yl}pyridin-2-amine (10). 10 was prepared according to general procedure 4 from intermediate 37 (250 mg, 833 μmol, 1.0 equiv) and boronic acid pinacol ester 64 (298 mg, 917 μmol, 1.1 equiv). Purification by column chromatography on silica gel (cyclohexane/EtOAc 1:0 → 1:3) gave compound 10 (248 mg, 609 μmol, 73%) as a colorless solid. ^{1}H NMR (400 MHz, CDCl$_3$): δ 9.03 (s, 1 H), 7.68 (t, $^2J_{H,F}$ = 55 Hz, 1 H), 6.84 (s, 1 H), 4.84 (br s, 2 H), 4.79−4.67 (m, 1 H), 4.46−4.43 (m, 1 H), 3.97 (dd, $J_{H,H}$ = 11, 3.6 Hz, 1 H), 3.90−3.63 (m, 10 H), 3.52 (td, $J_{H,H}$ = 12, 2.8 Hz, 1 H), 3.28 (td, $J_{H,H}$ = 13, 3.5 Hz, 1 H), 1.32 (d, $^3J_{H,H}$ = 6.9 Hz, 3 H). ^{13}C{^{1}H} NMR (101 MHz, CDCl$_3$): δ 169.3 (s, 1 C), 164.8 (s, 1 C), 164.4 (s, 1 C), 160.3 (s, 1 C), 152.4 (s, 1 C), 143.6 (t, $^2J_{C,F}$ = 22 Hz, 1 C), 121.4 (t, $^3J_{C,F}$ = 4.7 Hz, 1 C), 111.4 (t, $^1J_{C,F}$ = 239 Hz, 1 C), 104.1 (t, $^3J_{C,F}$ = 7.8 Hz, 1 C), 71.1 (s, 1 C), 67.1 (s, 1 C), 66.9 (br s, 2 C), 46.5 (s, 1 C), 43.7 (br s, 2 C), 38.6 (s, 1 C), 14.4 (s, 1 C). ESI-HRMS (m/z): [M + H]$^+$ calcd for C$_{18}$H$_{24}$F$_2$N$_7$O$_2$ 408.1954, found 408.1948. HPLC: t_R = 7.73 min (99.9% purity).

4-(Difluoromethyl)-5-[4-(morpholin-4-yl)-6-{8-oxa-3-azabicyclo-[3.2.1]octan-3-yl}-1,3,5-triazin-2-yl]pyridin-2-amine (11). 11 was prepared according to general procedure 4 from intermediate 38 (93.0 mg, 299 μmol, 1.0 equiv) and boronic acid pinacol ester 64 (99.0 mg, 305 μmol, 1.0 equiv). Purification by column chromatography on silica gel (CH$_2$Cl$_2$/CH$_3$OH 40:1) gave compound 11 (39.1 mg, 93.2 μmol, 31%) as a colorless solid. ^{1}H NMR (400 MHz, CDCl$_3$): δ 9.02 (s, 1 H), 7.67 (t, $^2J_{H,F}$ = 55 Hz, 1 H), 6.83 (s, 1 H), 4.84 (br s, 2 H), 4.50−4.26 (m, 4 H), 3.91−3.68 (m, 8 H), 3.29−3.13 (m, 2 H), 1.99−1.89 (m, 2 H), 1.82−1.72 (m, 2 H). ^{13}C{^{1}H} NMR (101 MHz, CDCl$_3$): δ 169.1 (s, 1 C), 165.9 (s, 1 C), 164.7 (s, 1 C), 160.2 (s, 1 C), 152.5 (s, 1 C), 143.7 (t, $^2J_{C,F}$ = 22 Hz, 1 C), 121.6 (t,

$^3J_{C,F}$ = 3.7 Hz, 1 C), 111.4 (t, $^1J_{C,F}$ = 238 Hz, 1 C), 104.1 (t, $^3J_{C,F}$ = 7.5 Hz, 1 C), 74.0 (br s, 2 C), 66.9 (s, 2 C), 49.5 (s, 1 C), 49.2 (s, 1 C), 43.8 (br s, 2 C), 27.8 (br s, 2 C). ESI-HRMS (m/z): [M + H]$^+$ calcd for $C_{19}H_{24}F_2N_7O_2$ 420.1954, found 420.1945. HPLC: t_R = 7.34 min (99.6% purity).

4-(Difluoromethyl)-5-[4-(morpholin-4-yl)-6-{3-oxa-8-azabicyclo-[3.2.1]octan-8-yl}-1,3,5-triazin-2-yl]pyridin-2-amine (12). **12** was prepared according to general procedure 4 from intermediate **39** (150 mg, 482 μmol, 1.0 equiv) and boronic acid pinacol ester **64** (160 mg, 492 μmol, 1.0 equiv). Purification by column chromatography on silica gel (cyclohexane/EtOAc 2:3 → 3:7) gave compound **12** (115 mg, 274 μmol, 56%) as a colorless solid. ^{1}H NMR (400 MHz, CDCl$_3$): δ 9.02 (s, 1 H), 7.68 (t, $^2J_{H,F}$ = 55 Hz, 1 H), 6.83 (s, 1 H), 4.94 (br s, 2 H), 4.74−4.60 (m, 2 H), 3.90−3.58 (m, 12 H), 2.12−1.93 (m, 4 H). ^{13}C{^{1}H} NMR (101 MHz, CDCl$_3$): δ 169.6 (s, 1 C), 164.9 (s, 1 C), 163.0 (s, 1 C), 160.2 (s, 1 C), 152.4 (s, 1 C), 143.7 (t, $^2J_{C,F}$ = 23 Hz, 1 C), 121.5 (br s, 1 C), 111.5 (t, $^1J_{C,F}$ = 238 Hz, 1 C), 104.1 (t, $^3J_{C,F}$ = 7.9 Hz, 1 C), 72.0 (s, 1 C), 71.7 (s, 1 C), 66.9 (s, 2 C), 55.1 (s, 1 C), 54.6 (s, 1 C), 43.7 (s, 2 C), 27.1 (s, 1 C), 27.0 (s, 1 C). ESI-HRMS (m/z): [M + H]$^+$ calcd for $C_{19}H_{24}F_2N_7O_2$ 420.1954, found 420.1944. HPLC: t_R = 7.50 min (96.3% purity).

5-{4,6-Bis[(3R)-3-methylmorpholin-4-yl]-1,3,5-triazin-2-yl}-4-(difluoromethyl)pyridin-2-amine (13). **13** was prepared according to general procedure 5 from intermediate **41** (250 mg, 796 μmol, 1.0 equiv) and boronic acid pinacol ester **64** (285 mg, 876 μmol, 1.1 equiv). Purification by column chromatography on silica gel (cyclohexane/EtOAc 1:0 → 3:1) gave compound **13** (327 mg, 776 μmol, 97%) as a colorless solid. ^{1}H NMR (400 MHz, CDCl$_3$): δ 9.03 (s, 1 H), 7.69 (t, $^2J_{H,F}$ = 55 Hz, 1 H), 6.82 (s, 1 H), 5.00 (br s, 2 H), 4.81−4.62 (m, 2 H), 4.48−4.29 (m, 2 H), 3.96 (dd, $J_{H,H}$ = 11, 3.5 Hz, 2 H), 3.76 (d, $J_{H,H}$ = 11 Hz, 2 H), 3.67 (dd, $J_{H,H}$ = 11, 3.3 Hz, 2 H), 3.52 (td, $J_{H,H}$ = 12, 3.0 Hz, 2 H), 3.34−3.23 (m, 2 H), 1.32 (t, $^3J_{H,H}$ = 6.9 Hz, 6 H). ^{13}C{^{1}H} NMR (101 MHz, CDCl$_3$): δ 169.3 (s, 1C), 164.5 (br s, 2 C), 160.2 (s, 1 C), 152.4 (s, 1C), 143.6 (t, $^2J_{C,F}$ = 22 Hz, 1 C), 121.6 (t, $^3J_{C,F}$ = 4.8 Hz, 1 C), 111.5 (t, $^1J_{C,F}$ = 239 Hz, 1 C), 104.1 (t, $^3J_{C,F}$ = 7.9 Hz, 1 C), 71.2 (s, 2 C), 67.1 (s, 2 C), 46.5 (s, 2 C), 38.6 (s, 2 C), 14.4 (br s, 2 C). ESI-HRMS (m/z): [M + H]$^+$ calcd for $C_{19}H_{26}F_2N_7O_2$ 422.2111, found 422.2101. HPLC: t_R = 8.28 min (99.2% purity).

5-[4,6-Bis({8-oxa-3-azabicyclo[3.2.1]octan-3-yl})-1,3,5-triazin-2-yl]-4-(difluoromethyl)pyridin-2-amine (14). **14** was prepared according to general procedure 4 from intermediate **42** (100 mg, 296 μmol, 1.0 equiv) and boronic acid pinacol ester **64** (106 mg, 326 μmol, 1.1 equiv). Purification by column chromatography on silica gel (cyclohexane/EtOAc 3:7) gave compound **14** (118 mg, 265 μmol, 89%) as a colorless solid. ^{1}H NMR (400 MHz, CDCl$_3$): δ 9.03 (s, 1 H), 7.89 (t, $^2J_{H,F}$ = 55 Hz, 1 H), 6.83 (s, 1 H), 4.83 (br s, 2 H), 4.50−4.23 (m, 8 H), 3.27−3.11 (m, 4 H), 2.00−1.88 (m, 4 H), 1.82−1.71 (m, 4 H). ^{13}C{^{1}H} NMR (101 MHz, CDCl$_3$): δ 168.8 (s, 1 C), 165.5 (s, 2 C), 160.0 (s, 1 C), 152.3 (s, 1 C), 143.5 (t, 1 C), 121.5 (br s, 1 C), 111.3 (t, $^1J_{C,F}$ = 239 Hz, 1 C), 104.0 (t, $^3J_{C,F}$ = 7.9 Hz, 1 C), 73.9 (s, 4 C), 49.3 (s, 2 C), 49.1 (s, 2 C), 27.7 (s, 4 C). ESI-HRMS (m/z): [M + H]$^+$ calcd for $C_{21}H_{26}F_2N_7O_2$ 446.2111, found 446.2100. HPLC: t_R = 7.71 min (98.4% purity).

5-{4,6-Bis[(1S,4S)-2-oxa-5-azabicyclo[2.2.1]heptan-5-yl]-1,3,5-triazin-2-yl}-4-(difluoromethyl)pyridin-2-amine (15). **15** was prepared according to general procedure 5 from intermediate **44** (200 mg, 645 μmol, 1.0 equiv) and boronic acid pinacol ester **64** (231 mg, 710 μmol, 1.1 equiv). Purification by column chromatography on silica gel (cyclohexane/EtOAc 1:0 → 2:3) gave compound **15** (191 mg, 458 μmol, 71%) as a colorless solid. ^{1}H NMR (400 MHz, CDCl$_3$): δ 9.12−9.01 (m, 1 H), 8.05−7.55 (m, 1 H), 6.83 (br s, 1 H), 5.12−4.99 (m, 2 H), 4.87 (br s, 2 H), 4.74−4.62 (m, 2 H), 3.95−3.83 (m, 4 H), 3.67−3.46 (m, 4 H), 2.00−1.85 (m, 4 H). ^{13}C{^{1}H} NMR (101 MHz, CDCl$_3$): δ 169.5−168.3 (m, 1 C), 163.6−162.8 (m, 2 C), 160.2 (s, 1 C), 152.5−152.2 (m, 1 C), 144.4−143.4 (m, 1 C), 121.7−120.8 (m, 1 C), 111.5 (t, $^1J_{C,F}$ = 239 Hz, 1 C), 104.1 (t, $^3J_{C,F}$ = 7.8 Hz, 1 C), 76.5 (s, 1 C), 76.4 (s, 1 C), 74.2 (s, 1 C), 73.9 (s, 1 C), 56.7 (s, 1 C), 56.3 (s, 1 C), 55.1 (s, 2 C), 36.8 (s, 1 C), 36.6 (s, 1 C). ESI-HRMS (m/z): [M + H]$^+$ calcd for $C_{19}H_{22}F_2N_7O_2$ 418.1798, found

418.1787. HPLC: t_R = 6.55 min (96.7% purity). Compound **15** exists as a mixture of rotamers.

5-{4,6-Bis[(1R,4R)-2-oxa-5-azabicyclo[2.2.1]heptan-5-yl]-1,3,5-triazin-2-yl}-4-(difluoromethyl)pyridin-2-amine (16). **16** was prepared according to general procedure 5 from intermediate **45** (200 mg, 645 μmol, 1.0 equiv) and boronic acid pinacol ester **64** (231 mg, 710 μmol, 1.1 equiv). Purification by column chromatography on silica gel (cyclohexane/EtOAc 1:0 → 2:3) gave compound **16** (123 mg, 295 μmol, 46%) as a colorless solid. ^{1}H NMR (400 MHz, CDCl$_3$): δ 9.13−9.02 (m, 1 H), 8.05−7.51 (m, 1 H), 6.84 (br s, 1 H), 5.10−5.03 (m, 2 H), 4.84 (br s, 2 H), 4.72−4.66 (m, 2 H), 3.95−3.82 (m, 4 H), 3.70−3.42 (m, 4 H), 2.00−1.87 (m, 4 H). ^{13}C{^{1}H} NMR (101 MHz, CDCl$_3$): δ 169.5−168.5 (m, 1 C), 163.5−163.0 (m, 2 C), 160.2 (s, 1 C), 152.3 (t, $^3J_{C,F}$ = 8.8 Hz, 1 C), 144.3−143.3 (m, 1 C), 121.6−120.9 (m, 1 C), 111.5 (t, $^1J_{C,F}$ = 239 Hz, 1 C), 104.1 (t, $^3J_{C,F}$ = 8.0 Hz, 1 C), 76.5−76.3 (m, 2 C), 74.3−73.9 (m, 2 C), 56.9−56.0 (m, 2 C), 55.1 (s, 2 C), 36.9−36.4 (m, 2 C). ESI-HRMS (m/z): [M + H]$^+$ calcd for $C_{19}H_{22}F_2N_7O_2$ 418.1798, found 418.1788. HPLC: t_R = 6.57 min (98.4% purity). Compound **16** exists as a mixture of rotamers.

5-[4,6-Bis({3-oxa-6-azabicyclo[3.1.1]heptan-6-yl})-1,3,5-triazin-2-yl]-4-(difluoromethyl)pyridin-2-amine (17). **17** was prepared according to general procedure 4 from intermediate **46** (40.0 mg, 129 μmol, 1.0 equiv) and boronic acid pinacol ester **64** (50.0 mg, 155 μmol, 1.2 equiv). Purification by column chromatography on silica gel (cyclohexane/EtOAc 1:4 → 0:1) gave compound **17** (35.2 mg, 84.3 μmol, 65%) as a colorless solid. ^{1}H NMR (400 MHz, (CD$_3$)$_2$SO): δ 8.91 (br s, 1 H), 7.84 (t, $^2J_{H,F}$ = 55 Hz, 1 H), 6.90 (br s, 2 H), 6.75 (s, 1 H), 4.44 (br s, 2 H), 4.32 (br s, 2 H), 4.20−4.10 (m, 4 H), 3.80−3.70 (m, 4 H), 2.72−2.63 (m, 2 H), 1.79 (d, $J_{H,H}$ = 8.2 Hz, 2 H). ^{13}C{^{1}H} NMR (101 MHz, (CD$_3$)$_2$SO): δ 168.9 (s, 1 C), 165.6 (s, 1 C), 165.5 (s, 1 C), 161.8 (s, 1 C), 152.3 (s, 1 C), 142.4 (t, $^2J_{C,F}$ = 20 Hz, 1 C), 117.2 (br s, 1 C), 111.7 (t, $^1J_{C,F}$ = 237 Hz, 1 C), 103.2 (t, $^3J_{C,F}$ = 9.0 Hz, 1 C), 64.9 (s, 2 C), 64.6 (s, 2 C), 61.3 (s, 2 C), 61.0 (s, 2 C), 27.7 (s, 2 C). ESI-HRMS (m/z): [M + H]$^+$ calcd for $C_{19}H_{22}F_2N_7O_2$ 418.1798, found 418.1784. HPLC: t_R = 6.44 min (99.7% purity).

5-{4,6-Bis[(3R)-3-ethylmorpholin-4-yl]-1,3,5-triazin-2-yl}-4-(difluoromethyl)pyridin-2-amine (18). **18** was prepared according to general procedure 4 from intermediate **47** (303 mg, 897 μmol, 1.0 equiv) and boronic acid pinacol ester **64** (288 mg, 886 μmol, 1.0 equiv). Purification by column chromatography on silica gel (cyclohexane/EtOAc 1:0 → 7:3) gave compound **18** (245 mg, 545 μmol, 61%) as a colorless solid. ^{1}H NMR (400 MHz, CDCl$_3$): δ 9.03 (s, 1 H), 7.69 (t, $^2J_{H,F}$ = 55 Hz, 1 H), 6.84 (s, 1 H), 4.84 (br s, 2 H), 4.63−4.36 (m, 4 H), 3.98−3.83 (m, 4 H), 3.64−3.46 (m, 4 H), 3.30−3.13 (m, 2 H), 1.93−1.71 (m, 4 H), 0.94 (t, $^3J_{H,H}$ = 7.4 Hz, 6 H). ^{13}C{^{1}H} NMR (101 MHz, CDCl$_3$): δ 169.2 (s, 1 C), 164.7 (s, 2 C), 160.2 (s, 1 C), 152.4 (s, 1 C), 143.6 (t, $^2J_{C,F}$ = 22 Hz, 1 C), 121.7 (t, $^3J_{C,F}$ = 4.7 Hz, 1 C), 111.4 (t, $^1J_{C,F}$ = 239 Hz, 1 C), 104.1 (t, $^3J_{C,F}$ = 7.6 Hz, 1 C), 68.5 (s, 2 C), 67.1 (s, 2 C), 52.2 (s, 2 C), 39.0 (br s, 2 C), 21.6 (s, 2 C), 11.0 (br s, 2 C). ESI-HRMS (m/z): [M + H]$^+$ calcd for $C_{21}H_{30}F_2N_7O_2$ 450.2424, found 450.2412. HPLC: t_R = 9.18 min (99.1% purity).

5-{4,6-Bis[(3R,5S)-3,5-dimethylmorpholin-4-yl]-1,3,5-triazin-2-yl}-4-(difluoromethyl)pyridin-2-amine (19). **19** was prepared according to general procedure 5 from intermediate **48** (200 mg, 585 μmol, 1.0 equiv) and boronic acid pinacol ester **64** (191 mg, 587 μmol, 1.0 equiv). Purification by column chromatography on silica gel (cyclohexane/EtOAc 1:0 → 1:1) gave compound **19** (110 mg, 245 μmol, 42%) as a colorless solid. ^{1}H NMR (400 MHz, CDCl$_3$): δ 9.10 (s, 1 H), 7.79 (t, $^2J_{H,F}$ = 55 Hz, 1 H), 6.84 (s, 1 H), 4.82 (br s, 2 H), 4.64−4.53 (m, 4 H), 3.87−3.79 (m, 4 H), 3.69−3.61 (m, 4 H), 1.38 (d, $^3J_{H,H}$ = 6.9 Hz, 12 H). ^{13}C{^{1}H} NMR (101 MHz, CDCl$_3$): δ 169.1 (s, 1 C), 164.1 (s, 2 C), 160.1 (s, 1 C), 152.6 (s, 1 C), 143.8 (t, $^2J_{C,F}$ = 22 Hz, 1 C), 121.8 (t, $^3J_{C,F}$ = 4.8 Hz, 1 C), 111.5 (t, $^1J_{C,F}$ = 239 Hz, 1 C), 104.0 (t, $^3J_{C,F}$ = 8.1 Hz, 1 C), 71.6 (s, 4 C), 45.9 (s, 4 C), 19.3 (s, 4 C). ESI-HRMS (m/z): [M + H]$^+$ calcd for $C_{21}H_{30}F_2N_7O_2$ 450.2424, found 450.2410. HPLC: t_R = 9.48 min (97.1% purity).

5-{4,6-Bis[(3R,5R)-3,5-dimethylmorpholin-4-yl]-1,3,5-triazin-2-yl}-4-(difluoromethyl)pyridin-2-amine (20). 20 was prepared according to general procedure 5 from intermediate 49 (247 mg, 723 μmol, 1.0 equiv) and boronic acid pinacol ester 64 (235 mg, 723 μmol, 1.0 equiv). Purification by column chromatography on silica gel (cyclohexane/EtOAc 1:0 → 3:2) gave compound 20 (156 mg, 347 μmol, 48%) as a colorless solid. ^{1}H NMR (400 MHz, (CD$_3$)$_2$SO): δ 8.91 (s, 1 H), 7.86 (t, $^2J_{H,F}$ = 55 Hz, 1 H), 6.83 (br s, 2 H), 6.76 (s, 1 H), 4.36–4.24 (m, 4 H), 4.13 (dd, $^2J_{H,H}$ = 11 Hz, $^3J_{H,H}$ = 3.4 Hz, 4 H), 3.69 (dd, $^2J_{H,H}$ = 11 Hz, $^3J_{H,H}$ = 2.2 Hz, 4 H), 1.38 (d, $^3J_{H,H}$ = 6.6 Hz, 12 H). ^{13}C{^{1}H} NMR (101 MHz, CDCl$_3$): δ 168.6 (s, 1 C), 163.6 (s, 2 C), 160.0 (s, 1 C), 152.5 (s, 1 C), 143.8 (t, $^2J_{C,F}$ = 22 Hz, 1 C), 121.4 (t, $^3J_{C,F}$ = 4.6 Hz, 1 C), 111.3 (t, $^1J_{C,F}$ = 239 Hz, 1 C), 103.8 (t, $^3J_{C,F}$ = 8.0 Hz, 1 C), 67.8 (s, 4 C), 48.1 (s, 4 C), 19.8 (s, 4 C). ESI-HRMS (m/z): [M + H]$^+$ calcd for C$_{21}$H$_{30}$F$_2$N$_7$O$_2$ 450.2424, found 450.2415. HPLC: t_R = 8.99 min (99.8% purity).

5-{4,6-Bis[(3S,5S)-3,5-dimethylmorpholin-4-yl]-1,3,5-triazin-2-yl}-4-(difluoromethyl)pyridin-2-amine (21). 21 was prepared according to general procedure 5 from intermediate 50 (232 mg, 679 μmol, 1.0 equiv) and boronic acid pinacol ester 64 (221 mg, 680 μmol, 1.0 equiv). Purification by column chromatography on silica gel (cyclohexane/EtOAc 1:0 → 3:2) gave compound 21 (171 mg, 380 μmol, 56%) as a colorless solid. ^{1}H NMR (400 MHz, (CD$_3$)$_2$SO): δ 8.91 (s, 1 H), 7.86 (t, $^2J_{H,F}$ = 55 Hz, 1 H), 6.83 (br s, 2 H), 6.76 (s, 1 H), 4.36–4.24 (m, 4 H), 4.13 (dd, $^2J_{H,H}$ = 11 Hz, $^3J_{H,H}$ = 3.0 Hz, 4 H), 3.69 (dd, $^2J_{H,H}$ = 11 Hz, $^3J_{H,H}$ = 1.9 Hz, 4 H), 1.38 (d, $^3J_{H,H}$ = 6.6 Hz, 12 H). ^{13}C{^{1}H} NMR (101 MHz, CDCl$_3$): δ 168.7 (s, 1 C), 163.8 (s, 2 C), 160.1 (s, 1 C), 152.6 (s, 1 C), 143.7 (t, $^2J_{C,F}$ = 22 Hz, 1 C), 121.6 (t, $^3J_{C,F}$ = 4.7 Hz, 1 C), 111.5 (t, $^1J_{C,F}$ = 239 Hz, 1 C), 104.0 (t, $^3J_{C,F}$ = 8.0 Hz, 1 C), 67.8 (s, 4 C), 48.1 (s, 4 C), 19.9 (s, 4 C). ESI-HRMS (m/z): [M + H]$^+$ calcd for C$_{21}$H$_{30}$F$_2$N$_7$O$_2$ 450.2424, found 450.2413. HPLC: t_R = 9.00 min (99.5% purity).

5-{4,6-Bis[(2R,6S)-2,6-dimethylmorpholin-4-yl]-1,3,5-triazin-2-yl}-4-(difluoromethyl)pyridin-2-amine (22). 22 was prepared according to general procedure 5 from intermediate 51 (209 mg, 612 μmol, 1.0 equiv) and boronic acid pinacol ester 64 (200 mg, 615 μmol, 1.0 equiv). Purification by column chromatography on silica gel (cyclohexane/EtOAc 1:0 → 3:2) gave compound 22 (206 mg, 458 μmol, 75%) as a colorless solid. ^{1}H NMR (400 MHz, CDCl$_3$): δ 9.02 (s, 1 H), 7.62 (t, $^2J_{H,F}$ = 55 Hz, 1 H), 6.84 (s, 1 H), 4.83 (br s, 2 H), 4.71–4.45 (m, 4 H), 3.67–3.55 (m, 4 H), 2.67–2.52 (m, 4 H), 1.29–1.22 (m, 12 H). ^{13}C{^{1}H} NMR (101 MHz, CDCl$_3$): δ 169.2 (s, 1 C), 164.5 (s, 2 C), 160.2 (s, 1 C), 152.3 (s, 1 C), 143.6 (t, $^2J_{C,F}$ = 22 Hz, 1 C), 121.7 (t, $^3J_{C,F}$ = 4.7 Hz, 1 C), 111.4 (t, $^1J_{C,F}$ = 239 Hz, 1 C), 104.2 (t, $^3J_{C,F}$ = 7.7 Hz, 1 C), 71.9 (s, 4 C), 48.9 (br s, 4 C), 19.0 (s, 4 C). ESI-HRMS (m/z): [M + H]$^+$ calcd for C$_{21}$H$_{30}$F$_2$N$_7$O$_2$ 450.2424, found 450.2431. HPLC: t_R = 11.34 min (98.4% purity).

5-[4,6-Bis(2,2-dimethylmorpholin-4-yl)-1,3,5-triazin-2-yl]-4-(difluoromethyl)pyridin-2-amine (23). 23 was prepared according to general procedure 4 from intermediate 52 (93.0 mg, 272 μmol, 1.0 equiv) and boronic acid pinacol ester 64 (89.0 mg, 273 μmol, 1.0 equiv). Purification by column chromatography on silica gel (cyclohexane/EtOAc 1:0 → 3:2) gave compound 23 (77.0 mg, 171 μmol, 63%) as a colorless solid. ^{1}H NMR (400 MHz, CDCl$_3$): δ 9.03 (s, 1 H), 7.64 (t, $^2J_{H,F}$ = 55 Hz, 1 H), 6.84 (s, 1 H), 4.83 (br s, 2 H), 3.91–3.56 (m, 12 H), 1.25 (s, 12 H). ^{13}C{^{1}H} NMR (101 MHz, CDCl$_3$): δ 169.3 (s, 1 C), 165.0 (s, 2 C), 160.2 (s, 1 C), 152.4 (s, 1 C), 143.7 (t, $^2J_{C,F}$ = 22 Hz, 1 C), 121.7 (br s, 1 C), 111.4 (t, $^1J_{C,F}$ = 238 Hz, 1 C), 104.1 (t, $^3J_{C,F}$ = 7.7 Hz, 1 C), 71.7 (s, 2 C), 60.8 (br s, 2 C), 52.6 (s, 1 C), 52.4 (s, 1 C), 43.5 (s, 1 C), 43.1 (s, 1 C), 24.4 (br s, 4 C). ESI-HRMS (m/z): [M + H]$^+$ calcd for C$_{21}$H$_{30}$F$_2$N$_7$O$_2$ 450.2424, found 450.2426. HPLC: t_R = 8.77 min (96.6% purity).

5-[4,6-Bis({8-oxa-5-azaspiro[3.5]nonan-5-yl})-1,3,5-triazin-2-yl]-4-(difluoromethyl)pyridin-2-amine (24). 24 was prepared according to general procedure 4 from intermediate 53 (300 mg, 820 μmol, 1.0 equiv) and boronic acid pinacol ester 64 (267 mg, 821 μmol, 1.0 equiv). Purification by column chromatography on silica gel (cyclohexane/EtOAc 1:0 → 4:1) gave compound 24 (229 mg, 484 μmol, 59%) as a colorless solid. ^{1}H NMR (400 MHz, CDCl$_3$): δ 8.93 (s, 1 H), 7.64 (t, $^2J_{H,F}$ = 55 Hz, 1 H), 6.82 (s, 1 H), 4.81 (br s, 2 H), 3.83–3.77 (m, 4 H), 3.76 (s, 4 H), 3.60–3.54 (m, 4 H), 2.61–2.47 (m, 4 H), 2.42–2.30 (m, 4 H), 1.87–1.64 (m, 4 H). ^{13}C{^{1}H} NMR (101 MHz, CDCl$_3$): δ 169.2 (s, 1 C), 165.7 (s, 2 C), 160.0 (s, 1 C), 152.5 (s, 1 C), 143.5 (t, $^2J_{C,F}$ = 22 Hz, 1 C), 121.8 (t, $^3J_{C,F}$ = 4.9 Hz, 1 C), 111.3 (t, $^1J_{C,F}$ = 239 Hz, 1 C), 104.0 (t, $^3J_{C,F}$ = 7.7 Hz, 1 C), 70.9 (s, 2 C), 66.2 (s, 2 C), 60.8 (s, 2 C), 43.5 (s, 2 C), 31.4 (s, 4 C), 15.0 (s, 2 C). ESI-HRMS (m/z): [M + H]$^+$ calcd for C$_{23}$H$_{30}$F$_2$N$_7$O$_2$ 474.2424, found 474.2428. HPLC: t_R = 9.86 min (98.7% purity).

5-[4,6-Bis({3,7-dioxa-9-azabicyclo[3.3.1]nonan-9-yl})-1,3,5-triazin-2-yl]-4-(difluoromethyl)pyridin-2-amine (25). 25 was prepared according to general procedure 5 from intermediate 54 (180 mg, 487 μmol, 1.0 equiv) and boronic acid pinacol ester 64 (159 mg, 489 μmol, 1.0 equiv). Purification by column chromatography on silica gel (cyclohexane/EtOAc/CH$_3$OH 1:1:0 → 0:100:5) gave compound 25 (102 mg, 214 μmol, 44%) as a colorless solid. ^{1}H NMR (400 MHz, (CD$_3$)$_2$SO): δ 8.87 (s, 1 H), 7.70 (t, $^2J_{H,F}$ = 55 Hz, 1 H), 6.89 (br s, 2 H), 6.76 (s, 1 H), 4.55–4.44 (m, 4 H), 4.07–3.96 (m, 8 H), 3.81–3.68 (m, 8 H). ^{13}C{^{1}H} NMR (101 MHz, (CD$_3$)$_2$SO): δ 169.7 (s, 1 C), 163.4 (s, 2 C), 161.7 (s, 1 C), 152.3 (s, 1 C), 142.1 (t, $^2J_{C,F}$ = 22 Hz, 1 C), 118.0 (t, $^3J_{C,F}$ = 4.5 Hz, 1 C), 111.9 (t, $^1J_{C,F}$ = 237 Hz, 1 C), 103.1 (t, $^3J_{C,F}$ = 8.3 Hz, 1 C), 68.7 (s, 4 C), 68.5 (s, 4 C), 48.3 (s, 2 C), 47.8 (s, 2 C). ESI-HRMS (m/z): [M + H]$^+$ calcd for C$_{21}$H$_{26}$F$_2$N$_7$O$_4$ 478.2009, found 478.2006. HPLC: t_R = 7.03 min (95.6% purity).

5-[4,6-Bis({3-oxa-9-azabicyclo[3.3.1]nonan-9-yl})-1,3,5-triazin-2-yl]-4-(difluoromethyl)pyridin-2-amine (26). 26 was prepared according to general procedure 5 from intermediate 55 (240 mg, 656 μmol, 1.0 equiv) and boronic acid pinacol ester 64 (213 mg, 655 μmol, 1.0 equiv). Purification by column chromatography on silica gel (cyclohexane/EtOAc 1:0 → 7:3) gave compound 26 (77.5 mg, 164 μmol, 25%) as a colorless solid. ^{1}H NMR (400 MHz, CDCl$_3$): δ 9.03–8.99 (m, 1 H), 7.82–7.51 (m, 1 H), 6.83 (br s, 1 H), 4.81 (br s, 2 H), 4.70 (br s, 2 H), 4.59 (br s, 2 H), 4.03–3.94 (m, 4 H), 3.88–3.80 (m, 4 H), 2.71–2.52 (m, 2 H), 1.98–1.78 (m, 8 H), 1.70–1.55 (m, 2 H). ^{13}C{^{1}H} NMR (101 MHz, CDCl$_3$): δ 169.8 (s, 1 C), 163.9 (s, 2 C), 160.1 (s, 1 C), 152.5–152.2 (m, 1 C), 143.6 (t, $^2J_{C,F}$ = 22 Hz, 1 C), 122.0–121.7 (m, 1 C), 111.5 (t, $^1J_{C,F}$ = 239 Hz, 1 C), 104.1 (t, $^3J_{C,F}$ = 7.7 Hz, 1 C), 71.5–71.2 (m, 4 C), 48.0–47.8 (m, 2 C), 47.4–47.2 (m, 2 C), 29.3–28.7 (m, 4 C), 20.7 (s, 2 C). ESI-HRMS (m/z): [M + H]$^+$ calcd for C$_{23}$H$_{30}$F$_2$N$_7$O$_2$ 474.2424, found 474.2418. HPLC: t_R = 9.70 min (97.0% purity). Compound 26 exists as a mixture of rotamers.

5-[2,6-Bis(morpholin-4-yl)pyrimidin-4-yl]-4-(trifluoromethyl)pyridin-2-amine (BKM120 (27)). 27 was prepared according to the literature.[24,34]

5-[2,6-Bis(morpholin-4-yl)pyrimidin-4-yl]-4-(difluoromethyl)pyridin-2-amine (28). 28 was prepared according to general procedure 5 from intermediate 57 (100 mg, 351 μmol, 1.0 equiv) and boronic acid pinacol ester 64 (125 mg, 384 μmol, 1.1 equiv). Purification by column chromatography on silica gel (cyclohexane/EtOAc 3:7) gave compound 28 (101 mg, 257 μmol, 73%) as a colorless solid. ^{1}H NMR (400 MHz, CDCl$_3$): δ 8.31 (s, 1 H), 7.30 (t, $^2J_{H,F}$ = 55 Hz, 1 H), 6.85 (s, 1 H), 6.04 (s, 1 H), 4.73 (br s, 2 H), 3.81–3.72 (m, 12 H), 3.65–3.59 (m, 4 H). ^{13}C{^{1}H} NMR (101 MHz, CDCl$_3$): δ 163.7 (s, 1 C), 162.6 (s, 1 C), 161.5 (s, 1 C), 159.3 (s, 1 C), 149.5 (s, 1 C), 142.6 (t, $^2J_{C,F}$ = 22 Hz, 1 C), 124.6 (t, $^3J_{C,F}$ = 5.3 Hz, 1 C), 111.5 (t, $^1J_{C,F}$ = 239 Hz, 1 C), 104.6 (t, $^3J_{C,F}$ = 6.8 Hz, 1 C), 91.5 (s, 1 C), 67.0 (s, 2 C), 66.7 (s, 2 C), 44.5 (s, 2 C), 44.4 (s, 2 C). ESI-HRMS (m/z): [M + H]$^+$ calcd for C$_{18}$H$_{22}$F$_2$N$_6$O$_2$ 393.1845; found: 393.1852. HPLC: t_R = 6.87 min (96.9% purity).

5-[4,6-Bis(morpholin-4-yl)pyrimidin-2-yl]-4-(trifluoromethyl)pyridin-2-amine (29). 29 was prepared according to the literature,[24] where the compound is referred to as BKM120-R1.

5-[4,6-Bis(morpholin-4-yl)pyrimidin-2-yl]-4-(difluoromethyl)pyridin-2-amine (30). 30 was prepared according to general procedure 5 from intermediate 58 (100 mg, 351 μmol, 1.0 equiv) and boronic acid pinacol ester 64 (125 mg, 384 μmol, 1.1 equiv). Purification by column chromatography on silica gel (cyclohexane/EtOAc 3:7) gave compound 30 (123 mg, 313 μmol, 89%) as a colorless solid. ^{1}H NMR (400 MHz, CDCl$_3$): δ 8.94 (br s, 1 H), 7.61 (t, $^2J_{H,F}$ = 55 Hz, 1 H), 6.83 (s, 1 H), 5.50 (s, 1 H), 4.74 (br s, 2 H),

3.82−3.78 (m, 8 H), 3.61−3.57 (m, 8 H). $^{13}C\{^1H\}$ NMR (101 MHz, $(CD_3)_2SO$): δ 163.4 (s, 2 C), 160.8 (s, 1 C), 160.7 (s, 1 C), 151.4 (s, 1 C), 141.4 (t, $^2J_{C,F}$ = 22 Hz, 1 C), 120.5 (t, $^3J_{C,F}$ = 4.8 Hz, 1 C), 112.0 (t, $^1J_{C,F}$ = 237 Hz, 1 C), 102.8 (t, $^3J_{C,F}$ = 7.7 Hz, 1 C), 79.6 (s, 1 C), 65.9 (s, 4 C), 44.3 (s, 4 C). ESI-HRMS (m/z): [M + H]$^+$ calcd for $C_{18}H_{23}F_2N_6O_2$ 393.1845, found 393.1848. HPLC: t_R = 6.58 min (96.4% purity).

5-[2,6-Bis({3-oxa-8-azabicyclo[3.2.1]octan-8-yl})pyrimidin-4-yl]-4-(trifluoromethyl)pyridin-2-amine (31). 31 was prepared according to general procedure 5 from intermediate 59 (108 mg, 321 μmol, 1.0 equiv) and boronic acid pinacol ester 72 (121 mg, 353 μmol, 1.1 equiv). Purification by column chromatography on silica gel (cyclohexane/EtOAc 1:0 → 1:4) gave compound 31 (110 mg, 238 μmol, 74%) as a yellowish solid. ^1H NMR (400 MHz, CDCl$_3$): δ 8.27 (s, 1 H), 6.78 (s, 1 H), 5.91 (s, 1 H), 4.77 (br s, 2 H), 4.63 (br s, 2 H), 4.52−4.31 (m, 2 H), 3.87−3.78 (m, 4 H), 3.63−3.55 (m, 4 H), 2.13−1.90 (m, 8 H). $^{13}C\{^1H\}$ NMR (101 MHz, CDCl$_3$): δ 163.0 (s, 1 C), 161.4 (s, 1 C), 161.1 (s, 1 C), 158.8 (s, 1 C), 150.9 (s, 1 C), 137.9 (q, $^2J_{C,F}$ = 32 Hz, 1 C), 124.4 (br s, 1 C), 123.0 (q, $^1J_{C,F}$ = 275 Hz, 1 C), 105.3 (q, $^3J_{C,F}$ = 5.5 Hz, 1 C), 94.4 (br s, 1 C), 71.6 (s, 2 C), 71.0 (s, 2 C), 55.4 (s, 2 C), 55.2 (s, 2 C), 27.1 (s, 2 C), 27.0 (s, 2 C). ESI-HRMS (m/z): [M + H]$^+$ calcd for $C_{22}H_{26}F_3N_6O_2$ 463.2064, found 463.2046. HPLC: t_R = 8.16 min (96.5% purity).

5-[2,6-Bis({3-oxa-8-azabicyclo[3.2.1]octan-8-yl})pyrimidin-4-yl]-4-(difluoromethyl)pyridin-2-amine (32). 32 was prepared according to general procedure 5 from intermediate 59 (82.9 mg, 246 μmol, 1.0 equiv) and boronic acid pinacol ester 64 (80 mg, 246 μmol, 1.0 equiv). Purification by column chromatography on silica gel (EtOAc/CH3OH 50:1) gave compound 32 (66.7 mg, 150 μmol, 61%) as a colorless solid. ^1H NMR (400 MHz, CDCl$_3$): δ 8.31 (s, 1 H), 7.33 (t, $^2J_{H,F}$ = 55 Hz, 1 H), 6.84 (s, 1 H), 5.98 (s, 1 H), 4.75 (br s, 2 H), 4.62 (br s, 2 H), 4.53−4.36 (m, 2 H), 3.86−3.76 (m, 4 H), 3.67−3.56 (m, 4 H), 2.15−1.91 (m, 8 H). $^{13}C\{^1H\}$ NMR (101 MHz, $(CD_3)_2SO$): δ 162.4 (s, 1 C), 161.3 (s, 1 C), 160.6 (s, 1 C), 160.2 (s, 1 C), 149.7 (s, 1 C), 141.0 (t, $^2J_{C,F}$ = 22 Hz, 1 C), 121.1 (br s, 1 C), 112.0 (t, $^1J_{C,F}$ = 236 Hz, 1 C), 103.3 (t, $^3J_{C,F}$ = 8.1 Hz, 1 C), 92.3 (s, 1 C), 70.5 (s, 2 C), 70.3 (s, 2 C), 54.7 (s, 2 C), 54.3 (s, 2 C), 26.6 (s, 2 C), 26.5 (s, 2 C). ESI-HRMS (m/z): [M + H]$^+$ calcd for $C_{22}H_{27}F_2N_6O_2$ 445.2158, found 445.2152. HPLC: t_R = 8.01 min (99.2% purity).

5-[4,6-Bis({3-oxa-8-azabicyclo[3.2.1]octan-8-yl})pyrimidin-2-yl]-4-(trifluoromethyl)pyridin-2-amine (33). 33 was prepared according to general procedure 5 from intermediate 60 (150 mg, 445 μmol, 1.0 equiv) and boronic acid pinacol ester 72 (169 mg, 492 μmol, 1.1 equiv). Purification by column chromatography on silica gel (EtOAc 100%) gave compound 33 (96.1 mg, 208 μmol, 47%) as a colorless solid. ^1H NMR (400 MHz, CDCl$_3$): δ 8.65 (s, 1 H), 6.77 (s, 1 H), 5.41 (s, 1 H), 4.76 (br s, 2 H), 4.45 (br s, 4 H), 3.83 (d, $J_{H,H}$ = 11 Hz, 4 H), 3.59 (d, $J_{H,H}$ = 11 Hz, 4 H), 2.14−1.96 (m, 8 H). $^{13}C\{^1H\}$ NMR (101 MHz, CDCl$_3$): δ 163.2 (s, 1 C), 161.6 (s, 2 C), 158.8 (s, 1 C), 152.6 (s, 1 C), 138.1 (q, $^2J_{C,F}$ = 32 Hz, 1 C), 124.3 (br s, 1 C), 123.2 (q, $^1J_{C,F}$ = 274 Hz, 1 C), 105.2 (q, $^3J_{C,F}$ = 5.2 Hz, 1 C), 82.5 (s, 1 C), 70.9 (s, 4 C), 55.3 (s, 4 C), 27.0 (s, 4 C). ESI-HRMS (m/z): [M + H]$^+$ calcd for $C_{22}H_{26}F_3N_6O_2$ 463.2064, found 463.2064. HPLC: t_R = 7.64 min (95.7% purity).

5-[4,6-Bis({3-oxa-8-azabicyclo[3.2.1]octan-8-yl})pyrimidin-2-yl]-4-(difluoromethyl)pyridin-2-amine (34). 34 was prepared according to general procedure 5 from intermediate 60 (137 mg, 407 μmol, 1.0 equiv) and boronic acid pinacol ester 64 (133 mg, 409 μmol, 1.0 equiv). Purification by column chromatography on silica gel (EtOAc 100%) gave compound 34 (79.4 mg, 179 μmol, 44%) as a colorless solid. ^1H NMR (400 MHz, $(CD_3)_2SO$): δ 8.77 (s, 1 H), 7.73 (t, $^2J_{H,F}$ = 55 Hz, 1 H), 6.72 (s, 1 H), 6.59 (br s, 2 H), 5.85 (s, 1 H), 4.52 (br s, 4 H), 3.64 (d, $J_{H,H}$ = 11 Hz, 4 H), 3.52 (d, $J_{H,H}$ = 11 Hz, 4 H), 1.99−1.82 (m, 8 H). $^{13}C\{^1H\}$ NMR (101 MHz, $(CD_3)_2SO$): δ 161.8 (s, 1 C), 161.0 (s, 2 C), 160.7 (s, 1 C), 151.5 (s, 1 C), 114.4 (t, $^2J_{C,F}$ = 21 Hz, 1 C), 120.4 (t, $^3J_{C,F}$ = 4.5 Hz, 1 C), 112.1 (t, $^1J_{C,F}$ = 237 Hz, 1 C), 102.8 (t, $^3J_{C,F}$ = 7.9 Hz, 1 C), 82.4 (s, 1 C), 70.0 (s, 4 C), 54.5 (s, 4 C), 26.5 (s, 4 C). ESI-HRMS (m/z): [M + H]$^+$ calcd for $C_{22}H_{27}F_2N_6O_2$ 445.2158, found 445.2145. HPLC: t_R = 7.45 min (98.1% purity).

2,4-Dichloro-6-(morpholin-4-yl)-1,3,5-triazine (35) and 2-Chloro-4,6-bis(morpholin-4-yl)-1,3,5-triazine (36). 35 and 36 were prepared according to the literature.[24]

2-Chloro-4-[(3R)-3-methylmorpholin-4-yl]-6-(morpholin-4-yl)-1,3,5-triazine (37). 37 was prepared according to general procedure 3 from (R)-3-methylmorpholine (370 mg, 3.66 mmol, 1.1 equiv) and 4-(4,6-dichloro-1,3,5-triazin-2-yl)morpholine (35, 820 mg, 3.49 mmol, 1.0 equiv) in the presence of N,N-diisopropylethylamine (1.34 mL, 7.69 mmol, 2.1 equiv). Purification by column chromatography on silica gel (cyclohexane/EtOAc 1:0 → 4:1) gave compound 37 (953 mg, 3.18 mmol, 91%) as a colorless solid. ^1H NMR (400 MHz, CDCl$_3$): δ 4.76−4.56 (m, 1 H), 4.39−4.23 (m, 1 H), 3.93 (dd, $J_{H,H}$ = 11, 3.6 Hz, 1 H), 3.86−3.65 (m, 9 H), 3.63 (dd, $J_{H,H}$ = 12, 3.2 Hz, 1 H), 3.48 (td, $J_{H,H}$ = 12, 3.0 Hz, 1 H), 3.30−3.19 (m, 1 H), 1.30 (d, $^3J_{H,H}$ = 6.8 Hz, 3 H). $^{13}C\{^1H\}$ NMR (101 MHz, CDCl$_3$): δ 169.8 (s, 1 C), 164.6 (s, 1 C), 164.3 (s, 1 C), 71.0 (s, 1 C), 67.0 (s, 1 C), 66.8 (br s, 2 C), 46.8 (s, 1 C), 44.0 (s, 2 C), 39.0 (s, 1 C), 14.6 (br s, 1 C). MALDI-MS: m/z = 300.3 ([M + H]$^+$).

3-[4-Chloro-6-(morpholin-4-yl)-1,3,5-triazin-2-yl]-8-oxa-3-azabicyclo[3.2.1]octane (38). 38 was prepared according to general procedure 3 from 8-oxa-3-azabicyclo[3.2.1]octane hydrochloride (67.0 mg, 448 μmol, 1.1 equiv) and 4-(4,6-dichloro-1,3,5-triazin-2-yl)morpholine (35, 100 mg, 425 μmol, 1.0 equiv) in the presence of N,N-diisopropylethylamine (148 μL, 850 μmol, 2.0 equiv). Purification by column chromatography on silica gel (cyclohexane/EtOAc 1:0 → 3:2) gave compound 38 (107 mg, 343 μmol, 81%) as a colorless solid. ^1H NMR (400 MHz, CDCl$_3$): δ 4.44−4.37 (m, 2 H), 4.29 (d, $J_{H,H}$ = 13 Hz, 1 H), 4.22 (d, $J_{H,H}$ = 13 Hz, 1 H), 3.89−3.66 (m, 8 H), 3.23−3.12 (m, 2 H), 1.99−1.87 (m, 2 H), 1.83−1.68 (m, 2 H). $^{13}C\{^1H\}$ NMR (101 MHz, CDCl$_3$): δ 169.6 (s, 1 C), 165.7 (s, 1 C), 164.4 (s, 1 C), 73.8 (s, 1 C), 73.7 (s, 1 C), 66.8 (s, 1 C), 66.6 (s, 1 C), 49.6 (s, 1 C), 49.5 (s, 1 C), 43.9 (br s, 2 C), 27.7 (s, 1 C), 27.6 (s, 1 C). MALDI-MS: m/z = 312.2 ([M + H]$^+$).

8-[4-Chloro-6-(morpholin-4-yl)-1,3,5-triazin-2-yl]-3-oxa-8-azabicyclo[3.2.1]octane (39). 39 was prepared according to general procedure 3 from 3-oxa-8-azabicyclo[3.2.1]octane (159 mg, 1.40 mmol, 1.1 equiv) and 4-(4,6-dichloro-1,3,5-triazin-2-yl)morpholine (35, 300 mg, 1.28 mmol, 1.0 equiv) in the presence of N,N-diisopropylethylamine (470 μL, 2.69 mmol, 2.1 equiv). Purification by column chromatography on silica gel (cyclohexane/EtOAc 1:0 → 4:1) gave compound 39 (312 mg, 1.00 mmol, 78%) as a colorless solid. ^1H NMR (400 MHz, CDCl$_3$): δ 4.70−4.55 (m, 2 H), 3.88−3.57 (m, 12 H), 2.09−1.91 (m, 4 H). $^{13}C\{^1H\}$ NMR (101 MHz, CDCl$_3$): δ 169.9 (s, 1 C), 164.7 (s, 1 C), 162.4 (s, 1 C), 72.3 (s, 1 C), 71.7 (s, 1 C), 66.8 (br s, 2 C), 55.0 (s, 1 C), 54.9 (s, 1 C), 43.9 (br s, 2 C), 27.0 (s, 1 C), 26.8 (s, 1 C). MALDI-MS: m/z = 312.6 ([M + H]$^+$).

2-Chloro-4,6-bis[(3R)-3-methylmorpholin-4-yl]-1,3,5-triazine (41). 41 was prepared according to general procedure 1 from cyanuric chloride (40, 508 mg, 2.75 mmol, 1.0 equiv) and (R)-3-methylmorpholine (558 mg, 5.52 mmol, 2.0 equiv) in the presence of N,N-diisopropylethylamine (1.06 mL, 6.07 mmol, 2.2 equiv). Purification by column chromatography on silica gel (cyclohexane/EtOAc 1:0 → 3:1) gave compound 41 (781 mg, 2.49 mmol, 91%) as a colorless solid. ^1H NMR (400 MHz, CDCl$_3$): δ 4.75−4.55 (m, 2 H), 4.41−4.21 (m, 2 H), 3.93 (dd, $J_{H,H}$ = 11, 3.7 Hz, 2 H), 3.73 (d, $J_{H,H}$ = 12 Hz, 2 H), 3.63 (dd, $J_{H,H}$ = 12, 3.3 Hz, 2 H), 3.48 (td, $J_{H,H}$ = 12, 3.0 Hz, 2 H), 3.29−3.18 (m, 2 H), 1.30 (d, $^3J_{H,H}$ = 6.9 Hz, 6 H). $^{13}C\{^1H\}$ NMR (101 MHz, CDCl$_3$): δ 169.8 (s, 1 C), 164.3 (s, 2 C), 71.0 (s, 2 C), 67.0 (s, 2 C), 46.8 (s, 2 C), 38.9 (s, 2 C), 14.6 (br s, 2 C). MALDI-MS: m/z = 314.3 ([M + H]$^+$).

3-(4-Chloro-6-{8-oxa-3-azabicyclo[3.2.1]octan-3-yl}-1,3,5-triazin-2-yl)-8-oxa-3-azabicyclo[3.2.1]octane (42). 42 was prepared according to general procedure 1 from cyanuric chloride (40, 1.63 g, 8.84 mmol, 1.0 equiv) and 8-oxa-3-azabicyclo[3.2.1]octane hydrochloride (2.65 g, 17.7 mmol, 2.0 equiv) in the presence of N,N-diisopropylethylamine (3.40 mL, 19.5 mmol, 2.2 equiv). Purification by column chromatography on silica gel (cyclohexane/EtOAc 4:1) gave compound 42 (2.80 g, 8.29 mmol, 94%) as a colorless solid. ^1H NMR (400 MHz, CDCl$_3$): δ 4.45−4.35 (m, 4 H),

4.33−4.16 (m, 4 H), 3.24−3.10 (m, 4 H), 2.10−1.85 (m, 4 H), 1.85−1.66 (m, 4 H). ^{13}C{^{1}H} NMR (101 MHz, CDCl$_3$): δ 169.4 (s, 1 C), 165.6 (s, 2 C), 73.8 (s, 2 C), 73.7 (br s, 2 C), 49.7−49.4 (m, 4 C), 27.8−27.4 (m, 4 C). MALDI-MS: m/z = 338.3 ([M + H]$^+$).

8-(4-Chloro-6-{3-oxa-8-azabicyclo[3.2.1]octan-8-yl}-1,3,5-triazin-2-yl)-3-oxa-8-azabicyclo[3.2.1]octane (43). 43 was prepared according to general procedure 1 from cyanuric chloride (40, 1.23 g, 6.67 mmol, 1.0 equiv) and 3-oxa-8-azabicyclo[3.2.1]octane hydrochloride (2.00 g, 13.4 mmol, 2.0 equiv) in the presence of N,N-diisopropylethylamine (4.80 mL, 27.6 mmol, 4.1 equiv). Purification by column chromatography on silica gel (cyclohexane/EtOAc 4:1) gave compound 43 (1.79 g, 5.30 mmol, 79%) as a colorless solid. ^{1}H NMR (400 MHz, CDCl$_3$): δ 4.73−4.53 (m, 4 H), 3.78−3.57 (m, 8 H), 2.11−1.88 (m, 8 H). ^{13}C{^{1}H} NMR (101 MHz, CDCl$_3$): δ 169.9 (s, 1 C), 162.5 (s, 1 C), 162.4 (s, 1 C), 72.2 (s, 2 C), 71.6 (br s, 2 C), 54.9 (s, 2 C), 54.8 (s, 2 C), 26.9 (s, 2 C), 26.8 (s, 2 C). MALDI-MS: m/z = 338.2 ([M + H]$^+$).

(1S,4S)-5-{4-Chloro-6-[(1S,4S)-2-oxa-5-azabicyclo[2.2.1]heptan-5-yl]-1,3,5-triazin-2-yl}-2-oxa-5-azabicyclo[2.2.1]heptane (44). 44 was prepared according to general procedure 1 from cyanuric chloride (40, 200 mg, 1.09 mmol, 1.0 equiv) and (1S,4S)-2-oxa-5-azabicyclo[2.2.1]heptane hydrochloride (335 mg, 2.47 mmol, 2.3 equiv) in the presence of N,N-diisopropylethylamine (800 μL, 4.59 mmol, 4.2 equiv). Purification by column chromatography on silica gel (cyclohexane/EtOAc 1:1 →0:1) gave compound 44 (264 mg, 861 μmol, 79%) as a colorless solid. ^{1}H NMR (400 MHz, CDCl$_3$): δ 5.06 (br s, 1 H), 4.98 (br s, 1 H), 4.67 (br s, 2 H), 3.90−3.80 (m, 4 H), 3.64−3.41 (m, 4 H), 2.00−1.81 (m, 4 H). ^{13}C{^{1}H} NMR (101 MHz, CDCl$_3$): δ 169.5−168.5 (m, 1 C), 163.1−162.5 (m, 2 C), 76.5−76.1 (m, 2 C), 74.1 (br s, 1 C), 73.7 (s, 1 C), 56.8 (br s, 2 C), 55.2 (br s, 2 C), 36.7 (br s, 1 C), 36.5−36.4 (m, 1 C). MALDI-MS: m/z = 310.2 ([M + H]$^+$). Compound 44 exists as a mixture of rotamers.

(1R,4R)-5-{4-Chloro-6-[(1R,4R)-2-oxa-5-azabicyclo[2.2.1]heptan-5-yl]-1,3,5-triazin-2-yl}-2-oxa-5-azabicyclo[2.2.1]heptane (45). 45 was prepared according to general procedure 1 from cyanuric chloride (40, 200 mg, 1.09 mmol, 1.0 equiv) and (1R,4R)-2-oxa-5-azabicyclo[2.2.1]heptane hydrochloride (324 mg, 2.39 mmol, 2.2 equiv) in the presence of N,N-diisopropylethylamine (800 μL, 4.59 mmol, 4.2 equiv). Purification by column chromatography on silica gel (cyclohexane/EtOAc 1:1 →0:1) gave compound 45 (217 mg, 707 μmol, 65%) as a colorless solid. ^{1}H NMR (400 MHz, CDCl$_3$): δ 5.06 (br s, 1 H), 4.98 (br s, 1 H), 4.67 (br s, 2 H), 3.90−3.80 (m, 4 H), 3.64−3.41 (m, 4 H), 2.00−1.82 (m, 4 H). ^{13}C{^{1}H} NMR (101 MHz, CDCl$_3$): δ 169.5−168.5 (m, 1 C), 163.0−162.6 (m, 2 C), 76.4−76.1 (m, 2 C), 74.1 (br s, 1 C), 73.7 (s, 1 C), 56.8 (br s, 2 C), 55.2 (br s, 2 C), 36.7 (br s, 1 C), 36.6−36.3 (m, 1 C). MALDI-MS: m/z = 310.1 ([M + H]$^+$). Compound 45 exists as a mixture of rotamers.

6-(4-Chloro-6-{3-oxa-6-azabicyclo[3.1.1]heptan-6-yl}-1,3,5-triazin-2-yl)-3-oxa-6-azabicyclo[3.1.1]heptane (46). 46 was prepared according to general procedure 1 from cyanuric chloride (40, 200 mg, 1.09 mmol, 1.0 equiv) and 3-oxa-6-azabicyclo[3.1.1]heptane trifluoroacetate (511 mg, 2.40 mmol, 2.2 equiv) in the presence of N,N-diisopropylethylamine (1.14 mL, 6.54 mmol, 6.0 equiv). Purification by column chromatography on silica gel (cyclohexane/EtOAc 2:3) gave compound 46 (258 mg, 833 μmol, 77%) as a colorless solid. ^{1}H NMR (400 MHz, CDCl$_3$): δ 4.54−4.46 (m, 2 H), 4.41−4.22 (m, 6 H), 3.87−3.74 (m, 4 H), 2.75−2.68 (m, 2 H), 1.96 (d, $^3J_{H,H}$ = 8.2 Hz, 2 H). ^{13}C{^{1}H} NMR (101 MHz, CDCl$_3$): δ 169.6 (s, 1 C), 165.4 (s, 1 C), 165.2 (s, 1 C), 66.5 (s, 2 C), 65.8 (s, 2 C), 62.3 (s, 2 C), 62.2 (s, 2 C), 27.5 (s, 1 C), 27.4 (s, 1 C). MALDI-MS: m/z = 310.5 ([M + H]$^+$).

2-Chloro-4,6-bis[(3R)-3-ethylmorpholin-4-yl]-1,3,5-triazine (47). 47 was prepared according to general procedure 1 from cyanuric chloride (40, 290 mg, 1.57 mmol, 1.0 equiv) and (R)-3-ethylmorpholine hydrochloride (500 mg, 3.30 mmol, 2.1 equiv) in the presence of N,N-diisopropylethylamine (1.15 mL, 6.60 mmol, 4.2 equiv). Purification by column chromatography on silica gel (cyclohexane/EtOAc 1:0 → 7:3) gave compound 47 (303 mg, 886 μmol, 56%) as a colorless solid. ^{1}H NMR (400 MHz, CDCl$_3$): δ 4.61−4.25 (m, 4 H), 3.95−3.78 (m, 4 H), 3.56 (dd, $J_{H,H}$ = 12, 3.2 Hz, 2 H), 3.48 (dd, $J_{H,H}$ = 12, 3.0 Hz, 2 H), 3.26−3.10 (m, 2 H), 1.86−1.71 (m, 4 H), 0.90 (t, $^3J_{H,H}$ = 7.4 Hz, 6 H). ^{13}C{^{1}H} NMR (101 MHz, CDCl$_3$): δ 169.6 (s, 1 C), 164.7 (br s, 2 C), 68.7 (s, 1 C), 68.5 (s, 1 C), 67.0 (s, 1 C), 66.9 (s, 1 C), 52.5 (s, 1 C), 52.2 (s, 1 C), 39.3 (s, 1 C), 39.1 (s, 1 C), 21.7 (br s, 2 C), 11.0 (s, 1 C), 10.6 (s, 1 C). MALDI-MS: m/z = 342.2 ([M + H]$^+$).

2-Chloro-4,6-bis[(3R,5S)-3,5-dimethylmorpholin-4-yl]-1,3,5-triazine (48). 48 was prepared according to general procedure 2 from cyanuric chloride (40, 382 mg, 2.07 mmol, 1.0 equiv) and (3R,5S)-3,5-dimethylmorpholine (500 mg, 4.34 mmol, 2.1 equiv) in the presence of N,N-diisopropylethylamine (1.50 mL, 8.69 mmol, 4.2 equiv). Purification by column chromatography on silica gel (cyclohexane/EtOAc 1:0 → 9:1) gave compound 48 (286 mg, 837 μmol, 41%) as a colorless solid. ^{1}H NMR (400 MHz, (CD$_3$)$_2$SO): δ 4.44−4.33 (m, 4 H), 3.77−3.69 (m, 4 H), 3.57−3.48 (m, 4 H), 1.25 (d, $^3J_{H,H}$ = 6.9 Hz, 12 H). ^{13}C{^{1}H} NMR (101 MHz, CDCl$_3$): δ 169.6 (s, 1 C), 164.1 (s, 2 C), 71.4 (s, 4 C), 46.2 (s, 4 C), 19.2 (br s, 4 C). MALDI-MS: m/z = 342.7 ([M + H]$^+$).

2-Chloro-4,6-bis[(3R,5R)-3,5-dimethylmorpholin-4-yl]-1,3,5-triazine (49). 49 was prepared according to general procedure 2 from (3R,5R)-3,5-dimethylmorpholine hydrochloride (345 mg, 2.28 mmol, 2.1 equiv) and cyanuric chloride (40, 200 mg, 1.08 mmol, 1.0 equiv) in the presence of N,N-diisopropylethylamine (790 μL, 4.54 mmol, 4.2 equiv). Purification by column chromatography on silica gel (cyclohexane/EtOAc 1:0 → 9:1) gave compound 49 (247 mg, 723 μmol, 67%) as a colorless solid. ^{1}H NMR (400 MHz, CDCl$_3$): δ 4.36−4.25 (m, 4 H), 4.21 (dd, $^2J_{H,H}$ = 11 Hz, $^3J_{H,H}$ = 3.4 Hz, 4 H), 3.73 (dd, $^2J_{H,H}$ = 11 Hz, $^3J_{H,H}$ = 2.3 Hz, 4 H), 1.43 (d, $^3J_{H,H}$ = 6.7 Hz, 12 H). ^{13}C{^{1}H} NMR (101 MHz, CDCl$_3$): δ 169.0 (s, 1 C), 163.9 (br s, 2 C), 67.6 (s, 4 C), 48.4 (s, 4 C), 19.7 (s, 4 C). MALDI-MS: m/z = 342.3 ([M + H]$^+$).

2-Chloro-4,6-bis[(3S,5S)-3,5-dimethylmorpholin-4-yl]-1,3,5-triazine (50). 50 was prepared according to general procedure 2 from (3S,5S)-3,5-dimethylmorpholine hydrochloride (345 mg, 2.28 mmol, 2.1 equiv) and cyanuric chloride (40, 200 mg, 1.08 mmol, 1.0 equiv) in the presence of N,N-diisopropylethylamine (790 μL, 4.54 mmol, 4.2 equiv). Purification by column chromatography on silica gel (cyclohexane/EtOAc 1:0 → 9:1) gave compound 50 (232 mg, 679 μmol, 63%) as a colorless solid. ^{1}H NMR (400 MHz, (CD$_3$)$_2$SO): δ 4.26−4.14 (m 4 H), 4.14−4.04 (m, 4 H), 3.65 (dd, $^2J_{H,H}$ = 11 Hz, $^3J_{H,H}$ = 2.2 Hz, 4 H), 1.34 (d, $^3J_{H,H}$ = 2.2 Hz, 12 H). ^{13}C{^{1}H} NMR (101 MHz, CDCl$_3$): δ 169.0 (s, 1 C), 163.9 (br s, 2 C), 67.6 (s, 4 C), 48.4 (s, 4 C), 19.7 (s, 4 C). MALDI-MS: m/z = 342.7 ([M + H]$^+$).

2-Chloro-4,6-bis[(2R,6S)-2,6-dimethylmorpholin-4-yl]-1,3,5-triazine (51). 51 was prepared according to general procedure 2 from (2S,6R)-2,6-dimethylmorpholine (656 mg, 5.70 mmol, 2.1 equiv) and cyanuric chloride (40, 500 mg, 2.72 mmol, 1.0 equiv) in the presence of N,N-diisopropylethylamine (2.00 mL, 11.4 mmol, 4.2 equiv). Purification by column chromatography on silica gel (cyclohexane/EtOAc 1:0 → 9:1) gave compound 51 (478 mg, 1.40 mmol, 51%) as a colorless solid. ^{1}H NMR (400 MHz, CDCl$_3$): δ 4.59−4.38 (m, 4 H), 3.64−3.51 (m, 4 H), 2.61−2.51 (m, 4 H), 1.24 (br s, 12 H). ^{13}C{^{1}H} NMR (101 MHz, CDCl$_3$): δ 169.6 (s, 1 C), 164.3 (s, 2 C), 71.9 (s, 2 C), 71.6 (s, 2 C), 48.9 (s, 4 C), 19.0 (s, 2 C), 18.8 (s, 2 C). MALDI-MS: m/z = 342.2 ([M + H]$^+$).

2-Chloro-4,6-bis(2,2-dimethylmorpholin-4-yl)-1,3,5-triazine (52). 52 was prepared according to general procedure 1 from cyanuric chloride (40, 381 mg, 2.07 mmol, 1.0 equiv) and 2,2-dimethylmorpholine (500 mg, 4.34 mmol, 2.1 equiv) in the presence of N,N-diisopropylethylamine (1.50 mL, 8.69 mmol, 4.2 equiv). Purification by column chromatography on silica gel (cyclohexane/EtOAc 1:0 → 4:1) gave compound 52 (107 mg, 313 μmol, 15%) as a colorless solid. ^{1}H NMR (400 MHz, CDCl$_3$): δ 3.84−3.68 (m, 8 H), 3.65−3.52 (m, 4 H), 1.23 (s, 12 H). ^{13}C{^{1}H} NMR (101 MHz, CDCl$_3$): δ 169.8 (s, 1 C), 164.9 (s, 2 C), 71.6 (s, 1 C), 71.5 (s, 1 C), 60.7 (s, 1 C), 60.3 (s, 1 C), 52.6 (s, 2 C), 43.6 (s, 1 C), 43.4 (s, 1 C), 24.4 (s, 2 C), 24.2 (s, 2 C). MALDI-MS: m/z = 342.3 ([M + H]$^+$).

5-(4-Chloro-6-{8-oxa-5-azaspiro[3.5]nonan-5-yl}-1,3,5-triazin-2-yl)-8-oxa-5-azaspiro[3.5]nonane (53). 53 was prepared according to general procedure 1 from cyanuric chloride (40, 345 mg, 1.87 mmol,

1.0 equiv) and 8-oxa-5-azaspiro[3.5]nonane (500 mg, 3.93 mmol, 2.1 equiv) in the presence of *N,N*-diisopropylethylamine (1.40 mL, 7.85 mmol, 4.2 equiv). Purification by column chromatography on silica gel (cyclohexane/EtOAc 1:0 → 9:1) gave compound **53** (451 mg, 1.23 mmol, 66%) as a colorless solid. ^{1}H NMR (400 MHz, CDCl$_3$): δ 3.80−3.65 (m, 8 H), 3.60−3.50 (m, 4 H), 2.55−2.42 (m, 4 H), 2.36−2.24 (m, 4 H), 1.84−1.71 (m, 2 H), 1.17−1.60 (m, 2 H). ^{13}C{^{1}H} NMR (101 MHz, CDCl$_3$): δ 168.8 (s, 1 C), 165.3 (s, 2 C), 71.1 (s, 2 C), 66.3 (s, 2 C), 61.0 (s, 2 C), 43.6 (s, 2 C), 31.2 (s, 4 C), 14.9 (s, 2 C). MALDI-MS: m/z = 366.2 ([M + H]$^+$).

9-(4-Chloro-6-{3,7-dioxa-9-azabicyclo[3.3.1]nonan-9-yl}-1,3,5-triazin-2-yl)-3,7-dioxa-9-azabicyclo[3.3.1]nonane (54). **54** was prepared according to procedure 2 from 3,7-dioxa-9-azabicyclo[3.3.1]nonane (180 mg, 1.39 mmol, 2.0 equiv) and cyanuric chloride (**40**, 128 mg, 694 μmol, 1.0 equiv) in the presence of *N,N*-diisopropylethylamine (490 μL, 2.8 mmol, 4.0 equiv). Purification by column chromatography on silica gel (cyclohexane/EtOAc 1:1 → 0:1) gave compound **54** (191 mg, 516 μmol, 74%) as a colorless solid. ^{1}H NMR (400 MHz, (CD$_3$)$_2$SO): δ 4.42 (br s, 2 H), 4.32 (br s, 2 H), 4.05−3.91 (m, 8 H), 3.76−3.63 (m, 8 H). ^{13}C{^{1}H} NMR (101 MHz, CDCl$_3$): δ 170.6 (s, 1 C), 163.6 (s, 2 C), 69.8 (s, 4 C), 69.5 (s, 4 C), 48.9 (s, 2 C), 48.8 (s, 2 C). MALDI-MS: m/z = 370.2 ([M + H]$^+$).

9-(4-Chloro-6-{3-oxa-9-azabicyclo[3.3.1]nonan-9-yl}-1,3,5-triazin-2-yl)-3-oxa-9-azabicyclo[3.3.1]nonane (55). **55** was prepared according to general procedure 1 from cyanuric chloride (**40**, 185 mg, 1.00 mmol, 1.0 equiv) and 3-oxa-9-azabicyclo[3.3.1]nonane hydrochloride (360 mg, 2.20 mmol, 2.2 equiv) in the presence of *N,N*-diisopropylethylamine (1.00 mL, 5.74 mmol, 5.7 equiv). Purification by column chromatography on silica gel (cyclohexane/EtOAc 1:0 → 9:1) gave compound **55** (297 mg, 812 μmol, 81%) as a colorless solid. ^{1}H NMR (400 MHz, (CD$_3$)$_2$SO): δ 4.48 (br s, 2 H), 4.42 (br s, 2 H), 3.95−3.86 (m, 4 H), 3.68−3.60 (m, 4 H), 2.51−2.38 (m, 4 H), 1.88−1.63 (m, 8 H), 1.59−1.49 (m, 2 H). ^{13}C{^{1}H} NMR (101 MHz, CDCl$_3$): δ 170.2 (s, 1 C), 163.5 (s, 2 C), 71.4−71.3 (m, 2 C), 71.2 (s, 1 C), 71.1 (s, 1 C), 47.9 (br s, 2 C), 47.8 (s, 1 C), 47.7 (s, 1 C), 29.4 (s, 1 C), 29.3 (s, 1 C), 28.9 (s, 1 C), 28.8 (s, 1 C), 20.5 (s, 2 C). MALDI-MS: m/z = 366.2 ([M + H]$^+$).

4-[6-Chloro-2-(morpholin-4-yl)pyrimidin-4-yl]morpholine (57) and 4-[2-chloro-6-(morpholin-4-yl)pyrimidin-4-yl]morpholine (58). **57** and **58** were prepared according to the literature.[24]

8-(6-Chloro-2-{3-oxa-8-azabicyclo[3.2.1]octan-8-yl}pyrimidin-4-yl)-3-oxa-8-azabicyclo[3.2.1]octane (59) and 8-(2-Chloro-6-{3-oxa-8-azabicyclo[3.2.1]octan-8-yl}pyrimidin-4-yl)-3-oxa-8-azabicyclo[3.2.1]octane (60). To a solution of 2,4,6-trichloropyrimidine (**56**, 1.08 g, 5.88 mmol, 1.0 equiv) and 3-oxa-8-azabicyclo[3.2.1]octane hydrochloride (1.94 g, 13.0 mmol, 2.2 equiv) in ethanol (13 mL), *N,N*-diisopropylethylamine (4.51 mL, 25.9 mmol, 4.4 equiv) was added. The resulting mixture was stirred at reflux overnight. Then, the reaction mixture was allowed to cool down to room temperature, and the solvent was removed under reduced pressure. The residue was dissolved in CH$_2$Cl$_2$ and washed with an aq satd NaHSO$_4$ solution, dried over anhydrous Na$_2$SO$_4$ and filtered, and the solvent was evaporated under reduced pressure. The products were separated by column chromatography on silica gel (cyclohexane/EtOAc 3:1 →1:1). Compound **59** (1.10 g, 3.27 mmol, 56%) and compound **60** (212 mg, 629 μmol, 11%) were obtained in two separate fractions. Compound **59**: ^{1}H NMR (400 MHz, CDCl$_3$): δ 5.79 (s, 1 H), 4.59 (br s, 2 H), 4.52−4.15 (m, 2 H), 3.80−3.71 (m, 4 H), 3.62−3.55 (m, 4 H), 2.12−1.90 (m, 8 H). ^{13}C{^{1}H} NMR (101 MHz, CDCl$_3$): δ 161.5 (s, 1 C), 160.6 (s, 1 C), 160.2 (s, 1 C), 92.8 (s, 1 C), 71.7 (s, 2 C), 71.2 (s, 2 C), 55.4 (br s, 4 C), 27.1 (s, 2 C), 27.0 (s, 2 C). MALDI-MS: m/z = 337.1 ([M + H]$^+$). Compound **60**: ^{1}H NMR (400 MHz, CDCl$_3$): δ 5.25 (s, 1 H), 4.50−4.24 (m, 4 H), 3.76 (d, $J_{H,H}$ = 11 Hz, 4 H), 3.62−3.54 (m, 4 H), 2.12−1.92 (m, 8 H). ^{13}C{^{1}H} NMR (101 MHz, CDCl$_3$): δ 161.8 (s, 2 C), 160.9 (s, 1 C), 81.4 (s, 1 C), 71.1 (br s, 4 C), 55.5 (s, 4 C), 26.9 (s, 4 C). MALDI-MS: m/z = 337.1 ([M + H]$^+$).

4-(Difluoromethyl)pyridin-2-amine (61). Pd(OAc)$_2$ (275 mg, 1.22 mmol, 0.05 equiv) and 2-dicyclohexylphosphino-2′,4′,6′-triisopropyl-

biphenyl (XPhos, 1.17 g, 2.45 mmol, 0.10 equiv) were dissolved in dioxane (10 mL) under nitrogen atmosphere, and the resulting mixture was stirred at room temperature for 45 min. This solution was then added to a mixture of *tert*-butylcarbamate (4.30 g, 36.7 mmol, 1.5 equiv), Cs$_2$CO$_3$ (15.9 g, 48.8 mmol, 2.0 equiv), and 2-chloro-4-(difluoromethyl)pyridine (4.00 g, 24.5 mmol, 1.0 equiv) in dioxane (80 mL) under nitrogen atmosphere. The reaction mixture was stirred at 90 °C for 3 h. After this time, the mixture was allowed to cool down to room temperature, diluted with EtOAc, washed with an aq satd NH$_4$Cl solution (2×) and deionized H$_2$O. The organic layer was dried over anhydrous Na$_2$SO$_4$ and filtered, and the solvent was evaporated under reduced pressure. The brownish residue was mixed with 4 M HCl in dioxane (50 mL, excess) and CH$_3$OH (20 mL) and heated at 80 °C for 45 min. Deionized H$_2$O was added, and the aqueous layer was washed with EtOAc (3×). The aqueous layer was then basified to pH = 10, with solid NaOH. This aqueous layer was extracted with EtOAc (3×). The combined organic layers were dried over anhydrous Na$_2$SO$_4$, filtered, and concentrated to dryness under reduced pressure. The desired product **61** (3.47 g, 24.1 mmol, 98%) was obtained as a colorless solid, which was used in the next step without further purification. ^{1}H NMR (400 MHz, CDCl$_3$): δ 8.16 (d, [2]$J_{H,H}$ = 5.2 Hz, 1 H), 6.74 (d, [2]$J_{H,H}$ = 4.8 Hz, 1 H), 6.59 (s, 1 H), 6.51 (t, [2]$J_{H,F}$ = 56 Hz, 1 H), 4.61 (br s, 2 H). ^{13}C{^{1}H} NMR (101 MHz, CDCl$_3$): δ 159.0 (s, 1 C), 149.1 (s, 1 C), 144.0 (t, [2]$J_{C,F}$ = 23 Hz, 1 C), 113.2 (t, [1]$J_{C,F}$ = 240 Hz, 1 C), 109.9 (t, [3]$J_{C,F}$ = 5.5 Hz, 1 C), 104.8 (t, [3]$J_{C,F}$ = 6.6 Hz, 1 C).

5-Bromo-4-(difluoromethyl)pyridin-2-amine (62). To a solution of 4-(difluoromethyl)pyridin-2-amine (**61**, 3.00 g, 20.8 mmol, 1.0 equiv) in tetrahydrofuran (60 mL), *N*-bromosuccinimide (3.89 g, 21.9 mmol, 1.05 equiv) was added at 0 °C. The resulting mixture was stirred overnight, while it was allowed to warm up to room temperature. EtOAc was added, and the organic layer was washed with an aq 8% Na$_2$CO$_3$ solution. The organic layer was separated and acidified with an aq 3 M HCl solution. The aqueous layer was washed with EtOAc (3×) and then basified to pH = 10, with solid NaOH and extracted with EtOAc (3×). The combined organic layers were dried over anhydrous Na$_2$SO$_4$, filtered, and concentrated to dryness under reduced pressure. The desired product **62** (3.65 g, 16.4 mmol, 79%) was obtained as a brownish solid, which was used in the next step without further purification. ^{1}H NMR (400 MHz, CDCl$_3$): δ 8.20 (s, 1 H), 6.75 (s, 1 H), 6.71 (t, [2]$J_{H,F}$ = 54 Hz, 1 H), 4.62 (br s, 2 H). ^{13}C{^{1}H} NMR (101 MHz, CDCl$_3$): δ 158.1 (s, 1 C), 150.7 (s, 1 C), 142.1 (t, [2]$J_{C,F}$ = 23 Hz, 1 C), 112.4 (t, [1]$J_{C,F}$ = 241 Hz, 1 C), 106.3 (t, [3]$J_{C,F}$ = 6.5 Hz, 1 C), 106.0 (t, [3]$J_{C,F}$ = 5.7 Hz, 1 C).

N′-[5-Bromo-4-(difluoromethyl)pyridin-2-yl]-N,N-dimethylmethanimidamide (63). To a solution of 5-bromo-4-(difluoromethyl)pyridin-2-amine (**62**, 3.68 g, 16.5 mmol, 1.0 equiv) in tetrahydrofuran (50 mL), *N,N*-dimethylformamide dimethyl acetal (3.30 mL, 24.8 mmol, 1.5 equiv) was added, and the resulting mixture was stirred at 60 °C for 3 h. The mixture was allowed to cool down to room temperature, and the solvent was evaporated under reduced pressure. The crude product was purified by column chromatography on silica gel (cyclohexane/EtOAc 1:1) to afford the desired compound **63** as a yellowish solid (3.76 g, 13.5 mmol, 82%). ^{1}H NMR (400 MHz, CDCl$_3$): δ 8.43 (s, 1 H), 8.34 (br s, 1 H), 7.17 (s, 1 H), 6.73 (t, [2]$J_{H,F}$ = 54 Hz, 1 H), 3.12 (s, 3 H), 3.10 (s, 3 H). ^{13}C{^{1}H} NMR (101 MHz, CDCl$_3$): δ 162.1 (s, 1 C), 155.8 (s, 1 C), 150.5 (s, 1 C), 141.9 (t, [2]$J_{C,F}$ = 23 Hz, 1 C), 115.8 (t, [3]$J_{C,F}$ = 6.2 Hz, 1 C), 112.6 (t, [1]$J_{C,F}$ = 240 Hz, 1 C), 110.4 (t, [3]$J_{C,F}$ = 5.7 Hz, 1 C), 41.0 (s, 1 C), 34.8 (s, 1 C).

N′-[4-(Difluoromethyl)-5-(4,4,5,5-tetramethyl-1,3,2-dioxaborolan-2-yl)pyridin-2-yl]-N,N-dimethylmethanimidamide (64). Step 1: To a 2 M solution of isopropylmagnesium chloride (3.10 mL, 6.20 mmol, 1.2 equiv) in tetrahydrofuran (6 mL) was slowly added a solution of *N′*-[5-bromo-4-(difluoromethyl)pyridin-2-yl]-*N,N*-dimethylmethanimidamide (**63**, 1.50 g, 5.39 mmol, 1.0 equiv) in tetrahydrofuran (5 mL) at 0 °C. The resulting brownish mixture was stirred at 0 °C for 45 min and then at room temperature for 15 min. After this time, TLC analysis showed complete consumption of the starting material. Step 2: 2-Isopropoxy-4,4,5,5-tetramethyl-1,3,2-

dioxaborolane (1.43 mL, 7.00 mmol, 1.3 equiv) was added, and the mixture was stirred at 60 °C for 3 h. The mixture was then placed in an Erlenmeyer flask, cooled to 0 °C, and quenched with a 15% aq NH$_4$Cl solution. The layers were separated and the aqueous layer was extracted with EtOAc (3×). The combined organic layers were dried over anhydrous Na$_2$SO$_4$ and filtered, and the solvent was evaporated under reduced pressure. The residue was dissolved in heptanes and washed with an aq satd NaHCO$_3$ solution. The organic layer was dried over anhydrous Na$_2$SO$_4$ and filtered, and the solvents were evaporated under reduced pressure. The desired product **64** (1.64 g, 5.04 mmol, 94%) was obtained as a brownish oil, which was used in the next step without further purification. ^{1}H NMR (400 MHz, CDCl$_3$): δ 8.66 (s, 1 H), 8.51 (s, 1 H), 7.34−7.04 (m, 2 H), 3.12 (s, 3 H), 3.12 (s, 3 H), 1.34 (s, 12 H). ^{13}C{^{1}H} NMR (101 MHz, CDCl$_3$): δ 164.9 (s, 1 C), 156.3 (s, 1 C), 156.0 (s, 1 C), 149.2 (t, $^2J_{C,F}$ = 22 Hz, 1 C), 115.5−112.3 (br s, 1 C), 113.3 (t, $^2J_{C,F}$ = 6.4 Hz, 1 C), 112.6 (t, $^1J_{C,F}$ = 238 Hz, 1 C), 84.0 (s, 2 C), 41.0 (s, 1 C), 34.8 (s, 1 C), 24.8 (s, 4 C). MALDI-MS: *m/z* = 326.0 ([M + H]$^+$).

(2-Amino-5-bromopyridin-4-yl)methanol (65). (2-Aminopyridin-4-yl)methanol (2.00 g, 16.1 mmol, 1.0 equiv) was dissolved in acetonitrile (80 mL) at −15 °C. *N*-Bromosuccinimide (3.01 g, 16.9 mmol, 1.1 equiv) was added portionwise, and the resulting reaction mixture was stirred at −15 °C for 1 h. Then the solvent was removed under reduced pressure, the crude residue was dissolved in EtOAc, and an aq satd Na$_2$CO$_3$ solution was added. The organic layer was separated, and the aqueous layer was extracted with EtOAc (3×). The combined organic layers were dried over anhydrous Na$_2$SO$_4$ and filtered, and the solvent was evaporated under reduced pressure. The desired product **65** (2.30 g, 11.3 mmol, 70%) was obtained as a colorless solid, which was used in the next step without further purification. ^{1}H NMR (400 MHz, (CD$_3$)$_2$SO): δ 7.86 (s, 1 H), 6.67 (br s, 1 H), 6.11 (br s, 2 H), 5.45 (t, $^3J_{H,H}$ = 5.6 Hz, 1 H), 4.35 (dd, $^3J_{H,H}$ = 5.6 Hz, $^4J_{H,H}$ = 1.2 Hz, 2 H). ^{13}C{^{1}H} NMR (101 MHz, (CD$_3$)$_2$SO): δ 159.3 (s, 1 C), 150.1 (s, 1 C), 148.0 (s, 1 C), 106.7 (s, 1 C), 104.4 (s, 1 C), 61.8 (s, 1 C).

5-Bromo-4-(fluoromethyl)pyridin-2-amine (66). To a solution of compound **65** (200 mg, 985 μmol, 1.0 equiv) in CH$_2$Cl$_2$ (10 mL) at 0 °C under nitrogen atmosphere, *N,N*-diethyl-*S,S*-difluorosulfiliminium tetrafluoroborate (XtalFluor-E, 338 mg, 1.48 mmol, 1.5 equiv) and triethylamine trihydrofluoride (241 μL, 1.48 mmol, 1.5 equiv) were added. The resulting mixture was stirred overnight while it was allowed to warm up to room temperature. Then the mixture was poured onto aq satd NaHCO$_3$ solution at 0 °C and extracted with CH$_2$Cl$_2$ (3×). The combined organic layers were dried over anhydrous Na$_2$SO$_4$ and filtered, and the solvent was evaporated under reduced pressure. Purification by column chromatography on silica gel (CH$_2$Cl$_2$/EtOAc 1:0 → 7:3) gave compound **66** (70.9 mg, 346 μmol, 45%) as a colorless solid. ^{1}H NMR (400 MHz, CDCl$_3$): δ 8.09 (s, 1 H), 6.63 (s, 1 H), 5.35 (dd, $^2J_{H,F}$ = 47 Hz, $^4J_{H,H}$ = 1.1 Hz, 2 H), 4.52 (br s, 2 H). ^{13}C{^{1}H} NMR (101 MHz, (CD$_3$)$_2$SO): δ 159.4 (s, 1 C), 148.9 (s, 1 C), 144.3 (d, $^2J_{C,F}$ = 18 Hz, 1 C), 106.5 (d, $^3J_{C,F}$ = 11 Hz, 1 C), 103.2 (d, $^3J_{C,F}$ = 5.6 Hz, 1 C), 82.4 (d, $^1J_{C,F}$ = 169 Hz, 1 C).

N′-[5-Bromo-4-(fluoromethyl)pyridin-2-yl]-N,N-dimethylmethanimidamide (67). Compound **66** (57.0 mg, 278 μmol, 1.0 equiv) was dissolved in tetrahydrofuran (1.5 mL), and *N,N*-dimethylformamide dimethyl acetal (93.0 μL, 700 mmol, 2.5 equiv) was added. The reaction mixture was stirred at 70 °C overnight. Then the solvent was evaporated under reduced pressure. EtOAc and deionized H$_2$O was added to the residue. The organic layer was separated, and the aqueous layer was extracted with EtOAc (3×). The combined organic layers were dried over anhydrous Na$_2$SO$_4$, filtered, and reduced to dryness under reduced pressure. The desired product **67** (65.1 mg, 250 μmol, 90%) was obtained as a colorless solid, which was used in the next step without further purification. ^{1}H NMR (400 MHz, CDCl$_3$): δ 8.40 (s, 1 H), 8.25 (s, 1 H), 7.06 (s, 1 H), 5.37 (d, $^2J_{H,F}$ = 47 Hz, $^4J_{H,H}$ = 1.1 Hz, 2 H), 3.10 (s, 3 H), 3.09 (s, 3 H). ^{13}C{^{1}H} NMR (101 MHz, CDCl$_3$): δ 161.9 (s, 1 C), 155.7 (s, 1 C), 149.5 (s, 1 C), 145.9 (d, $^2J_{C,F}$ = 19 Hz, 1 C), 116.1 (d, $^3J_{C,F}$ = 11 Hz, 1 C), 110.5 (d, $^3J_{C,F}$ =

6.1 Hz, 1 C), 82.5 (d, $^1J_{C,F}$ = 173 Hz, 1 C), 41.0 (s, 1 C), 34.9 (s, 1 C).

N′-[5-Bromo-4-{[tert-butyl(dimethyl)silyl]oxymethyl]-2-pyridyl]-N,N-dimethyl-formamidine (68). Step 1: (2-Amino-5-bromopyridin-4-yl)methanol (**65**, 2.20 g, 10.8 mmol, 1.0 equiv) was dissolved in tetrahydrofuran (50 mL), and *N,N*-dimethylformamide dimethyl acetal (2.70 mL, 20.2 mmol, 1.9 equiv) was added. The reaction mixture was stirred at 70 °C overnight. Then the solvent was evaporated under reduced pressure. EtOAc and deionized H$_2$O was added to the residue. The organic layer was separated, and the aqueous layer was extracted with EtOAc (3×). The combined organic layers were dried over anhydrous Na$_2$SO$_4$, filtered, and reduced to dryness under reduced pressure. Step 2: The above residue and imidazole (2.21 g, 32.4 mmol, 3.0 equiv) were dissolved in *N,N*-dimethylformamide (90 mL), and *tert*-butyldimethylsilyl chloride (1.86 g, 12.3 mmol, 1.1 equiv) was added. The reaction mixture was stirred for 1 h at room temperature. An aq satd NaHCO$_3$ solution and EtOAc were added. The organic layer was separated, and the aqueous layer was extracted with EtOAc (3×). The combined organic layers were dried over anhydrous Na$_2$SO$_4$, filtered, and reduced to dryness under reduced pressure. Purification by column chromatography on silica gel (cyclohexane/EtOAc 1:0 →1:1) gave compound **68** (1.82 g, 4.89 mmol, 45%) as a colorless semisolid. ^{1}H NMR (400 MHz, CD$_3$OD): δ 8.36 (s, 1 H), 8.17 (s, 1 H), 7.18 (s, 1 H), 4.70 (d, $^4J_{H,H}$ = 1.2 Hz, 2 H), 3.15 (s, 3 H), 3.07 (s, 3 H), 0.99 (s, 9 H), 0.17 (s, 6 H). ^{13}C{^{1}H} NMR (101 MHz, CD$_3$OD): δ 162.8 (s, 1 C), 157.9 (s, 1 C), 152.3 (s, 1 C), 149.7 (s, 1 C), 116.9 (s, 1 C), 112.8 (s, 1 C), 65.1 (s, 1 C), 41.4 (s, 1 C), 35.2 (s, 1 C), 26.4 (s, 3 C), 19.3 (s, 1 C), − 5.35 (s, 2 C). MALDI-MS: *m/z* = 372.0 ([M + H]$^+$).

5-Bromo-4-(dimethoxymethyl)pyridin-2-amine (69). 4-(Dimethoxymethyl)pyridine-2-amine (2.00 g, 11.9 mmol, 1.0 equiv) was dissolved in 2-methyltetrahydrofuran (24 mL) at 0 °C. *N*-Bromosuccinimide (2.23 g, 12.5 mmol, 1.1 equiv) was added portionwise, and the resulting reaction mixture was stirred at 0 °C for 1 h. The cooling bath was removed, and the reaction mixture was further stirred at room temperature overnight. Then an aq satd Na$_2$CO$_3$ solution was added. The organic layer was separated, and the aqueous layer was extracted with 2-methyltetrahydrofuran (2×). The combined organic layers were dried over anhydrous Na$_2$SO$_4$ and filtered, and the solvent was evaporated under reduced pressure. Purification by column chromatography on silica gel (cyclohexane/EtOAc 1:0 → 4:1) gave compound **69** (2.59 g, 10.5 mmol, 88%) as a yellowish solid. ^{1}H NMR (400 MHz, (CD$_3$)$_2$SO): δ 7.98 (s, 1 H), 6.65 (s, 1 H), 6.23 (br s, 2 H), 5.28 (s, 1 H), 3.28 (s, 6 H). ^{13}C{^{1}H} NMR (101 MHz, CDCl$_3$): δ 157.9 (s, 1 C), 150.1 (s, 1 C), 146.0 (s, 1 C), 108.2 (s, 1 C), 108.0 (s, 1 C), 101.5 (s, 1 C), 53.9 (s, 2 C).

tert-Butyl N-[5-Bromo-4-(dimethoxymethyl)pyridin-2-yl]-N-[(tert-butoxy)carbonyl]carba-mate (70). **70** was prepared according to general procedure 7 from intermediate **69** (2.58 g, 10.4 mmol, 1.0 equiv). Purification by column chromatography on silica gel (cyclohexane/EtOAc 1:0 → 9:1) gave the desired product **70** (1.29 g, 2.88 mmol, 28%) as a yellowish oil. ^{1}H NMR (400 MHz, (CD$_3$)$_2$SO): δ 8.65 (s, 1 H), 7.44 (s, 1 H), 5.50 (s, 1 H), 3.32 (s, 6 H), 1.39 (s, 18 H). ^{13}C{^{1}H} NMR (101 MHz, CDCl$_3$): δ 151.6 (s, 1 C), 151.0 (s, 2 C), 150.9 (s, 1 C), 147.0 (s, 1 C), 121.7 (s, 1 C), 118.6 (s, 1 C), 100.7 (s, 1 C), 83.4 (s, 2 C), 53.4 (s, 2 C), 28.0 (s, 6 C).

tert-Butyl N-(5-Bromo-4-methoxypyridin-2-yl)-N-[(tert-butoxy)carbonyl]carbamate (71). **71** was prepared according to general procedure 7 from 5-bromo-4-methoxypyridin-2-amine (2.00 g, 9.85 mmol, 1.0 equiv). Purification by column chromatography on silica gel (cyclohexane/EtOAc 1:0 → 4:1) gave the desired product **71** (914 mg, 2.27 mmol, 23%) as a colorless solid. ^{1}H NMR (400 MHz, (CD$_3$)$_2$SO): δ 8.44 (s, 1 H), 7.26 (s, 1 H), 3.93 (s, 3 H), 1.40 (s, 18 H). ^{13}C{^{1}H} NMR (101 MHz, (CD$_3$)$_2$SO): δ 162.7 (s, 1 C), 152.8 (s, 1 C), 150.5 (s, 1 C), 149.7 (s, 2 C), 107.5 (s, 1 C), 106.2 (s, 1 C), 82.8 (s, 2 C), 57.0 (s, 1 C), 27.5 (s, 6 C).

N,N-Dimethyl-N′-[5-(4,4,5,5-tetramethyl-1,3,2-dioxaborolan-2-yl)-4-(trifluoromethyl)pyridin-2-yl]methanimidamide (72). **72** was prepared according to the literature.[24]

Determination of Inhibitor Dissociation Constants. Dissociation constants of compounds (K_i) for p110α and mTOR were determined by commercial LanthaScreen (Life Technologies) and evaluated as described in detail in ref 24. In brief, AlexaFluor647-labeled Kinase Tracer314 (no PV6087) with a K_d of 2.2 nM was used at 20 nM for p110α, and at a final concentration of 10 nM for mTOR (K_d of 19 nM). Recombinant N-terminally (His)$_6$-tagged p110α was detected with biotinylated anti-(His)$_6$-tag antibody (2 nM, no. PV6089) and LanthaScreen Eu-Steptavidin (2 nM, no. PV5899); N-terminal GST fused to truncated mTOR (amino acids 1360−2549; no. PR8683B) was detected with a LanthaScreen Eu-labeled anti-GST antibody (2 nM, no. PV5594). The p110α assay buffer was composed of 50 mM HEPES pH 7.5, 10 mM MgCl$_2$, 1 mM EGTA, and 0.01% (v/v) Brij-35, and the mTOR assay buffer contained 50 mM HEPES, 5 mM MgCl$_2$, 1 mM EGTA, and 0.01% Pluronic F-127.

Structure Modeling of PI3K and mTOR Kinase Complexes. The coordinates of the PQR309 (**1**)−PI3Kγ complex (PDB 5OQ4; resolution of 2.7 Å) and mTOR kinase bound to PI103 (PDB 4JT6; 3.6 Å) were used as starting points to dock molecules into the ATP-binding sites. Docking of inhibitors was performed using SwissDock (swissdock.ch), and energy minimization was performed using YASARA's default settings. Alternatively, ligands in crystal structures were manually replaced or substituted. Further measurements and figures were generated in PyMOL 1.7 and Maestro 11.1.

Kinome Profiling. Selectivity and kinase cross-reactivities of indicated compounds were assessed with the ScanMax platform from DiscoverX.[35] Binding of immobilized ligand to DNA-tagged kinases was completed with 10 μM compound, and kinase bound to the immobilized ligand was determined by quantitative PCR of the respective DNA tags. Binding constants were determined by competing immobilized ligand kinase interactions with an 11-point 3-fold serial dilution of compound starting from 30 μM. Binding constants were calculated by a dose−response curve using the Hill equation with Hill Slope set to −1.[23]

Cell Cycle Analysis. A2058 cells ($1-2 \times 10^5$ cells/mL) or SKOV3 cells ($0.25-0.5 \times 10^5$ cells/mL) were seeded in DMEM supplemented with 10% heat-inactivated FCS, 1% L-glutamine, and 1% penicillin−streptomycin (2 mL/well of 6-well plates). The day after, inhibitors (5 μM for A2058, 2 μM for SKOV3) were added for 24 h. Subsequently, nonadherent cells were collected by centrifugation, adherent cells were detached, fixed, and permeabilized, combined with the previously nonadherent cells, in PBS supplemented with 4% paraformaldehyde/1% bovine serum albumin/0.1% TritonX-100 for 30 min at 4 °C then washed with 1% bovine serum albumin/0.1% TritonX-100 in PBS followed by DNA-staining with 1 μg/mL Hoechst33342 in 1% bovine serum albumin/0.1% TritonX-100 in PBS (>1 h, RT, in the dark). Cell cycle profiles were acquired by fluorescence activated cell sorting (FACSCanto II, Becton Dickinson) and analyzed with FlowJo (Treestar) software.

Viability Studies on 66 Cell Lines. The NTRC Oncolines 66 cell lines were exposed for 72 h to 9-point 3-fold serial dilutions of PQR620 (**3**) as described in ref 24. The IC$_{50}$s were calculated by nonlinear regression using IDBS XLfit 5. The percentage growth after 72 h (%-growth) was normalized as follows: 100% × (luminescence$_{t=72h}$/luminescence$_{untreated, t=72h}$). This was fitted to a four-parameter logistics curve: % growth = bottom + (top − bottom)/(1+ $10^{[(\log IC_{50}-\log x)\times HillSlope]}$), where bottom and top are the asymptotic minimum and maximum cell growth that the compound allows in that assay.

Microscopy-Based Proliferation Assay for A2058 and SKOV3 Cells. IC$_{50}$s of A2058 or SKOV3 cell proliferation were determined and calculated as in ref 24.

Cellular PI3K and mTOR Signaling. Downstream signals emerging from TORC2 (phosphorylation of Ser473 of PKB/Akt; rabbit polyclonal antibody from Cell Signaling Technology (CST), no. 4058) and TORC1 (phosphorylation of Ser235/236 on the ribosomal protein S6; rabbit monoclonal antibody from CST, no. 4856) were measured by In-Cell Western plating 2×10^4 A2058 or 1.6×10^4 SKOV3 cells/well in 96-well plates (Cell Carrier, PerkinElmer) for 24 h (37 °C, 5% CO$_2$) before exposing cells for 1

h to inhibitors or DMSO. Then, cells were fixed (4% PFA in PBS for 30 min at RT), blocked (1% BSA/0.1% Triton X-100/5% goat serum in PBS for 30 min, RT), and stained with CST primary antibodies (1:500). Tubulin staining (mouse anti-α-tubulin, 1:2000, Sigma no. T9026) was assessed as an internal standard. Secondary antibody [IRDye680-conjugated goat antimouse, and IRDye800-conjugated goat antirabbit antibodies (LICOR no. 926-68070 and no. 926-32211), both 1:500] fluorescence was detected on an Odyssey CLx infrared imaging scanner (LICOR). Percentage of remaining phospho-substrate signals were calculated in relation to cellular tubulin.[24]

Western Blotting. Cells were lysed in lysis buffer (20 mM Tris-HCl pH 8, 138 mM NaCl, 2.7 mM KCl, 5% glycerol, 1% NP-40), and cleared supernatants were denatured by boiling (96 °C, 6 min) after adding 5× sample buffer. Cellular protein amounts were adjusted and subjected to SDS-PAGE and transferred to Immobilon FL membranes (Millipore). Primary antibodies to pSer473-PKB/Akt (no. 4058L), pThr308-PKB/Akt (no. 4056L), PKB/AKT (no. 2929S), pT389-S6K1 (no. 9206S), and pS235/236 ribosomal protein S6 (no. 4856S); S6K1 (no. 9202S), ribosomal protein S6 (no. 2317S), pSer65 4EBP1 (no. 9456), and 4EBP1 (no. 9452S) were all from CST; α-tubulin (no. T9026) was from Sigma. HRP-conjugated secondary antibodies were detected by chemiluminescence on a Fusion FX (Vilber Lourmat) imaging system.

Formulation of Compounds and in Vivo Pharmacology. PQR620 (**3**) and PQR309 (**1**) (12.5 mg) were dissolved in DMSO (0.25 mL) by vortexing and sonication. After the addition of 2.25 mL of 20% HP-β-CD (hydroxypropyl-β-cyclodextrin/water), the mixture was vortexed and sonicated to get 2.5 mL dosing solution (dose volume: 10 μL/g). Formulations were homogeneous at the time of application. Experimental procedures in male C57BL/6J mice were in accordance with regulations of the Landesamt für Gesundheit und Verbraucherschutz, Saarbrücken); female Sprague−Dawley (SD) rat studies were carried out according to the NRC Guide for the Care and Use of Laboratory Animals, authorized by the French authorities (Agreement no. A21231011EA) and overviewed by the Animal Care and Use Committee of Oncodesign (CNREEA agreement no. 91).

OVCAR-3 Xenograft Mouse Tumor Model. *OVCAR-3 Cell cCulture.* Cells were cultured as monolayer in DMEM medium supplemented with 10% fetal bovine serum at 37 °C and 5% CO$_2$. Cells were passaged by trypsin-EDTA treatment and harvested in the exponential growth phase tumor inoculation.

Tumor Inoculation and Group Assignments. Each mouse (female BALB/c nude; age: 8−9 weeks) was inoculated subcutaneously with 5×10^6 cells (in 0.1 mL PBS) into the right flank. At treatment start mean tumor size was ca. 157 mm^3, body weight and tumor volume were assessed, and randomized groups using a randomized block design based on tumor volumes were established. Tumor cell inoculation is depicted as day 0.

Data Collection and Termination. Animals were monitored daily for mobility, visual estimation of food and water consumption, eye/hair matting, morbidity, mortality, tumor growth and potential macroscopic adverse effects of drug treatment. Body weight and tumor volumes were determined three times weekly. The latter was determined in two dimensions using a caliper, and the volume was expressed in mm^3 using the formula:

$$V = 0.5 \times a \times b^2$$

where a and b are the long and short diameters of the tumor. All mice were terminated on day 45 after the tumor inoculation, when the excised tumor was weighted. BALB/c nude mice were from Shanghai Lingchang Bio-Technology Co. Ltd. All animal procedures were approved by the Institutional Animal Care and Use Committee (IACUC) of CrownBio. Care and use of animals was in accordance with the regulations of the Association for Assessment and Accreditation of Laboratory Animal Care (AAALAC).

Determination of Seizures in *Tsc1*^{GFAP} Conditional Knock-out Mice. A previously established mouse model of TSC with conditional inactivation of the Tsc1 gene in glial fibrillary acidic protein (GFAP)-positive cells (*Tsc1*^{GFAP} conditional knockout mice),

which develops progressive epilepsy, encephalopathy, and premature death, was used.[33]

Animals. Tsc1[flox/flox]/GFAP-Cre mice of either sex were bred at PsychoGenics using breeding pairs obtained from M. Wong's Laboratory (Washington University, St. Louis, MO) to generate a tissue-specific knockout of Tsc1 in GFAP-positive cells. All mice were handled according to the PsychoGenics ethical guidelines. Light/dark cycles were maintained at 12 h/12 h, temperature was 20−23 °C, and humidity ∼50%. Food and water ad libitum. Mice were randomly assigned to designated treatment groups, and dosing was performed during the light cycle phase. Assessment and approval of the study by the Association for Assessment and Accreditation of Laboratory Animal Care (approval IACUC 282_0616).

Surgery. Aseptic techniques were used throughout all surgery. Mice were anesthetized with isoflurane with homeostatic heating to maintain core temperature at 37 ± 1 °C. An 8201-EEG head mount (Pinnacle Technology, Inc., Lawrence, KS) with bihemispheric leads in the frontal and parietal cortices and an indwelling local field potential electrode targeting the region above the CA1 were used. Before, during, and after surgery, animals were administered fluids, nutrition, antibiotics, and analgesics as required/recommended by the Program of Veterinary Care (PVC) team and IACUC, in concert with the Attending Veterinarian and/or according to IACUC Guidelines. Mice were implanted with electrodes at the age of postnatal day (PND) 22 to PND27 and allowed to recover for up to 4 weeks of age (PND35).

EEG Recording. EEG was recorded continuously using the Pinnacle Technology 8206 data conditioning and acquisition system (DCAS), and real-time visualization of all EEG channels from all mice was observed using Sirenia or PAL-8400 software. Synchronized video recordings were collected for the duration of the EEG recordings.

Test Compound and Treatments. Vehicle (sulfobutyl-ether-β-cyclodextrin, Captisol, Dexolve; SBECD) was obtained from DavosPharma (Liberty, MO). Compounds were initially dissolved in acidified 23.5% SBECD (5.0 mL of 40% SBECD + 3.5 mL of H_2O + 0.2 M HCl as needed). Solution pH was adjusted to be within 2.2 and 2.7 using 0.2 M NaOH and diluted to a final volume of 10.0 mL to yield a Vehicle of 20% SBECD (pH 3.0 ± 0.1). Mice in the study were randomly assigned to one of the following treatment groups: Vehicle 10 mL/kg (20% SBECD; PND21-53; po qd), PQR620 (**3**) (100 mg/kg; group B; PND21-53; po qd), and PQR309 (**1**) (50 mg/kg; group C; PND21-53; po qd). Stock 40% SBECD was stored at 4 °C. Vehicle and compound solutions were prepared fresh weekly.

ASSOCIATED CONTENT

Ⓢ Supporting Information

The Supporting Information is available free of charge on the ACS Publications website at DOI: 10.1021/acs.jmedchem.8b01262.

> Information on amino acid conservation of PI3K/mTOR structural elements influencing the −CHF₂ dipole and structural elements of PI3K/mTOR close to morpholine bridge; a docking model of mTOR kinase with bound PQR620 (**3**); SD errors of mTOR and lipid kinase binding; a TREEspot data visualization of KINOMEScan interactions (of PQR620 (**3**), INK128 (**73**), SB2602 (**74**), and PP242 (**75**), selectivity profile analyses, and the raw date of kinase interactions (KINOMEscan of PQR620 (**3**)); in vitro pharmacology, enzyme and uptake assays, cancer cell line panel for compound PQR620 (**3**); quantification of cell cycle distribution of A2058 and SKOV3 cells after exposure to PQR620 (**3**), INK128 (**73**), PP242 (**75**), SB2602 (**74**), rapamycin, and GDC0941 (**76**) and phosphoprotein levels in A2058 and SKOV3 cells after drug exposure; correlation of cancer mutations and sensitivity to PQR620 (**3**) in cancer cell line panel; mouse PK data;

unspecific rat brain tissue binding values for PQR620 (**3**); MDCK permeability data and P-gp dependence; collection of compound activity data, clogP and PSA; compound structures overview; ^{1}H NMR spectra; ^{13}C{[1]} NMR spectra; MALDI-MS spectra. ESI-HRMS spectra; and HPLC chromatograms (PDF)

Molecular formula strings and selected data (CSV)

Accession Codes

PDB 5OQ4 was used for docking of compound PQR620 (**3**) into PI3Kγ. PDB 4JT6 was used for docking of compound PQR620 (**3**) into mTOR kinase.

AUTHOR INFORMATION

Corresponding Author

*Phone: +41 61 207 5046. Fax: +41 61 207 3566. E-mail: matthias.wymann@unibas.ch.

ORCID Ⓞ

Denise Rageot: 0000-0002-2833-5481
Chiara Borsari: 0000-0002-4688-8362
Alexander M. Sele: 0000-0002-4903-7934
John Burke: 0000-0001-7904-9859
Matthias P. Wymann: 0000-0003-3349-4281

Author Contributions

D.R., T.B., and A.M. contributed equally. The manuscript was written through contributions of all authors. All authors have given approval to the final version of the manuscript.

Notes

The authors declare the following competing financial interest(s): PHe, FB, and DF are current or past employees of PIQUR Therapeutics AG, Basel; and PHi, PHe, DF, and MPW are shareholders of PIQUR Therapeutics AG.

ABBREVIATIONS USED

ESI, electrospray ionization; GPCR, G-protein coupled receptor; mTOR, mechanistic (or mammalian) target of rapamycin; TORC1, mTOR complex 1; TSC, tuberous sclerosis complex; PI3K, phosphoinositide 3-kinase; PKB/Akt, protein kinase B/Akt; PTEN, phosphatase and tensin homologue; PtdIns(3,4,5)P_3, phosphatidylinositol(3,4,5)-trisphosphate; PyBpin, pyridine boronic acid pinacol ester; S6RP, ribosomal protein S6; S6K, p70 S6 kinase; VPS34, vacuolar protein sorting 34, the class III PI3K

REFERENCES

(1) Wymann, M. P.; Schneiter, R. Lipid signalling in disease. *Nat. Rev. Mol. Cell Biol.* **2008**, *9*, 162−176. Yang, H.; Rudge, D. G.; Koos, J.

D.; Vaidialingam, B.; Yang, H. J.; Pavletich, N. P. mTOR kinase structure, mechanism and regulation. *Nature* **2013**, *497*, 217−223. Shimobayashi, M.; Hall, M. N. Making new contacts: the mTOR network in metabolism and signalling crosstalk. *Nat. Rev. Mol. Cell Biol.* **2014**, *15*, 155−162. Saxton, R. A.; Sabatini, D. M. mTOR signaling in growth, metabolism, and disease. *Cell* **2017**, *168*, 960−976.

(2) Laplante, M.; Sabatini, D. M. mTOR signaling in growth control and disease. *Cell* **2012**, *149*, 274−293.

(3) Sarbassov, D. D.; Guertin, D. A.; Ali, S. M.; Sabatini, D. M. Phosphorylation and regulation of Akt/PKB by the rictor-mTOR complex. *Science* **2005**, *307*, 1098−1101.

(4) Liu, P.; Gan, W.; Chin, Y. R.; Ogura, K.; Guo, J.; Zhang, J.; Wang, B.; Blenis, J.; Cantley, L. C.; Toker, A.; Su, B.; Wei, W. PtdIns(3,4,5)P3-dependent activation of the mTORC2 kinase complex. *Cancer Discovery* **2015**, *5*, 1194−1209.

(5) Benjamin, D.; Colombi, M.; Moroni, C.; Hall, M. N. Rapamycin passes the torch: a new generation of mTOR inhibitors. *Nat. Rev. Drug Discovery* **2011**, *10*, 868−880.

(6) Choi, J.; Chen, J.; Schreiber, S. L.; Clardy, J. Structure of the FKBP12-rapamycin complex interacting with the binding domain of human FRAP. *Science* **1996**, *273*, 239−242.

(7) Eisen, H. J.; Tuzcu, E. M.; Dorent, R.; Kobashigawa, J.; Mancini, D.; Valantine-von Kaeppler, H. A.; Starling, R. C.; Sorensen, K.; Hummel, M.; Lind, J. M.; Abeywickrama, K. H.; Bernhardt, P. Everolimus for the prevention of allograft rejection and vasculopathy in cardiac-transplant recipients. *N. Engl. J. Med.* **2003**, *349*, 847−858. Jacob, S.; Nair, A. B. A review on therapeutic drug monitoring of the mTOR class of immunosuppressants: everolimus and sirolimus. *Drugs Ther Perspect* **2017**, *33*, 290−301. Alalawi, F.; Sharma, A.; Halawa, A. mTOR Inhibitors in the current practice. *J. Clin. Exp. Nephrol.* **2017**, *1*, 26.

(8) Costa, M. A.; Simon, D. I. Molecular basis of restenosis and drug-eluting stents. *Circulation* **2005**, *111*, 2257−2273.

(9) Motzer, R. J.; Escudier, B.; Oudard, S.; Hutson, T. E.; Porta, C.; Bracarda, S.; Grunwald, V.; Thompson, J. A.; Figlin, R. A.; Hollaender, N.; Urbanowitz, G.; Berg, W. J.; Kay, A.; Lebwohl, D.; Ravaud, A. Efficacy of everolimus in advanced renal cell carcinoma: a double-blind, randomised, placebo-controlled phase III trial. *Lancet* **2008**, *372*, 449−456.

(10) Jerusalem, G.; Rorive, A.; Collignon, J. Use of mTOR inhibitors in the treatment of breast cancer: an evaluation of factors that influence patient outcomes. *Breast Cancer: Targets Ther.* **2014**, *6*, 43−57.

(11) Arachchige Don, A. S.; Zheng, X. F. S. Recent clinical trials of mTOR-targeted cancer therapies. *Rev. Recent Clin. Trials* **2011**, *6*, 24−35.

(12) Shor, B.; Gibbons, J. J.; Abraham, R. T.; Yu, K. Targeting mTOR globally in cancer: thinking beyond rapamycin. *Cell Cycle* **2009**, *8*, 3831−3837.

(13) Slotkin, E. K.; Patwardhan, P. P.; Vasudeva, S. D.; de Stanchina, E.; Tap, W. D.; Schwartz, G. K. MLN0128, an ATP-competitive mTOR kinase inhibitor with potent in vitro and in vivo antitumor activity, as potential therapy for bone and soft-tissue sarcoma. *Mol. Cancer Ther.* **2015**, *14*, 395−406. Hsieh, A. C.; Liu, Y.; Edlind, M. P.; Ingolia, N. T.; Janes, M. R.; Sher, A.; Shi, E. Y.; Stumpf, C. R.; Christensen, C.; Bonham, M. J.; Wang, S.; Ren, P.; Martin, M.; Jessen, K.; Feldman, M. E.; Weissman, J. S.; Shokat, K. M.; Rommel, C.; Ruggero, D. The translational landscape of mTOR signalling steers cancer initiation and metastasis. *Nature* **2012**, *485*, 55−61.

(14) Mortensen, D. S.; Fultz, K. E.; Xu, S.; Xu, W.; Packard, G.; Khambatta, G.; Gamez, J. C.; Leisten, J.; Zhao, J.; Apuy, J.; Ghoreishi, K.; Hickman, M.; Narla, R. K.; Bissonette, R.; Richardson, S.; Peng, S. X.; Perrin-Ninkovic, S.; Tran, T.; Shi, T.; Yang, W. Q.; Tong, Z.; Cathers, B. E.; Moghaddam, M. F.; Canan, S. S.; Worland, P.; Sankar, S.; Raymon, H. K. CC-223, a potent and selective inhibitor of mTOR kinase: in vitro and in vivo characterization. *Mol. Cancer Ther.* **2015**, *14*, 1295−1305. Jin, Z.; Niu, H.; Wang, X.; Zhang, L.; Wang, Q.;

Yang, A. Preclinical study of CC223 as a potential anti-ovarian cancer agent. *Oncotarget* **2017**, *8*, 58469−58479.

(15) Pike, K. G.; Malagu, K.; Hummersone, M. G.; Menear, K. A.; Duggan, H. M.; Gomez, S.; Martin, N. M.; Ruston, L.; Pass, S. L.; Pass, M. Optimization of potent and selective dual mTORC1 and mTORC2 inhibitors: the discovery of AZD8055 and AZD2014. *Bioorg. Med. Chem. Lett.* **2013**, *23*, 1212−1216.

(16) Crino, P. B.; Nathanson, K. L.; Henske, E. P. The tuberous sclerosis complex. *N. Engl. J. Med.* **2006**, *355*, 1345−1356.

(17) Meikle, L.; Pollizzi, K.; Egnor, A.; Kramvis, I.; Lane, H.; Sahin, M.; Kwiatkowski, D. J. Response of a neuronal model of tuberous sclerosis to mammalian target of rapamycin (mTOR) inhibitors: effects on mTORC1 and Akt signaling lead to improved survival and function. *J. Neurosci.* **2008**, *28*, 5422−5432.

(18) Krueger, D. A.; Wilfong, A. A.; Mays, M.; Talley, C. M.; Agricola, K.; Tudor, C.; Capal, J.; Holland-Bouley, K.; Franz, D. N. Long-term treatment of epilepsy with everolimus in tuberous sclerosis. *Neurology* **2016**, *87*, 2408−2415.

(19) MacKeigan, J. P.; Krueger, D. A. Differentiating the mTOR inhibitors everolimus and sirolimus in the treatment of tuberous sclerosis complex. *Neuro Oncol* **2015**, *17*, 1550−1559.

(20) McCormack, F. X.; Inoue, Y.; Moss, J.; Singer, L. G.; Strange, C.; Nakata, K.; Barker, A. F.; Chapman, J. T.; Brantly, M. L.; Stocks, J. M.; Brown, K. K.; Lynch, J. P.; Goldberg, H. J.; Young, L. R.; Kinder, B. W.; Downey, G. P.; Sullivan, E. J.; Colby, T. V.; McKay, R. T.; Cohen, M. M.; Korbee, L.; Taveira-DaSilva, A. M.; Lee, H. S.; Krischer, J. P.; Trapnell, B. C.; National Institutes of Health Rare Lung Diseases Consortium; MILES Trial Group. Efficacy and safety of sirolimus in lymphangioleiomyomatosis. *N. Engl. J. Med.* **2011**, *364*, 1595−1606.

(21) Talboom, J. S.; Velazquez, R.; Oddo, S. The mammalian target of rapamycin at the crossroad between cognitive aging and Alzheimer's disease. *NPJ. Aging Mech. Dis.* **2015**, *1*, 15008.

(22) Ravikumar, B.; Vacher, C.; Berger, Z.; Davies, J. E.; Luo, S.; Oroz, L. G.; Scaravilli, F.; Easton, D. F.; Duden, R.; O'Kane, C. J.; Rubinsztein, D. C. Inhibition of mTOR induces autophagy and reduces toxicity of polyglutamine expansions in fly and mouse models of Huntington disease. *Nat. Genet.* **2004**, *36*, 585−595. Floto, R. A.; Sarkar, S.; Perlstein, E. O.; Kampmann, B.; Schreiber, S. L.; Rubinsztein, D. C. Small molecule enhancers of rapamycin-induced TOR inhibition promote autophagy, reduce toxicity in Huntington's disease models and enhance killing of mycobacteria by macrophages. *Autophagy* **2007**, *3*, 620−622.

(23) Beaufils, F.; Cmiljanovic, N.; Cmiljanovic, V.; Bohnacker, T.; Melone, A.; Marone, R.; Jackson, E.; Zhang, X.; Sele, A.; Borsari, C.; Mestan, J.; Hebeisen, P.; Hillmann, P.; Giese, B.; Zvelebil, M.; Fabbro, D.; Williams, R. L.; Rageot, D.; Wymann, M. P. 5-(4,6-dimorpholino-1,3,5-triazin-2-yl)-4-(trifluoromethyl)pyridin-2-amine (PQR309), a potent, brain-penetrant, orally bioavailable, pan-class I PI3K/mTOR inhibitor as clinical candidate in oncology. *J. Med. Chem.* **2017**, *60*, 7524−7538.

(24) Bohnacker, T.; Prota, A. E.; Beaufils, F.; Burke, J. E.; Melone, A.; Inglis, A. J.; Rageot, D.; Sele, A. M.; Cmiljanovic, V.; Cmiljanovic, N.; Bargsten, K.; Aher, A.; Akhmanova, A.; Díaz, J. F.; Fabbro, D.; Zvelebil, M.; Williams, R. L.; Steinmetz, M. O.; Wymann, M. P. Deconvolution of Buparlisib's mechanism of action defines specific PI3K and tubulin inhibitors for therapeutic intervention. *Nat. Commun.* **2017**, *8*, 14683.

(25) Sessler, C. D.; Rahm, M.; Becker, S.; Goldberg, J. M.; Wang, F.; Lippard, S. J. CF$_2$H, a Hydrogen Bond Donor. *J. Am. Chem. Soc.* **2017**, *139*, 9325−9332. Zafrani, Y.; Yeffet, D.; Sod-Moriah, G.; Berliner, A.; Amir, D.; Marciano, D.; Gershonov, E.; Saphier, S. Difluoromethyl Bioisostere: examining the "lipophilic hydrogen bond donor" concept. *J. Med. Chem.* **2017**, *60*, 797−804.

(26) Zask, A.; Kaplan, J.; Verheijen, J. C.; Richard, D. J.; Curran, K.; Brooijmans, N.; Bennett, E. M.; Toral-Barza, L.; Hollander, I.; Ayral-Kaloustian, S.; Yu, K. Morpholine derivatives greatly enhance the selectivity of mammalian target of rapamycin (mTOR) inhibitors. *J. Med. Chem.* **2009**, *52*, 7942−7945.

(27) Walker, E. H.; Pacold, M. E.; Perisic, O.; Stephens, L.; Hawkins, P. T.; Wymann, M. P.; Williams, R. L. Structural determinants of phosphoinositide 3-kinase inhibition by wortmannin, LY294002, quercetin, myricetin, and staurosporine. *Mol. Cell* **2000**, *6*, 909−919.

(28) Davis, M. I.; Hunt, J. P.; Herrgard, S.; Ciceri, P.; Wodicka, L. M.; Pallares, G.; Hocker, M.; Treiber, D. K.; Zarrinkar, P. P. Comprehensive analysis of kinase inhibitor selectivity. *Nat. Biotechnol.* **2011**, *29*, 1046−1051.

(29) Brandt, C.; Hillmann, P.; Noack, A.; Römermann, K.; Öhler, L. A.; Rageot, D.; Beaufils, F.; Melone, A.; Sele, A. M.; Wymann, M. P.; Fabbro, D.; Löscher, W. The novel, catalytic mTORC1/2 inhibitor PQR620 and the PI3K/mTORC1/2 inhibitor PQR530 effectively cross the blood-brain barrier and increase seizure threshold in a mouse model of chronic epilepsy. *Neuropharmacology* **2018**, *140*, 107−120.

(30) Marone, R.; Erhart, D.; Mertz, A. C.; Bohnacker, T.; Schnell, C.; Cmiljanovic, V.; Stauffer, F.; Garcia-Echeverria, C.; Giese, B.; Maira, S. M.; Wymann, M. P. Targeting melanoma with dual phosphoinositide 3-kinase/mammalian target of rapamycin inhibitors. *Mol. Cancer Res.* **2009**, *7*, 601−613.

(31) O'Reilly, K. E.; Rojo, F.; She, Q. B.; Solit, D.; Mills, G. B.; Smith, D.; Lane, H.; Hofmann, F.; Hicklin, D. J.; Ludwig, D. L.; Baselga, J.; Rosen, N. mTOR inhibition induces upstream receptor tyrosine kinase signaling and activates Akt. *Cancer Res.* **2006**, *66*, 1500−1508.

(32) Kleinert, M.; Sylow, L.; Fazakerley, D. J.; Krycer, J. R.; Thomas, K. C.; Oxbøll, A. J.; Jordy, A. B.; Jensen, T. E.; Yang, G.; Schjerling, P.; Kiens, B.; James, D. E.; Ruegg, M. A.; Richter, E. A. Acute mTOR inhibition induces insulin resistance and alters substrate utilization in vivo. *Mol. Metab.* **2014**, *3*, 630−641.

(33) Zeng, L. H.; Xu, L.; Gutmann, D. H.; Wong, M. Rapamycin prevents epilepsy in a mouse model of tuberous sclerosis complex. *Ann. Neurol.* **2008**, *63*, 444−453.

(34) Burger, M. T.; Pecchi, S.; Wagman, A.; Ni, Z. J.; Knapp, M.; Hendrickson, T.; Atallah, G.; Pfister, K.; Zhang, Y.; Bartulis, S.; Frazier, K.; Ng, S.; Smith, A.; Verhagen, J.; Haznedar, J.; Huh, K.; Iwanowicz, E.; Xin, X.; Menezes, D.; Merritt, H.; Lee, I.; Wiesmann, M.; Kaufman, S.; Crawford, K.; Chin, M.; Bussiere, D.; Shoemaker, K.; Zaror, I.; Maira, S. M.; Voliva, C. F. Identification of NVP-BKM120 as a potent, selective, orally bioavailable class I PI3 kinase inhibitor for treating cancer. *ACS Med. Chem. Lett.* **2011**, *2*, 774−779.

(35) Fabian, M. A.; Biggs, W. H.; Treiber, D. K.; Atteridge, C. E.; Azimioara, M. D.; Benedetti, M. G.; Carter, T. A.; Ciceri, P.; Edeen, P. T.; Floyd, M.; Ford, J. M.; Galvin, M.; Gerlach, J. L.; Grotzfeld, R. M.; Herrgard, S.; Insko, D. E.; Insko, M. A.; Lai, A. G.; Lélias, J. M.; Mehta, S. A.; Milanov, Z. V.; Velasco, A. M.; Wodicka, L. M.; Patel, H. K.; Zarrinkar, P. P.; Lockhart, D. J. A small molecule-kinase interaction map for clinical kinase inhibitors. *Nat. Biotechnol.* **2005**, *23*, 329−336.